ISSN 1173-5996

Ignition Properties of New Zealand Timber

by
Chu Kang Ngu

Supervised by

Dr Charley Fleischmann

Fire Engineering Research Report 01/5
March 2001

This report was presented as a project report as part of the
M.E. (Fire) degree at the University of Canterbury

School of Engineering
University of Canterbury
Private Bag 4800
Christchurch, New Zealand

Phone 643 364-2250
Fax 643 364-2758
www.civil.canterbury.ac.nz

Abstract

This project investigated the ignition properties of New Zealand Timbers and timber products. The ignition test on the wood was according to the British Standard BS 476: Part 13, 1987 using ISO ignitability apparatus. The ignition time for each sample was recorded and correlated by seven correlations. These seven correlations are:

1) Mikkola and Wichman
2) Tewarson
3) Quintiere and Harkleroad
4) Janssens
5) Toal, Silcock and Shields
6) Delichatsios, Panagiotou and Kiley
7) Spearpoint and Quintiere

Six types of wood, Macrocarpa, Beech, Rimu, Radiata Pine, Plywood and medium density fiberboard (mdf) were tested at constant heat flux lower than 40 kW/m^2 until ignition did not occur within 20 minutes. Each type of wood was tested at two different thicknesses, 20 mm and 40 mm. The repeatability and reproducibility were also determined.

It was found that the results such as critical heat flux, thermal inertia, ignition temperature, Thermal Response Parameter (TRP), Flux Time Product (FTP) and so on were different from one correlation to another. It is hard to say which one is the best technique in estimating the ignition properties of New Zealand wood, but one can get an idea of which methods will give higher or lower results. Another words: the tendency of each method to under-predict or over-predict the results. Both the 20-mm and 40-mm wood behaved as thermally thick (some thermally intermediate) solids and they have very close values of minimum heat flux and critical heat flux.

Acknowledgements

I would first like to thank you Dr Charley Fleishmann my supervisor for all of his guidance, suggestions, precious ideas and lecturing during the year either in this project or in the course work. Thanks a lot!

Thank you to my other lecturers Andy Buchanan and Michael Spearpoint for their supports and advice.

Thanks to Grant Dunlop for helping me to cut the wood samples and for his technical service and advice.

Thanks to Civil Engineering Workshop for building the ISO ignitability apparatus.

To all of the Fire Engineering class this year. Shao, Richard, Flora, Linus, Baven, Adeline, Ruth, Jenny, Andrew and Angela, thank you. Hope all of you will become fire engineers.

Finally, big thank you to Mum and Dad, and Sindy for your financial and spiritual support. May God bless you all.

Table of Contents Page

ABSTRACT.....1

ACKNOWLEDGEMENTS.....2

TABLE OF CONTENTS.....3

LIST OF FIGURES.....6

LIST OF TABLES.....9

CHAPTER 1: INTRODUCTION.....11

CHAPTER 2: EXPERIMENTAL METHODOLOGY
BS 476: PART 13

2.1) DEFINITIONS.....13
2.2) PRINCIPLES OF THE TEST.....14
2.3) SPECIMEN PREPARATION.....15
2.4) BASEBOARD PREPARATION.....16
2.5) ALUMINIUM FOIL PREPARATION.....16
2.6) TEST APPARATUS.....17
2.7) CALIBRATION.....18
2.8) TEST PROCEDURE.....19

CHAPTER 3: LITERATURE SURVEY

3.1) THEORETICAL BACKGROUND.....24
3.2) MIKKOLA & WICHMAN.....27
3.3) TEWARSON.....29
3.4) QUINTIERE & HARKLEROAD.....31
3.5) JANSSENS.....34
3.6) TOAL, SILCOCK & SHIELDS.....36
3.7) DELICHATSIOS, PANAGIOTOU & KILEY.....37
3.8) SPEARPOINT & QUINTIERE.....40

CHAPTER 4: DATA ANALYSIS

4.1) CALIBRATION OF THE CONE ELEMENT.....43
4.2) CALCULATION OF DENSITY AND MOISTURE CONTENT.....45
4.3) DETERMINATION OF THERMAL PROPERTIES.....46
4.4) DETERMINE THE IGNITION TEMPERATURE.....47
4.5) CONDITIONING OF THE SAMPLES AND BASEBOARD.....49
4.6) DETERMINE THE REPEATABILITY AND REPRODUCIBLITY.....50

CHAPTER 5: RESULTS AND DISCUSSION

5.1) DENSITY AND MOISTURE CONTENT.....54
5.2) OBSERVATION DURING TEST.....56
5.3) GOODNESS OF THE BEST-FIT LINE.....58
5.4) THERMALLY THIN OR THERMALLY THICK BEHAVIOUR?.....62
5.5) IGNITION TEMPERATURE AND THERMAL INERTIA.....64
5.6) MINIMUM HEAT FLUX AND CRITICAL HEAT FLUX.....68
5.7) REPEATABILITY AND REPRODUCIBILITY.....72
5.8) WHICH IS THE BEST METHOD?.....75

CHAPTER 6: SOURCES OF ERROR.....78

CHAPTER 7: CONCLUSION.....79

NOMENCLATURE.....82

REFERENCES.....85

APPENDICES

APPENDIX A.....88
APPENDIX B: RESULTS OF EACH CORRELATION.....89
APPENDIX C: MACROCARPA.....93
APPENCIX D: BEECH.....96
APPENDIX E: MEDIUM DENSITY FIBERBOARD.....99
APPENDIX F: RADIATA PINE.....103
APPENDIX G: RIMU.....106
APPENDIX H: PLYWOOD.....109
APPENDIX I: RAW DATA.....112
APPENDIX J: REPEATIBILITY AND REPRODUCIBILITY.....114
APPENDIX K: PLOT OF MEASURED t_{ig} VS PREDICTED t_{ig} 120

List of Figures

Figure 4.1: Calibration Curve of the Cone heater
Figure 4.2: Sensitivity of h_c to the change in T_{ig}
Figure 5.1: Ignition data of mdf plotted by Tewarson (same as Figure E2 in Appendix E)
Figure 5.2: Ignition data of Rimu plotted by Quintiere & Harkleroad (same as Figure G3)
Figure 5.3: Ignition data of Beech plotted by Janssens (same as Figure D4)
Figure 5.4: Relationship between r, R and m
Figure 5.5: Predicted ignition time versus Measured ignition time for Beech (same as Figure K5)
Figure 5.6: Predicted ignition time versus Measured ignition time at $t_{ig} < 200$ s for Beech

Figure A1: ISO Ignitability test apparatus
Figure A2: Wrapping of the specimen

Figure C1: Ignition data of Macrocarpa plotted by Mikkola & Wichman, Delichatsios et. al. and Spearpoint et. al.
Figure C2: Ignition data of Macrocarpa plotted by Tewarson
Figure C3: Ignition data of Macrocarpa plotted by Quintere and Harkleroad
Figure C4: Ignition data of Macrocarpa plotted by Janssens
Figure C5: Ignition data of 20-mm Macrocarpa plotted by Toal, Silcock & Shields
Figure C6: Ignition data of 40-mm Macrocarpa plotted by Toal, Silcock

Figure D1: Ignition data of Beech plotted by Mikkola & Wichman, Delichatsios et. al. and Spearpoint et. al.
Figure D2: Ignition data of Beech plotted by Tewarson
Figure D3: Ignition data of Beech plotted by Quintiere and Harkleroad
Figure D4: Ignition data of Beech plotted by Janssens
Figure D5: Ignition data of 20-mm Beech plotted by Toal, Silcock and Shields
Figure D6: Ignition data of 40-mm Beech plotted by Toal, Silcock and Shields

Figure E1: Ignition data of mdf plotted by Mikkola & Wichman, Delichatsios et. al. and Spearpoint et. al.
Figure E2: Ignition data of mdf plotted by Tewarson
Figure E3: Ignition data of mdf plotted by Quintiere and Harkleroad
Figure E4: Ignition data of mdf plotted by Janssens
Figure E5: Ignition data of 20-mm mdf plotted by Toal, Silcock and Shields
Figure E6: 40-mm mdf plotted by Toal, Silcock and Shields, earlier done based on calibration scale on 5/12/2000
Figure E7: 40-mm mdf plotted by Toal, Silcock and Shields, redone based on calibration scale on 20/12/2000

Figure F1: Ignition data of Radiata Pine plotted by Mikkola et. al., Delichatsios et. al. & Spearpoint
Figure F2: Ignition data of Radiata Pine plotted by Tewarson
Figure F3: Ignition data of Radiata Pine plotted by Quintiere and Harkleroad
Figure F4: Ignition data of Radiata Pine plotted by Janssens
Figure F5: Ignition data of 20-mm Radiata Pine plotted by Toal, Silcock and Shields
Figure F6: Ignition data of 40-mm Radiata Pine plotted by Toal, Silcock and Shields

Figure G1: Ignition data of Rimu plotted by Mikkola & Wichman
Figure G2: Ignition data of Rimu plotted by Tewarson
Figure G3: Ignition data of Rimu plotted by Quintiere and Harkleroad
Figure G4: Ignition data of Rimu plotted by Janssens
Figure G5: Ignition data of 20-mm Rimu plotted by Toal, Silcock and Shields
Figure G6: Ignition data of 20-mm Rimu plotted by Toal, Silcock and Shields

Figure H1: Ignition data of Plywood plotted by Mikkola & Wichman, Delichatsios et. al. and Spearpoint et. al.
Figure H2: Ignition data of Plywood plotted by Tewarson
Figure H3: Ignition data of Plywood plotted by Quintiere and Harkleroad
Figure H4: Ignition data of Plywood plotted by Janssens
Figure H5: Ignition data of 20-mm Plywood plotted by Toal, Silcock and Shields
Figure H6: Ignition data of 40-mm Plywood plotted by Toal, Silcock and Shields

Figure K1: Predicted ignition time versus Measured ignition time for 40-mm Radiata Pine
Figure K2: Predicted ignition time versus Measured ignition time for 20-mm Radiata Pine
Figure K3: Predicted ignition time versus Measured ignition time for 40-mm Rimu
Figure K4: Predicted ignition time versus Measured ignition time for 20-mm Rimu
Figure K5: Predicted ignition time versus Measured ignition time for 40-mm Beech
Figure K6: Predicted ignition time versus Measured ignition time for 20-mm Beech
Figure K7: Predicted ignition time versus Measured ignition time for 40-mm Macrocarpa
Figure K8: Predicted ignition time versus Measured ignition time for 20-mm Macrocarpa
Figure K9: Predicted ignition time versus Measured ignition time for 40-mm mdf
Figure K10: Predicted ignition time versus Measured ignition time for 20-mm mdf
Figure K11: Predicted ignition time versus Measured ignition time for 40-mm Plywood
Figure K12: Predicted ignition time versus Measured ignition time for 20-mm Plywood

List of Tables

Table 3.1: Summary of the correlations' plots

Table 5.1: Density and Moisture Content of the 40-mm samples
Table 5.2: Density and Moisture Content of the 20-mm samples
Table 5.3: The ranges of ignition temperature, T_{ig}, of each wood
Table 5.4: The ranges of thermal inertia, kρc, of each wood
Table 5.5: The ranges of minimum heat flux of each wood
Table 5.6: Comparison between the calculated r (and R) and the limits
Table 7.1: Recommendation of Best and Worst Correlations
Table 7.2: Values of thermal inertia, critical heat flux and ignition temperature

Table B1: Results of 40-mm wood from Mikkola & Wichman
Table B2: Results of 20-mm wood from Mikkola & Wichman
Table B3: Results of 40-mm wood from Tewarson
Table B4: Results of 20-mm wood from Tewarson
Table B5: Results of 40-mm wood from Quintiere & Harkleroad
Table B6: Results of 20-mm wood from Quintiere & Harkleroad
Table B7: Results of 40-mm wood from Janssens
Table B8: Results of 20-mm wood from Janssens
Table B9: Results of 40-mm wood from Toal, Silcock & Shields
Table B10: Results of 20-mm wood from Toal, Silcock & Shields
Table B11: Results of 40-mm wood from Delichatsios et. al
Table B12: Results of 20-mm wood from Delichatsios et. al.

Table I1: Ignition Data of 40-mm samples
Table I2: Ignition Data of 20-mm samples

Table J1: Δ of 40-mm Rimu

Table J2: Δ of 20-mm Rimu

Table J3: Δ of 40-mm Radiata Pine

Table J4: Δ of 20-mm Radiata Pine

Table J5: Δ of 40-mm Beech

Table J6: Δ of 20-mm Beech

Table J7: Δ of 40-mm Macrocarpa

Table J8: Δ of 20-mm Macrocarpa

Table J9: Δ of 40-mm Plywood

Table J10: Δ of 20-mm Plywood

Table J11: Δ of 20-mm mdf

Table J12: Original data, y_i

Table J13: y_i^2

Table J14: $(1/n)*(\text{sum of } y_i)^2$

Table J15: Intra-cell standard deviation, s_i

Table J16: Cell averages, y_i bar

Table J17: y bar bar

Table J18: n bar bar

Table J19: Between-lab variance, s_L^2

Table J20: Calculation of r and R values

CHAPTER 1: INTRODUCTION

Fire is one of the most unpredictable and hence dangerous accidents that occur in our surroundings, especially in residential buildings. Its occurrence, development, behaviour and effects are very complex. In order for a fire to occur, the material needs to be ignited. The term "ignitability" is defined in ISO 3261 as the capability of a material to be ignited. Ignition is one of the essential fire properties, which must or always be considered in any assessment of fire hazard.

Ignition depends on various interrelated factors. As the surface is exposed to heat flux, initially most of the heat is transferred into the interior of the specimen. The rate of this heat transfer is dependent on the thermal properties of the material including ignition temperature, T_{ig}; ambient temperature, T_{∞}; material thermal conductivity, k; material specific heat, c; and the density of the material, ρ. The ignition of wood is more complex than other materials, especially when a layer of char is formed. It also depends on the species, moisture content, inherent variability of wood as a natural material, the orientation of the specimen when exposed to the incident heat flux (mounted vertically or horizontally) [2] and the grain orientation (along or across the grain) [15].

The objective of this paper is to examine the ignition properties of some New Zealand timbers and timber products using simple thermal models. Six types of timber or timber products were tested to get their time to ignition, t_{ig}. The six different types of timber are Radiata Pine, Rimu, Beech, Macrocarpa, and New Zealand made timber products: medium density fiberboard (mdf) and plywood. Seven simple thermal correlations developed by various researchers are used and compared to find out the best way to predict the ignition time. This paper will also be looking at another important ignition property of a material: minimum heat flux, $\dot{q}''_{min}$, which is the lowest incident heat flux that can ignite a material. Ignition will not occur at a heat flux lower than the minimum heat flux, $\dot{q}''_{min}$.

The methodology of ignition test used in this paper is based on the British Standard BS 476: Part 13 [14]; also called ISO Ignitability Test. The wood samples are to be exposed to 11 levels of constant irradiances. The tested wood samples have two thicknesses, 20 mm and 40 mm. The experimental method and equipment used with respect to BS 476: Part 13 are discussed in detail in Chapter 2.

The duration of the ignition test will influence the determination of the minimum heat flux. According to BS 476: Part 13, each test should be terminated if no sustained surface ignition occurs within 15 minutes. However, in this research the specimens were given a period of 20 minutes to be ignited. A specimen is ignited if it has a continuous flame at its surface for an uninterrupted period of at least 10 seconds.

CHAPTER 2: EXPERIMENTAL METHODOLOGY BS 476: PART 13

The fire tests on the wood specimens are based on the British Standard BS 476: Part 13: "Method of measuring the ignitability of products subjected to thermal irradiance" [14]. This part of the BS 476 is similar to ISO 5657 – 1986: "Fire Tests – Reaction to Fire – Ignitability of Building Products". The units of irradiance are given in kW/m^2.

2.1) Definitions

Some of the terms used in this report need to be well defined in order to avoid misunderstanding and confusion. The terms in the brackets have the same meanings as the preceding terms.

Product:
Material, composite or assembly about which information is required.

Material:
Single substance or uniformly dispersed mixture, for example, metal, timber (wood), concrete, polymers, etc.

Specimen (Sample):
Representative piece of product which is to be tested together with any substrate or treatment. In this report, the specimen (or sample) refers to the wood (timber) specimen that is to be tested.

Irradiance (Heat flux):
(at a point of a surface) Quotient of the radiant flux incident on an infinitesimal element of surface containing the point, by the area of that element.

Sustained surface ignition:

Inception of a flame on the surface of the specimen which is still present at the next application of the pilot flame. It can be simplified by saying "Ignition" only.

Standards:

Referring to BS 476: 1987: Part 13 unless specified.

2.2) Principles of the Test

The specimens are mounted horizontally on a sample holder (also called specimen insertion and location tray) during the test. Their upper surfaces are exposed to constant thermal irradiance at certain levels of irradiance released by the radiator cone heater, within the range of 10 kW/m^2 to 50 kW/m^2. In this research, the levels of irradiance ranged from 10 kW/m^2 to 40 kW/m^2. The term irradiance indicates the essentially radiative mode of heat transfer. A pilot flame is then applied at certain intervals to a position of 10 mm above the centre of each specimen to ignite any volatile gases that are given off near the surface of the specimens. The pilot flame is widely used due to its simplicity. The time at which sustained surface ignition occurs is recorded. The test does not measure the ignition temperature, T_{ig}.

2.3) Specimen Preparation

Five specimens are tested at each level of irradiance. In this research, there are 11 levels of heat flux in total (10, 11, 12, 13, 14, 15, 20, 25, 30, 35, 40 kW/m^2). The specimens shall have a size of 165 × 165 mm squares according to BS 476: Part 13, with thicknesses of 20 mm and 40 mm. The following shows the total number of specimens to be tested for each type of timber in the tests at one thickness:

Number of specimen:

- Radiata Pine = 11 irradiance level × 5 specimens = 55
- Rimu = 55
- Beech = 55
- Macrocarpa = 55
- Medium density fiberboard = 55
- Plywood = 55

Total = 330 specimens

Before the test, all the specimens are conditioned to constant mass at a temperature of 23 ± 2 deg C, humidity of 50 ± 5 % for a duration of 1-2 weeks, with free access of air to both end sides of the specimens. The reason for doing this is that cellulosic materials require sufficient time to reach equilibrium with the conditioning atmosphere. Constant mass is proof of satisfactory conditioning.

2.4) Baseboard Preparation

The square specimens will be backed by a baseboard during the test. The baseboard are square with the same size as the specimen: that is, 165 × 165 mm^2. The baseboard shall be made of non-combustible insulation board with a nominal thickness of 6 mm. According to the Standards, the baseboards need to be oven-dried to a density of 825 ± 125 kg/m^3. In this research, the baseboards are made of Fyreline GIB board with good enough insulation properties. Like the specimens, the baseboards are to be conditioned for at least 24 hours at a temperature of 23 ± 2 °C and humidity of 50 ± 5 %, with free of access air to both sides of the baseboards. The number of baseboards depends on the frequency of testing and probably the type of product being tested. This is because some of the baseboards can be re-used after the test.

2.5) Aluminium Foil Preparation

A conditioned specimen placed on the baseboard is wrapped in a piece of aluminium foil to ensure an airtight fit at the rear surface. The aluminium foil shall have a thickness of 0.02 mm from which a circular hole of 140-mm diameter has been previously cut before the tests. The circular cut-out zone is centrally positioned over the upper surface of the specimen. Such an arrangement exposes a constant area of the specimen to irradiation and protects the apparatus from becoming soiled by any melting or intumescing products. A specimen-baseboard combination wrapped in aluminium foil is shown in figure A1 in Appendix A.

2.6) Test Apparatus

The ISO ignitability apparatus is a readily setup of the cone calorimeter which includes:

- specimen support framework
- masking plate
- pressing plate
- radiator cone
- pilot flame application mechanism
- specimen insertion and location tray
- specimen screening plate
- additional equipment (temperature controller, radiometer, millivolt measuring device, calibration board, etc).

The general arrangement of suitable apparatus is shown in Figure 2 in BS 476: Part 13: 1988, which is also shown in the Figure A2 in Appendix A of this report. The apparatus are placed in an environment free of draughts. The tests were carried out in a fume cupboard with no induced airflow draughts over the specimen. The airflow must be less than 0.02 m/s to satisfy this condition. This is because if the induced airflow is more than 0.02 m/s, it may disturb the natural airflow near the surface of the specimen and hence cause excessive unwanted convection cooling.

2.7) Calibration

For the purpose of calibration, a radiometer shall be installed in the hole or groove of the calibration board. The radiometer is used to measure the irradiance incident on the surface of a specimen. The apparatus, as explained above, is already set up, except the spark igniter should be turned off throughout the calibration procedure. The calibration board is then placed in the apparatus in the specimen position.

Electric supply is switched on and the temperature settings of the temperature controller are established to produce the required irradiances at the centre of the circular opening in the masking plate, hence the exposed circular upper surface of the specimen of 10, 11, 12, etc kW/m^2. Adjustments near the final setting for the cone heater temperature should be followed by a 5-min period without further adjustment to ensure that the remainder of the apparatus has achieved sufficient temperature equilibrium. At each full equilibrium, the average temperature of the thermocouple monitors located in the cone heater are read and recorded.

These procedures are carried out at least twice, the first time at settings of increasing temperature and the second time at decreasing temperatures. The values should be repeatable to within $\pm$ 5 °C. Values outside these limits indicate possible defects in control of monitoring equipment, or significant changes in the test environment, which must be corrected before further calibrations are carried out.

2.8) Test Procedure

The following procedure is basically similar to BS 476, with some modifications. The most important modification is the use of a spark igniter instead of gas flame supplier as specified in the Standards. The purpose of doing so is to reduce the long interval gas flame application according to the Standards. The Standards require the gas flame application mechanism to ignite the specimens once every four seconds, but by using the spark igniter, one can apply the ignition source to the specimens twice per second. Therefore the spark ignition can increase the accuracy of the recorded time to ignition, t_{ig} and therefore reduce uncertainty.

Just before the test:

a) Once the specimens reach constant mass, remove the specimens from conditioning cabinet and weigh them

b) Record the mass and other relevant information

c) Wrap the specimens and baseboards with aluminium foil

During the Test:

d) Turn on the fan of the fume cupboard

e) Set up and check the apparatus

f) Before starting check the following equipment is in the lab and readily available:

1. CO_2 fire extinguisher
2. Safety glass
3. Stop watches
4. Insertion and location tray (Sample holder)
5. Dummy specimen board (Insulation board) for cone calorimeter
6. Specimen screening plate (Cone shield)
7. Metal bucket half full of water

g) Get ready with the prepared specimen-baseboard combination and make sure it has been weighed

h) Adjust the counterweight to give a force of 20 ± 2 N between the upper surface of the specimen and the underside of the masking plate

i) Turn on the power to the ISO ignitability apparatus at wall

j) On the apparatus front panel, turn on the main power to the apparatus

k) Then turn on the power to the cone heater on the apparatus front panel as well

l) Place the dummy specimen board on the pressing plate

m) Adjust the temperature setting of the controller to the appropriate value established by the calibration procedure to correspond to 400 degrees Celsius (or other level as required)

n) Allow the apparatus to heat up to equilibrium. When the heater has attained temperature equilibrium, a further 5 minutes should be allowed to elapse before commencing exposure of a specimen

o) Remove a prepared specimen from conditioning cabinet and place the prepared specimen on the insertion and location tray

p) After the radiator cone is preheated, set the cone to the desired irradiance level.

q) Once the cone has reached the desired temperature, conduct the next seven steps in rapid succession (15 seconds) wearing safety glass and gloves:

1. Place the specimen screening plate on top of the masking plate
2. Lower the pressing plate, remove the dummy specimen board
3. Place the insertion and location tray containing the specimen on the pressing plate
4. Release the pressing plate
5. Remove the specimen screening plate and start timer (stopwatch)
6. Turn on the spark igniter

r) Record the time to ignition on the prepared information sheet

s) Place extinguishing board on top of the masking plate

t) Turn off the spark igniter

u) Remove the insertion and location tray

v) Place the dummy specimen board on the pressing plate

w) Remove the extinguishing board as quickly as possible

x) Remove the specimen from the insertion and location tray and place the specimen in the water bucket

y) Operations l) to t) should be repeated for the remaining four specimens

Repeat the Test:

z) A further set of five specimens are tested at the next lower level of irradiance

aa) If no sustained surface ignition occurs with all specimens in a batch of five at a given irradiance, tests are not carried out at lower irradiances

bb) When adjusting the heater to the next level of irradiance, sufficient time (3 minutes) must be allowed for the apparatus to reach thermal equilibrium following the change in temperature

Observation during Test:

cc) Several important observations during the test need to be recorded are:

- Time, position and nature of other ignitions
- Glowing decomposition of the specimen
- Melting, foaming, spalling, cracking, expansion or shrinkage of the exposed surface of the specimen

When finished the Test:

dd) When finished with all testing, reduce the cone temperature to 400 degrees Celsius and let it cool for 5 minutes

ee) Turn off the power to the cone heater and the ISO ignitability apparatus on the apparatus front panel

ff) Turn off the main power on the wall

gg) Check all of the equipment listed in step b) is left in a neat and orderly fashion

hh) In control room turn off fan in the fume cupboard and lights

ii) First thing the next day, remove the specimens from water and place it in the rubbish bin.

CHAPTER 3: LITERATURE SURVEY

As stated before, seven different techniques that relate the ignition time to the incident heat flux are used to analyse the experimental results; that is, to calculate the time to ignition under constant radiative heat flux. A number of articles give a good description and explanation of how these seven correlations work in terms of their origins and assumptions. It will be a great advantage to briefly review the seven Ignition time/Irradiance correlations. These are:

1) Mikkola and Wichman[11]
2) Tewarson [10]
3) Quintiere and Harkleroad [5]
4) Janssens [3],[4]
5) Toal, Silcock and Shields [1],[2],[3]
6) Delichatsios, Panagiotou and Kiley [13]
7) Spearpoint and Quintiere [15]

3.1) Theoretical Background [3]

Before going into any details of these correlations, there are some definitions one has to be aware of. This research considers only the ignition of timber caused by piloted ignition. Piloted ignition occurs when a material is heated with an ignition source present. The ignition source can be a small flame, a spark, an electric arc, a burning ember and so on. When the material is heated, it decomposes and releases mass in the form of pyrolyzates. Ignition then occurs when the concentration of the gases released (pyrolysis) exceeds the lower flammable limit in the presence of an ignition source close to the irradiated surface.

All of these correlations have one thing in common; that is, the inclusion of a critical heat flux, $\dot{q}''_{cr}$. Critical heat flux, $\dot{q}''_{cr}$ is a theoretical lower limit for the incident flux necessary to create the conditions for ignition. The critical heat flux $\dot{q}''_{cr}$ should not be confused with minimum heat flux, $\dot{q}''_{\min}$. According to Janssens' [9] definitions, these two terms have the same meanings, except that $\dot{q}''_{cr}$ is an estimate of $\dot{q}''_{\min}$ derived from a correlation of experimental data. The $\dot{q}''_{cr}$ is extrapolated from experimental correlation by making the time to ignition equal to infinity. Therefore $\dot{q}''_{cr}$ is dependent on the type of model used for correlating the ignition data. As a result, $\dot{q}''_{cr}$ is not the best way to estimate the minimum safe radiation level. The $\dot{q}''_{\min}$ is more reliable and is obtained experimentally from a series of decreasing flux levels until ignition does not occur, and it depends on the decision of the researcher as to how long the test should be run. Thus the minimum heat flux is somewhere between the lowest incident heat flux at which ignition occurred and highest incident heat flux at which ignition did not occur. The $\dot{q}''_{\min}$ should be greater than $\dot{q}''_{cr}$ ($\dot{q}''_{\min} > \dot{q}''_{cr}$) [2].

Note that all the specimens tested in this research are physically thermally thick. According to Mikkola and Wichman [11], wood specimens with a thickness greater than 15-20 mm may be considered as thermally thick. To say that a sample is thermally thick means that the unexposed surface temperature, T_s, has not begun to rise.

These correlations apply the same fundamental assumptions; that is, the material is chemically inert, has constant thermophysical properties, and is opaque. Another common assumption is that ignition occurs when the surface temperature, T_s, reaches a critical value, i.e. ignition temperature, T_{ig}. With these fundamental assumptions, the energy balance at the point of ignition may be expressed as follows:

$$-k\frac{dT}{dx}_{x=0} = \varepsilon.\dot{q}''_e - h_c(T_{ig} - T_\infty) - \varepsilon\sigma(T_{ig}^4 - T_\infty^4) \qquad (1)$$

where it has been assumed that the surface acts as a grey body.

Equation (1) shows the net heat conduction into the specimen due to the absorbed incident flux $\varepsilon \dot{q}_e''$, and the convective and radiative surface heat losses.

For a thermally thick material the boundary condition at the unexposed surface is:

$$-k\frac{dT}{dx}_{x\to\infty} = 0 \quad \text{for} \quad t > 0. \tag{2}$$

The initial conditions of the specimen before exposure to the incident flux are:

$$T = T_\infty \quad \text{at} \quad t = 0 \quad \text{for} \quad x \geq 0. \tag{3}$$

In relating the critical heat flux, $\dot{q}_{cr}''$ to the thermal properties of the material, when the net heat conduction into the material is zero, the following equations (4) and (5) can be expressed:

$$\varepsilon \dot{q}_{cr}'' = h_c(T_{ig} - T_\infty) + \varepsilon\sigma(T_{ig}^4 - T_\infty^4) \tag{4}$$

or $$\varepsilon \dot{q}_{cr}'' = h_{ig}(T_{ig} - T_\infty) \tag{5}$$

where $h_{ig} = h_c + \varepsilon\sigma(T^2_{ig} + T^2_\infty)(T_{ig} + T_\infty)$

The above theoretical concept, fundamental assumptions and boundary conditions were developed and used by researchers in developing the time-to-ignition/irradiance models, as briefly discussed below.

3.2) Mikkola and Wichman [11]

Mikkola and Wichman produced a functional relationship between the ignition time and the applied exterior heat flux on a material's surface. They considered two different methods for deducing the relationship that makes it possible to correlate the ignition data obtained experimentally. These two methods are a linearized thermal ignition model and a more general integral method. Both methods give an equivalent form of solution for ignition time, t_{ig}, in both thermally thick and thermally thin cases. Like other correlations, Mikkola and Wichman's correlation is based on a simple thermal ignition problem, which means the gas and solid phase problems are greatly idealised or simplified.

The technique enables correlation of experimental data by plotting a best-fit linear regression line through the ignition data, as t_{ig}^{-1} versus $\dot{q}_e''$. One has to determine whether the specimen tested is thermally thick or thermally thin before applying this correlation. Mikkola and Wichman suggest that a specimen can be considered to be thermally thin and thermally thick if:

$$L_0 / \sqrt{\alpha t_{ig}} \leq 0.4 \qquad \textit{for thermally thin} \qquad (6)$$

$$L_0 / \sqrt{\alpha t_{ig}} \geq 4.0 \qquad \textit{for thermally thick} \qquad (7)$$

α is the thermal diffusivity = k/ρc. Using the typical values for wood, k = 0.15 $Wm^{-1}K^{-1}$, c = 1500 $Jkg^{-1}K^{-1}$ with a characteristic ignition time of 120 seconds. The above equations give a practical limit for thermally thin wood of 1 mm and 15-20 mm for thermally thick wood.

The solution for time to ignition, t_{ig}, solved by Mikkola and Wichman is given below:

$$t_{ig} = \rho L_0 c \frac{(T_{ig} - T_\infty)}{(\dot{q}_e'' - \dot{q}_{cr}'')} \quad \textit{for thermally thin} \tag{8}$$

$$t_{ig} = \frac{\pi}{4} k\rho c \frac{(T_{ig} - T_\infty)^2}{(\dot{q}_e'' - \dot{q}_{cr}'')^2} \quad \textit{for thermally thick} \tag{9}$$

Note that the ignition temperature (T_{ig}), density (ρ), specific heat (c), and critical heat flux, $\dot{q}_{cr}''$ are determined experimentally. Ignition temperature, specific heat and density are very difficult to measure experimentally, especially when the specimen is thermally thin. Hence it is easier to calculate the product of $\rho L_0 c$ from the equation (8) for thermally thin samples, by using the following expression:

$$\rho L_0 c = \frac{1}{slope\,(T_{ig} - T_\infty)} \tag{10}$$

$k\rho c$ in equation (9) for thermally thick samples can be calculated using the equation as shown below:

$$k\rho c = \frac{4}{\pi}\left[\frac{1}{slope\,(T_{ig} - T_\infty)}\right]^2 \tag{11}$$

The ignition temperature can be estimated using the obtained critical heat flux, $\dot{q}_{cr}''$ and equation (4) with appropriate convective heat transfer coefficient, h_c. This method plots the ignition data as t_{ig}^{-1} versus $\dot{q}_e''$ for thermally thin solids, and $t_{ig}^{-1/2}$ versus $\dot{q}_e''$ for thermally thick solids. The critical heat is simply the intercept divided by the slope of the plots:

$\dot{q}''_{cr}$ = Intercept / Slope (12)

Limitations:

The correlation can be used for both thermally thin and thermally thick wood samples. Thus one has to determine carefully whether the specimen is thermally thick or thermally thin to avoid the wrong application of this correlation. There is no precise limit for defining the thermally thick and thermally thin. Mikkola and Wichman defined a solution for thermally intermediate thickness by averaging the sample thickness, L_0 and the characteristic conduction length. For more detailed information, one can refer to the paper written by Mikkola and Wichman in reference [11].

3.3) Tewarson [10]

Tewarson [10] has collected a huge amount of ignition data for his method of analysing the ignition time due to different levels of irradiances. In his analysis, he simplified the thermally thick equation (9) above. Tewarson defined a new single parameter named Thermal Response Parameter (TRP), which combines the ignition temperature, T_{ig} and the thermal inertia, kρc, as shown in the expression below:

$$TRP = \Delta T_{ig} \sqrt{k\rho c} \quad (13)$$

$\Delta T_{ig} = T_{ig} - T_{\infty}$, ignition temperature above ambient. TRP is determined experimentally from ignition results of Factory Mutual Research Corporation Flammability Apparatus and the cone calorimeter. This method can also be applied to other experimental methods. The relationship between the ignition time and the incident irradiance is shown in the equation (14) below. From the equation, the ignition data collected is plotted as $t_{ig}^{-1/2}$ versus $(\dot{q}''_e - \dot{q}''_{\min})$.

$$\sqrt{\frac{1}{t_{ig}}} = \frac{\sqrt{\pi/4}(\dot{q}''_e - \dot{q}''_{\min})}{TRP} \tag{14}$$

Notice that Tewarson uses $\dot{q}''_{\min}$ instead of $\dot{q}''_{cr}$ that was used in thermally thick equation (9). The $\dot{q}''_{\min}$ is calculated from a series of decreasing heat flux tests until the specimen does not ignite. TRP can be computed from the slope of the best-fit linear regression through the data points using equation (15) below. The best-fit line should pass through the origin.

$$TRP = \sqrt{\frac{4}{\pi}}\left(\frac{1}{Slope}\right) \tag{15}$$

Time to ignition, t_{ig} can be calculated by rearranging the equation (15) above as expressed in the following equation (16):

$$t_{ig} = \frac{\pi}{4}\frac{(TRP)^2}{(\dot{q}''_e - \dot{q}''_{\min})} \tag{16}$$

Tewarson's correlation has an advantage of not requiring the surface temperature. This is because the measurement of surface temperature in practice is very difficult, although the principle of critical surface temperature is simple and easy to understand. In addition, there is no easy or widely accepted way of measuring surface temperature. Therefore from an experimental point of view, not having to measure the surface temperature is advantageous.

Limitations:

Tewarson's correlation is applied to thermally thick solids only. It is prudent for the engineer to check that the thickness of the material is at least as thick as the experimental specimen.

3.4) Quintiere and Harkleroad [5]

Quintiere and Harkleroad used a thermal conduction model to analyse and interpret the ignition data obtained from the Lateral Ignition and Flame spread Test (LIFT). This thermal conduction model is fully discussed by Kanury [6] and Simms [7] in ignition studies of wood materials. Their results suggest that the surface temperature (T_s) under constant external radiant heat flux, $\dot{q}_e''$ can be given as:

$$T_s - T_\infty = \frac{\dot{q}_e''}{h_{ig}} F(t) \qquad (17)$$

where h_{ig} = overall heat transfer coefficient accounting for both radiation and convection

$F(t)$ = a function of time and thermal properties of the solid

T_s = T_{ig} at ignition

Although an exact expression can be found for F(t) under conditions of constant properties and a thermally thick solid, F(t) was determined empirically due to the limits of the thermally thick solid solution and the predominant form of their results. The empirical values for F(t) have been found to describe all of the ignition results from the LIFT apparatus successfully and are as follows:

$$F(t) = \frac{\dot{q}''_{\min}}{\dot{q}_e''} =\geq \begin{Bmatrix} b\sqrt{t}, & t \leq t_m \\ 1, & t \geq t_m \end{Bmatrix} \qquad (18)$$

b in the above equation (18) is a constant related to kρc and t_m is a characteristic time indicative of the time taken to reach thermal equilibrium. Hence after a long time, t $\geq t_m$, F(t) becomes 1.

The Quintiere and Harkleroad correlation plots the ignition data as $\dot{q}''_{min} / \dot{q}''_e$ versus $t_{ig}^{1/2}$. A best-fit linear regression line is drawn through the data points and it must pass through the origin. Some of the data points can be ignored, for example $\dot{q}''_{min} / \dot{q}''_e > 0.8$, in order to obtain a reasonable fit for the majority of the data. A certain amount of judgement is required when doing this. The slope of the best-fit line is b, and t_m is the intercept, where $\dot{q}''_{min} / \dot{q}''_e = 1$. The minimum heat flux $\dot{q}''_{min}$ is obtained from a series of decreasing flux tests until ignition does not occur. This method does not actually give the ignition temperature, T_{ig}. The ignition temperature can be determined by the equation (4) above, assuming ε of the incident heat flux is 1, and $\dot{q}''_{cr}$ is replaced with $\dot{q}''_{min}$.

$$\dot{q}''_{min} = h_c(T_{ig} - T_\infty) + \varepsilon\sigma(T_{ig}^4 - T_\infty^4) = h_{ig}(T_{ig} - T_\infty) \qquad (19)$$

From equations (17) and (18), the time to ignition, t_{ig} can be calculated from the following expression:

$$t_{ig} = \left(\frac{\dot{q}''_{min}}{b\dot{q}''_e} \right) \quad for \quad t \le t_m \qquad (20)$$

The h_{ig} can be easily obtained by rearranging equation (19) with the known T_{ig}. An effective kρc value can be calculated from the following expression:

$$k\rho c = \frac{4}{\pi}\left(\frac{h_{ig}}{b} \right)^2 \qquad (21)$$

This correlation is not theoretically justified, but Quintiere and Harkleroad believe that it considers the effects of variable properties, which are significant for the range of temperatures encountered, and accounts for the heat loss effects from the back of the sample and the baseboard. Application of this technique has been done on LIFT

apparatus results only. However, there is no reason the technique cannot be used on other apparatus.

In LIFT apparatus, Quintiere and Harkleroad place the specimens vertically as opposed to the typical horizontal setup in the cone calorimeter or ISO ignitability apparatus. The vertical specimens take longer to be ignited and have a higher $\dot{q}''_{cr}$. This is due to the difference in the convective boundary layer [8] or changes in the convective heat transfer coefficient [2].

Limitations:

This method is derived for thermally thick solids only. The ignition time must be less than t_m. It is important to check that the thickness of the material is at least as thick as the experimental sample when applying this correlation.

3.5) Janssens [3],[4]

Janssens developed a simplified thermal model for piloted ignition of wood. The model is applicable even if the thermal properties k and c are temperature dependent, and the surface heat losses are nonlinear, and $\varepsilon \leq 1$ due to reradiation. Janssens used a numerical (finite difference) technique to develop a functional relationship. Using experimental data from a series of ignition tests on wood products, the functional form of Janssens' correlation is found to be:

$$\dot{q}_e'' = \dot{q}_{cr}'' \left[1 + 0.73 \left(\frac{kc\rho}{h_{ig}^2 t_{ig}} \right)^{0.547} \right] \tag{22}$$

The above equation (22) can also be expressed in a non-dimensional form [4]. Janssens' correlation plots the data as $(t_{ig})^{-0.547}$ versus $\dot{q}_e''$. The critical heat flux in the equation above can be obtained from equation (12), which is the same as Mikkola and Wichman's correlation. The kρc can be calculated using the following relationship derived from equation (22) above.

$$k\rho c = h_{ig}^2 (0.73 \times slope \times \dot{q}_{cr}'')^{-1.83} \tag{23}$$

The h_{ig} is calculated using the following relationship:

$$h_{ig} = \frac{\varepsilon \, \dot{q}_{cr}''}{(T_{ig} - T_\infty)} \tag{24}$$

T_{ig} in the above equation (24) can be measured experimentally or from equation (4) above with known $\dot{q}''_{cr}$. Wesson [12] measured absorptivity for a large number of wood species at ambient temperature, T_∞. He found the value for $\varepsilon = 0.76$. However, as wood is heated, its surface darkens and emissivity, ε, is close to 1 just prior to ignition. Hence Janssens suggested that $\varepsilon = 0.88$, an average value, be used as typical for wood. Equation (22) can be rearranged to get a solution for ignition time, t_{ig}:

$$t_{ig} = 0.563\left[\frac{k\rho c}{h_{ig}^2}\right]\left[\frac{\dot{q}''_e}{\dot{q}''_{cr}} - 1\right]^{-1.83} \qquad (25)$$

Limitations:

The greatest limitation of this method is it applies only to thermally thick wood samples. Therefore one has to carefully check that the specimen is thermally thick. The 0.547 power and 0.73 in equation (22) were determined using a numerical model of ignition experimental data of cellulosic material and has not been verified for other materials.

3.6) Toal, Silcock and Shields [1],[2],[3]

This correlation was originally developed by Smith and Green [3], who defined the flux-time product, FTP as follows:

$$FTP = \sum_{0}^{t_{ig}} (\dot{q}_e'' - \dot{q}_{cr}'')_{\Delta t}^{n} \Delta t \qquad (26)$$

The FTP can be assumed to be the excess absorbed energy up to the point of ignition of a combustible specimen. If the exterior flux, $\dot{q}_e''$ is constant, the above equation can be simplified to:

$$FTP = (\dot{q}_e'' - \dot{q}_{cr}'')^n t_{ig} \qquad (27)$$

The original FTP concept is to predict the time to ignition within a thermally closed system; that is, the OSU apparatus. Toal, Silcock and Shields recommended that the Flux Time Product, FTP be extended to accommodate the ignition time data obtained from the cone calorimeter and the ISO ignitibilty cone apparatus. In equation (27) above, n is flux time product index. Notice that if n = 1, equation (27) is equivalent to the thermally thin equation (8), where $FTP_1 = \rho L_0 c(T_{ig} - T_\infty)$ and similarly if n = 2, equation (27) is equivalent to the thermally thick equation (9), where $FTP_2 = (\pi/4)k\rho c(T_{ig} - T_\infty)^2$. Again when n = 1.83, equation (27) compares well with Janssens' equation (25).

The correlation determines the FTP by plotting $\dot{q}_e''$ versus $(t_{ig})^{-1/n}$ using the rearranged form of equation (27):

$$\dot{q}_e'' = \dot{q}_{cr}'' + \frac{FTP^{1/n}}{t_{ig}^{1/n}} \qquad (28)$$

The value n is found by trial and error to get a best-fit line through the ignition data points, typically $1 \leq n \leq 2$. The intercept of the plot $\dot{q}_e''$ versus $(t)^{-1/n}$ is the critical heat flux, $\dot{q}_{cr}''$. The slope of the line is $FTP^{1/n}$.

Limitations:

It is important to bear in mind that the power n in equations (27) and (28) is dependent on the thickness of the tested specimen. Therefore, before the application of this correlation, it is essential to make sure that the specimen thickness to be modelled is consistent with the data being applied in the correlation.

3.7) Delichatsios, Panagiotou and Kiley [13]

Delichatsios, Panagiotou and Kiley have developed approximate solutions for interpreting time to ignition data, based on asymptotic analysis. The approximate solutions were compared with detailed surface temperature histories and the exact solutions, as well as with the experimental data. In their experiments, they adopt a procedure for covering the exposed surface of a specimen with a thin layer (50 μm) of carbon black. This is to ensure that all the incident heat is absorbed by the tested specimens by suppressing the effects of the spectral characteristics of the source and/or the material. Another purpose of doing this is to make sure that all the heat is absorbed at the surface by conduction, not by in-depth radiation absorption. Therefore this method accurately accounts for the heat losses, especially surface reradiation, that may affect the

thermal response of a material when exposed to an external heat flux, $\dot{q}_e''$. Compared to the above correlations, the researchers have assumed that:

(a) the heat losses can be represented by a linearized convection term [4], [5],
(b) they used a general integral model to treat the reradiation losses (i.e. non-linear heat losses) [11] or
(c) they used a numerical (finite difference) solutions to account for the reradiation losses [4].

Delichatsios, Panagiotou and Kiley suggest that when the incident heat flux is high, about three times greater than the critical heat flux, i.e. $\dot{q}_e'' > 3.0\dot{q}_{cr}''$, the relationship between ignition time, t_{ig} and incident irradiance, $\dot{q}_e''$, is:

$$\frac{1}{\sqrt{t_{ig}}} = \frac{2}{\sqrt{\pi k\rho c}(T_{ig} - T_\infty)}[\dot{q}_e'' - 0.64\dot{q}_{cr}''] \tag{28}$$

where, $$\dot{q}_{cr}'' = \sigma(T_{ig}^4 - T_\infty^4) \tag{29}$$

For low incident heat flux where the imposed heat flux is close to the critical heat flux, i.e. $\dot{q}_e'' < 1.1\dot{q}_{cr}''$, then:

$$\frac{1}{\sqrt{t_{ig}}} = \frac{\pi}{\sqrt{\pi k\rho c}} \frac{\dot{q}_e'' - \dot{q}_{cr}''}{T_{ig} - T_\infty} \tag{30}$$

It is notable that the critical heat flux in equation (29) does not consider convective heat irradiance. The reason is that convective heat fluxes are negligible compared to the radiative heat fluxes. The above expressions (28) and (30) can also be expressed in a dimensionless form [13]. The details on how the above equations (28) and (30) are obtained and compared with the exact solutions are published elsewhere [13]. This technique plots the ignition data as $t^{-1/2}$ versus $\dot{q}_e''$. This should not be confused with the plot given by Mikkola and Wichmans' correlation [11], which plots the same ordinate and abscissa.

The critical irradiance, $\dot{q}_{cr}''$ can be determined either by equation (29) or by $(\dot{q}_e'')_{\text{int}} = 0.64\,\dot{q}_{cr}''$ from equation (28). The $(\dot{q}_e'')_{\text{int}}$ is the intercept with the abscissa. One can get the thermal inertia, kρc, from the slope of the best-fit regression line as below:

$$\frac{2}{\sqrt{\pi\, k\rho c}(T_{ig} - T_{\infty})} = slope \qquad (31)$$

Limitation:

This method of correlating the ignition data is applicable only to thermally thick materials and it is used on experiments with carbon-covered material only. As a result, the method involves some experimental uncertainties such as surface absorptivity, in-depth radiation losses, and so on. Experiments with both carbon-covered and carbon-free materials should be carried out to evaluate these effects.

3.8) M.J. Spearpoint and Quintiere [15]

Spearpoint and Quintiere [15] examined an integral model initially developed by Quintiere [16]. The integral model is a one-dimensional model for charring materials. With the fundamental assumptions and boundary conditions as discussed in section 3.1, Spearpoint and Quintiere [15] derived a dimensionless parameter β, which is a ratio of the magnitude of radiation and convective losses to the incident flux, $\dot{q}_e^{"}$.

$$\beta = \frac{\sigma (T_{ig}^4 - T_\infty^4) + h_c (T_{ig} - T_\infty)}{\dot{q}_e^{"}} \tag{32}$$

From equation (4) where ε = 1.0 at ignition, β_{ig} can be expressed as the critical heat flux divided by the incident heat flux:

$$\beta_{ig} = \frac{\dot{q}_{cr}^{"}}{\dot{q}_e^{"}} \tag{33}$$

They obtained a relationship between the ignition time, t_{ig} and the external heat flux, $\dot{q}_e^{"}$ which is shown in equation (34).

$$t_{ig} = C_{ig} k \rho c \frac{(T_{ig} - T_\infty)^2}{(\dot{q}_e^{"})^2} \tag{34}$$

where, $C_{ig} = \frac{4}{3}\left[\frac{1}{(2-\beta_{ig})(1-\beta_{ig})}\right]$ (35)

When the incident heat flux is large, $\dot{q}_e'' \gg \dot{q}_{cr}''$, β_{ig} approaches zero. Hence equation (34) becomes:

$$t_{ig} \approx \frac{2}{3} k\rho c \frac{(T_{ig} - T_\infty)^2}{(\dot{q}_e'')^2} \tag{36}$$

Equation (36) is comparable with the relationship developed by Mikkola and Wichman [11] as expressed in equation (9). As in Mikkola and Wichmans [11], and in Delichatsios, Panagiotou and Kiley [13], this correlation plots the $(t_{ig})^{-1/2}$ against $\dot{q}_e''$. The critical heat flux can be obtained by using the intercept along the x-axis of a linear extrapolation of the high heat flux plot $(t_{ig})^{-1/2}$ versus $\dot{q}_e''$ from equation (36). This is exactly the same method used by Mikkola and Wichman's correlation to determine the $\dot{q}_{cr}''$, except this intercept value needs to be modified by a constant factor of 0.76 to obtain an estimate of the critical heat flux that is consistent with the integral model. Such value a (0.76) is different from that used by Delichatsios, Panagiotou and Kiley [15], which is 0.64. Therefore both the Delichatsios et al.[13], and Spearpoint et al.[15] correlation have a critical heat flux higher than Mikkola and Wichman's [11]correlation.

$$\dot{q}_{cr}'' = \frac{(\dot{q}_e'')_{\text{int}}}{0.76} \tag{37}$$

$$k\rho c = \frac{3}{2}\left[\frac{1}{slope\,(T_{ig} - T_\infty)}\right]^2 \tag{38}$$

Thermal inertia is calculated from the slope of the linear best-fit regression line of the plot, as shown in equation (38). The ignition temperature, T_{ig}, can be measured experimentally or calculated from equation (4): $\dot{q}_{cr}'' = \sigma(T_{ig}^4 - T_\infty^4) + h_c(T_{ig} - T_\infty)$, with an appropriate value for convective heat transfer coefficient, h_c. Spearpoint and Quintiere [15] used a value of 18 W/m^2K for h_c. The details of the development and derivations of these equations (32) to (36) are published elsewhere [15].

Limitation:

This technique of correlating the ignition data is limited to the use of thermally thick materials only. It gives a very good match with the experimental data at high incident fluxes (> 20 kW/m^2), but not at low heat fluxes.

The following table shows the summary of how all the above correlations plot their ignition data. All the correlations have one thing in common, that is, they all require a best-fit linear regression line to be drawn through the ignition data obtained experimentally.

Correlation	x - axis	y - axis	Application
1) Mikkola & Wichman[11]	$\dot{q}_e''$	$t_{ig}^{-1/2}$	Thermally thick & thin
2) Tewarson [10]	$\dot{q}_e'' - \dot{q}_{\min}''$	$t_{ig}^{-1/2}$	Thermally thick
3) Quintiere & Harkleroad [5]	$t_{ig}^{1/2}$	$\dot{q}_{\min}'' / \dot{q}_e''$	Thermally thick
4) Janssens [3],[4]	$\dot{q}_e''$	$t_{ig}^{-0.547}$	Thermally thick
5) Toal, Silcock & Shields [1],[2],[3]	$t_{ig}^{-1/n}$	$\dot{q}_e''$	Thermally thick & thin
6) Delichatsios, Panagiotou & Kiley [13]	$\dot{q}_e''$	$t_{ig}^{-1/2}$	Thermally thick
7) Spearpoint & Quintiere [15]	$\dot{q}_e''$	$t_{ig}^{-1/2}$	Thermally thick

Table 3.1: Summary of the correlations' plots

CHAPTER 4: DATA ANALYSIS

4.1) Calibration of the Cone Element

The heat flux released by the cone heater was calibrated to obtain a relationship between the temperature of the cone element and the level of irradiance released at the surface of the heat flux gauge. The level of heat flux is measured in terms of voltage (mV) by radiometer. By using the conversion factor supplied by the manufacturer of the cone heater, the proposed level of incident heat flux (kW/m^2) can be determined. According to the calibration scale of the manufacturer, 1 kW/m^2 = 0.187 mV. The following calibration curve of the cone heater allows one to know directly the temperature that the cone heater is set at to obtain the required level of incident heat flux during the test.

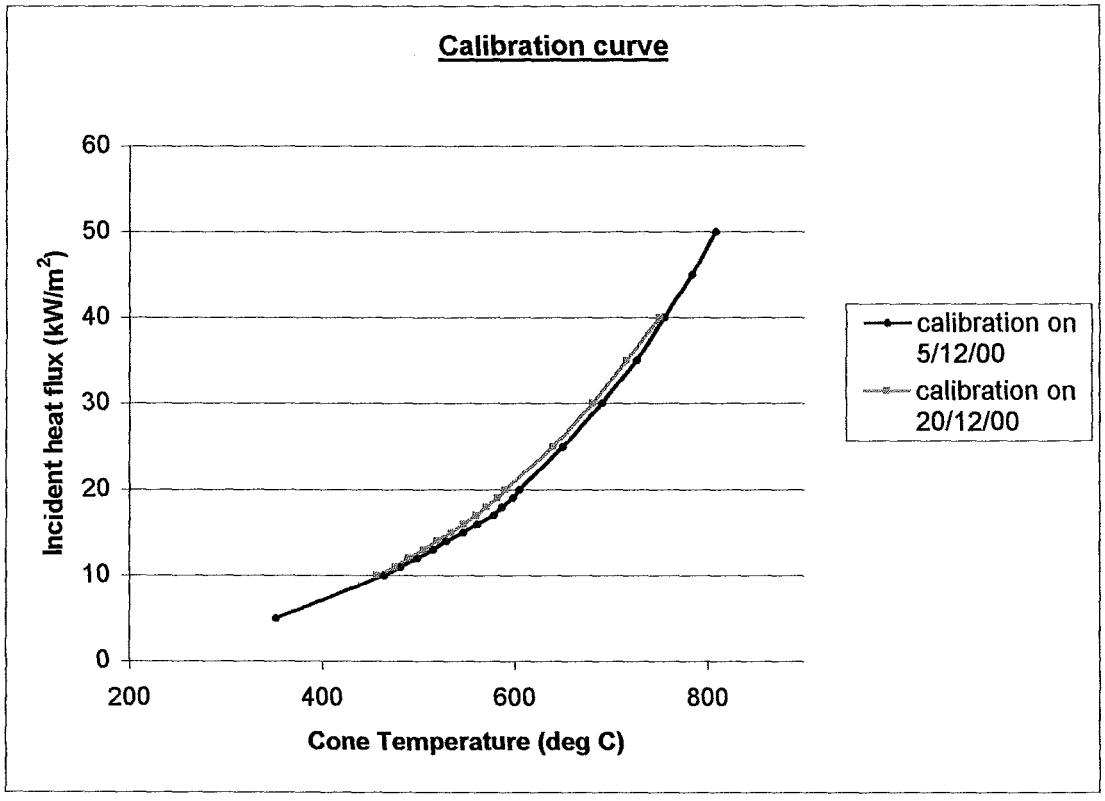

Figure 4.1: Calibration Curve of the Cone heater

Two calibrations were done: one on 5 December 2000 and one on 20 December 2000. The values of the temperature were out of the repeatable limit of ±5 °C after a period of 15 days. According to figure 4.1 above, one can notice that the variation of the temperature is greatest within the region of 15 kW/m^2 to 35 kW/m^2. Comparison of the calibrations done on 5 December and 20 December showed an average drop of about 2 %. There are a number of possible reasons for this.

The first possibility may relate to the position of the highest temperature point. The highest temperature point should be at the centre of the exposed area (circle) of the specimen. During the calibration process on 20 December, the highest temperature point was found to have fallen to the region in front of the centre point. Therefore the calibration scale obtained on 20 December was based on this greatest point, not on the midpoint of the radiator cone.

In fact the determination of the midpoint of the cone heater is very difficult. Using only the eyes to make adjustments, one can get different positions every time when locating the radiometer at the centre of the heater.

If there is nothing wrong with the cone heater and the temperature (irradiance) distribution, the radiometer may give the wrong readings. The backing board used to place the radiometer will affect the readings taken by the radiometer. The insulation properties of the backing board are questionable.

Fortunately the variation between the two calibration scales is small, only 2 %. Therefore such small variation is unlikely to affect the results greatly for this research.

4.2) Calibration of Density and Moisture Content

Only the dried density, ρ_d of the wood was recorded in this research. This is the density of the wood dried during the conditioning period. The dried density, ρ_d was calculated using the measured weight of the specimen after being dried in the conditioning room, W_d and the volume of the specimen, V:

$$\rho_d = \frac{W_d}{V} \tag{39}$$

The dried density for each sample was calculated to obtain an average dried density, ρ_{avg} for each wood species.

The evaluation of the moisture content was based on the weight of the specimens. Three different moisture contents were evaluated. They are:

$X_{initial}$ = initial moisture content in the species before conditioning
X_{loss} = loss of moisture content in the species during conditioning
X_{final} = final moisture content after being dried in the conditioning room

The following equations were used to determine the above moisture content for each sample. As before, the average moisture content for each wood species was considered for comparison.

$$X_{initial} = \frac{W - W_{od}}{W_{od}} \tag{40}$$

$$X_{loss} = \frac{W - W_d}{W_d} \tag{41}$$

$$X_{final} = X_{inital} - X_{loss} \qquad (42)$$

where W = initial weight of the specimen before conditioning

W_d = weight of the specimen after being dried in conditioning room

W_{od} = weight of the specimen after being oven-dried

4.3) Determination of Thermal Properties

The thermal properties of a material are often referred to as the thermal conductivity, k; density, ρ; and the specific heat, c. These values are very difficult to be measured during the test. Therefore in ignition experiments, the product kρc, called thermal inertia, is typically reported as a single quantity instead of the single values for k, ρ and c.

Among the seven correlations, five of them can be used to calculate the thermal inertia, kρc directly. The five correlations are:

1) Mikkola and Wichman – see equation (11)
2) Quintiere and Harkleroad – see equation (21)
3) Janssens – see equation (23)
4) Delichatsios, Panagiotou and Kiley – see equation (31)
5) Spearpoint and Quintiere – see equation (38)

Tewarson also measured the thermal inertia, kρc, indirectly by calculating the TRP, a parameter that combines the ignition temperature above ambient, ΔT_{ig} and the thermal inertia, kρc, (see equation (13)).

4.4) Determine the Ignition Temperature

The ignition temperature, T_{ig}, is determined by using equation (4), assuming the emissivity, $\varepsilon = 1$ and the obtained critical heat flux, $\dot{q}''_{cr}$. Most of the variables are easily known except the convective heat transfer coefficient, h_c. It is important to choose an appropriate value for the h_c. The h_c can vary depending on the geometry of the surface, the nature of the flow and the thickness of the boundary layer. Convective heat transfer calculations usually involve the heat transfer between the surface of a solid and a surrounding fluid, which either heats or cools the solid material. Therefore it actually changes with time as the temperature of the surrounding fluid varies with time. Since a single h_c could not be derived, most researchers used an average value of h_c in their calculations.

From the literature, the reported h_c used by the researchers are between 11 W/m^2K to 18 W/m^2K. For example, Mike Spearpoint [15] used h_c = 18 W/m^2K in his research in estimating the ignition temperature, T_{ig}. Quintiere and Harkleroad [5] used h_c = 15 W/m^2K, which is characteristic of the natural convection for the LIFT apparatus. Silcock and Shields [3] recommended a value of 11 W/m^2K for the h_c. Janssens [18] used a value of 13.5 kW/m^2K for h_c, representative of the Cone Calorimeter in the vertical orientation.

However, in this research, the h_c was evaluated by the methodology found in reference [17] written by Atreya. For a horizontal surface, the following general-purpose correlation is considered valid (see table 1-3.4 in reference [17]):

$$Nu_L = 0.54 Ra_L^{1/4}, \quad 10^5 \le \mathrm{Ra_L} \le 10^7 \tag{43}$$

$$Ra_L = Gr_L \,\mathrm{Pr} = \frac{g\beta(T_{ig} - T_\infty)L^3}{\nu\alpha} \tag{44}$$

where Ra_L = Rayleigh number

Gr_L = Grashof number

Nu_L = Nusselt number

Pr = Prandtl number

L = characteristic length

β = $1/T_{ig}$

Viscosity (ν) and α are the thermophysical constants of air at atmospheric pressure at hot gas temperature, T_f, which can be found in Table 1-3.5 in reference [17] as well. The T_f is defined as:

$$T_f = \frac{T_{ig} + T_\infty}{2} \tag{45}$$

L is the characteristic length equal to the surface area, A_s divided by the perimeter of the exposed area of the sample, P, to the incident heat flux. In this case, the exposed area, A_s is the area of a circle with a diameter of 140 mm. The next issue arising is the value of the T_{ig}. The T_{ig} is assumed to be 370 °C, although each species may have different T_{ig}. Figure 4.2 shows the values of h_c over the different ignition temperature values. According to the figure, the sensitivity of the h_c values is rather low in relation to the change in T_{ig}, especially when the T_{ig} is over 300 °C. Therefore at T_{ig} = 370 °C, the h_c = 12.2 W/m^2K. This value is reasonable, since it is within the range of values in the reported literature. Notice that Shields, Silcock and Murray [2] also used the same methodology from reference [17] to obtain the values for h_c as a comparison between the vertical and horizontal orientations of the samples.

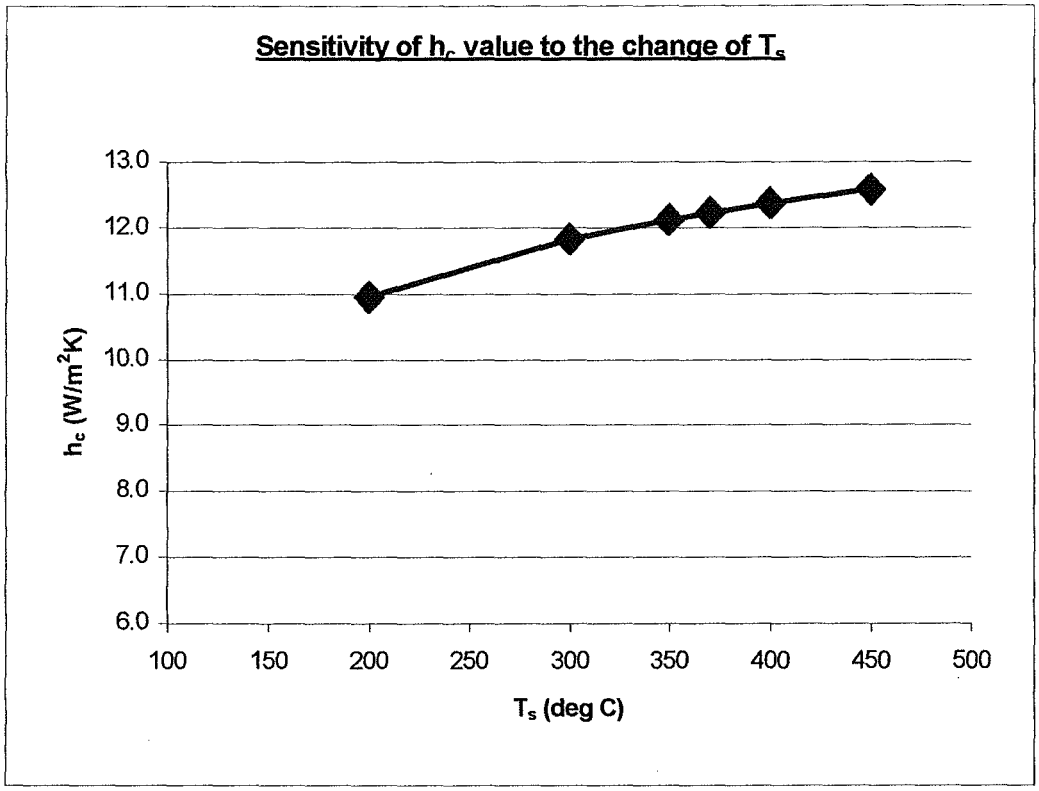

Figure 4.2: Sensitivity of h_c to the change in T_{ig}

4.5) Conditioning of the Samples and Baseboards

The specimens were conditioned as required by the Standards for two weeks to reach constant mass. In this research, the samples are said to reach constant mass when the mass loss rates of the samples are less than 1 g/day. Therefore the mass of the samples was measured to observe the mass loss rate during the conditioning period. From the mass loss rate observation, the thick samples reached constant mass after 21 days. To ensure the samples had really reached equilibrium condition, an extra 7-day period was allowed before the tests were carried out. The thin samples took a shorter period to reach the condition of constant mass: about 10 days. Again, for safety, the samples were conditioned for further 7-day period.

4.6) Determine the Repeatability and Reproducibility

Repeatability, r and reproducibility, R were determined by the method described in BS 5497 Part 1: 1987 [20], which is identical to ISO 5725-1986. Repeatability is defined as the closeness of agreement between mutually independent test results obtained using the same method on identical test material in the same lab by the same operator using the same equipment within short intervals of time. Reproducibility is the closeness of agreement between test results using the same method on identical material in different laboratories with different operators using different equipment.

The absolute difference, Δ, between the extreme values and the mean values was calculated for each wood species at each level of irradiance. This is shown in Tables J1 to J11 in Appendix J. This Δ parameter is expressed as a percentage (%) and is also a measure of the repeatability, r. The followings are the equations to calculate the absolute difference, Δ:

$$\Delta_{up} = \frac{t_{ig\,\max} - m}{m} \times 100\% \qquad (46)$$

$$\Delta_{low} = \frac{m - t_{ig\,\min}}{m} \times 100\% \qquad (47)$$

where, Δ_{up} = absolute difference between maximum t_{ig} and mean t_{ig}

Δ_{low} = absolute difference between minimum t_{ig} and mean t_{ig}

$t_{ig\,min}$ = minimum t_{ig} of the five tested specimens at certain irradiance level

$t_{ig\,max}$ = maximum t_{ig} of the five tested specimens at certain irradiance level

m = mean t_{ig} of the five specimens at certain irradiance level

Originally this research will only able to study the repeatability, r, of the samples, but as explained above, the problem of air draught over the surface of the tested 40-mm samples was found to be relatively large in the later stage of this research. Therefore there are two sets of experimental data here (see Table I1 in Appendix I); one obtained in the presence of air draught and one obtained without the air draught problem due to the cage. The former was done on the 40-mm sample with levels of irradiance between 20 kW/m^2 to $40kW/m^2$ and based on the calibration scale on 5 December 2000. However, the latter was done on the 40-mm samples below 20 kW/m^2 and on all the 20-mm woods based on the calibration curve on 20 December 2000. Therefore, the differences between the two sets of results are the calibration scales and the environmental conditions on the surface of the specimen.

In order to calculate the reproducibility, R, of the woods, the 40-mm mdf were retested based on the calibration scale done on 20 December 2000 and with the cage on to ensure a quiescent condition. This set of mdf data is called lab 1 and the previously obtained 40-mm mdf test results based on calibration scale done on 5 December 2000 is called lab 2 in calculating the R.

The following are the series of equations used to get the r and R for the mdf (between lab 1 and lab 2). The two experiments are considered as uniform level experiments.

$$s_i = \sqrt{\frac{1}{n_i - 1}\left[\sum_{k=1}^{n_i} y_i^2 - \frac{1}{n_i}\left(\sum_{k=1}^{n_i} y_i\right)^2\right]} \tag{48}$$

$$s_r^2 = \frac{\sum s_i^2}{p} \tag{49}$$

$$s_L^2 = \frac{\frac{1}{p-1}\left[\sum_{i=1}^{p} n_i \left(\bar{y}_i - \bar{\bar{y}}\right)^2\right] - s_r^2}{\bar{\bar{n}}} \tag{50}$$

$$s_R^2 = s_r^2 + s_L^2 \tag{51}$$

where n_i = number of replicates at each level of irradiance

p = number of laboratories

y_i = any one of the results (ignition time, t_{ig})

$\bar{y}_i$ = average ignition times of the n replicates

s_i = intra-cell standard deviation

s_r^2 = repeatability variance

s_L^2 = between-lab variance

s_R^2 = reproducibility variance

$$\bar{\bar{y}} = \frac{\sum_{i=1}^{p} n_i \bar{y}_i}{\sum_{i=1}^{p} n_i} \tag{52}$$

$$\bar{\bar{n}} = \frac{1}{p-1}\left[\sum_{i=1}^{p} n_i - \frac{\sum_{i=1}^{p} n_i^2}{\sum_{i=1}^{p} n_i}\right] \tag{53}$$

Repeatability, r, and reproducibility, R, are defined according to BS 5497 as:

$$r = 2.8\sqrt{s_r^2} \tag{54}$$

$$R = 2.8\sqrt{s_R^2} \tag{55}$$

The details of the r and R calculations are shown in Tables J12 to J20 in Appendix J. Note that one should refer to the BS 5497 Part 1: 1987 for further or greater understandings of the method of calculating the r and R values. By calculating the repeatability and reproducibility using the above method and equations, the closeness of agreement between test results can be known, and hence the accuracy of the test results.

CHAPTER 5: RESULTS AND DISCUSSION

5.1) Density and Moisture Content

The measured average density and moisture content for each species of wood are shown in Table 5.1 and Table 5.2 below.

	density	$X_{initial}$ (%)	X_{final} (%)
mdf	727	8.4	8.5
Beech	661	14.5	12.4
Rimu	593	15.1	12.3
Macrocarpa	550	18.2	12.1
Radiata Pine	524	14.4	12.3
Plywood	507	10.6	10.5

Table 5.1: Density and Moisture Content of the 40-mm samples

	density	$X_{initial}$ (%)	X_{final} (%)
mdf	727	8.4	8.5
Beech	586	13.5	12.6
Rimu	568	14.8	13.4
Macrocarpa	517	13.5	11.6
Plywood	507	10.6	10.5
Radiata Pine	454	11.9	11.4

Table 5.2: Density and Moisture Content of the 20-mm samples

From the above tables, both the 40-mm and 20-mm samples have the mdf as the highest density wood product, with ρ = 727 kg/m^3. The only difference in terms of density is that Plywood and Radiata Pine are the lowest density wood among the 40-mm and 20-mm samples respectively. The Plywood and the mdf have the same density values for both the 20-mm and the 40-mm specimens. This is because the 40-mm mdf and Plywood samples used in this research consisted of two 20-mm samples of mdf and Plywood. Therefore the mdf and Plywood used in each cases were actually originated from the same manufacturer.

Comparison between the thin and thick samples for species Beech, Rimu, Macrocarpa and Radiata Pine, showed that the thick samples had a density greater than the thin ones.

The 40-mm Macrocarpa samples have the highest initial moisture content, $X_{initial}$ of 18.2 %. Its final moisture content is not the highest, which indicates it suffered the greatest moisture loss during the conditioning period. The final moisture content, X_{final} of Beech, Radiata Pine, Rimu and Macrocarpa are very close (about 12 %). For mdf and Plywood, there is a slight difference between their initial and final moisture content. In fact, mdf had gained a small amount of moisture content (0.1 %) during the conditioning, and Plywood only lost 0.1 % moisture content. This effect reveals a uniform moisture content in the manufactured wood products and a low influence of the surrounding atmosphere conditions on these wood products.

The 20-mm Rimu samples had the greatest moisture content in both initial and final moisture content, 14.8 % and 13.4 % respectively. Macrocarpa, Beech and Radiata Pine have very close final moisture content. Similar to the 40-mm samples, the moisture lost in 20-mm Macrocarpa is the greatest. The final moisture content in mdf and Plywood is 8.5 % and 10.5 % respectively. The mdf has the lowest moisture content although its density is the highest among the wood species.

From both tables above, the moisture content of the wood species is within 8 % to 13 %. In general, the thin samples lost less moisture than the thick ones. This is why the thin samples took a shorter conditioning period to reach constant mass than the thick samples. One may find that the reported wood density in the literature varies quite significantly from the above results. This is because the density of wood varies significantly between species. It also varies between trees of the same species and even within individual trees.

5.2) Observation during Test

There were several important observations during the tests. The first, most obvious observation is the charring of the tested samples. The formation of a char layer will affect the ignition of a material. The pyrolysis of charring wood is a complex interplay of chemistry, heat and mass transfer. When wood chars, the surface shrinks and hence loses its composition, leaving a variable amount of residue when it burns. According to Mikkola and Wichman [11], once a char layer of the order of 1-mm thickness forms, ignition no longer occurs. However, this study does not show this: that is, the once the char layer exceeded 1-mm thickness, the ignition still occurred.

Often when the incident heat fluxes were high (30-40 kW/m^2) or low (< 13 kW/m^2), the specimens became lightly charred. This is because at high heat fluxes, the specimens were ignited very quickly before the samples had a chance to char further. At low heat fluxes, the produced incident heat on the surface of the samples was too low to char the specimens and there were no ignitions. The specimens were charred severely when the incident heat fluxes approached the minimum heat flux, $\dot{q}''_{min}$, which is around 15 kW/m^2.

Cracks were observed on some of the samples. These samples had either the tiny invisible internal or external defects (or cracks) that were further developed when exposed to the heat. The cracks can be grouped into two types: long, lateral and wide; and another short, tiny and numerous. The long, lateral and wide cracks were observed mostly on Rimu, whereas Plywood had short, thin and numerous cracks.

Flashing always occurred near the ignition time, t_{ig}. Flashing is the flame that goes off within 10 seconds. Therefore it cannot be considered as an ignition, because the Standards defined the ignition as a continuous flame that stayed for more than 10 seconds. This phenomenon increased the difficulty of recording the ignition time, t_{ig}. Therefore it is important for the researcher to decide whether an ignition has occurred or

not. Basically this is not difficult once the researcher has become experienced, as the flashing goes off very quickly.

Some of the samples also had moisture (sap) loss through the specimens' surfaces. Moisture (sap) was found to evaporate at the surface of the specimen during the tests. Such an observation was common when the samples had natural defects and cracks. This released moisture accelerates the ignition of the specimen. Therefore the specimens selected must be in reasonably flat and with evenly distributed surface irregularities, as specified by the Standards.

The thick and thin samples behaved quite differently when they were burned. The thin samples were easier and quicker to be heated up than the thick samples. Heat takes more time to travel through thick specimens. Therefore the baseboards in the 20-mm wood tests felt warm at high heat fluxes, when the ignition time, t_{ig} was short. The most significant difference between the two different thicknesses of samples tested is the bending of the thin samples when heated. With the formation of the char layer on the top of the specimens, the upper surface of the specimen will shrink. This induces a tensile force in the bottom portion of the specimen and causes the specimen to become concave.

5.3) Goodness of Best-Fit Line

Graphical presentations of the ignition data plotted by the seven correlations are shown in Appendix C to Appendix H. Generally, the plotted experimental results have a very good linear best-fit line, with R^2 greater than 0.96. The Tewarson's method has an R^2 value of 0.74 to 0.89 except for mdf. The ignition data of the mdf is very poorly correlated by using this method, in which the R^2 value is about 0.50 for 20-mm and 40-mm samples. Such a poor correlation is due to the requirement that the plotted linear regression line should pass through the origin. For example, the following Figure 5.1 shows the ignition data of mdf plotted by Tewarson's method. One can see clearly that the R^2 values for 20-mm and 40-mm samples are 0.53 and 0.49 respectively. The first 3 data points, at ($\dot{q}''_e - \dot{q}''_{min}$) equals to 0, 5 and 10, are very poor correlated as the best-fit line was drawn to pass through the origin.

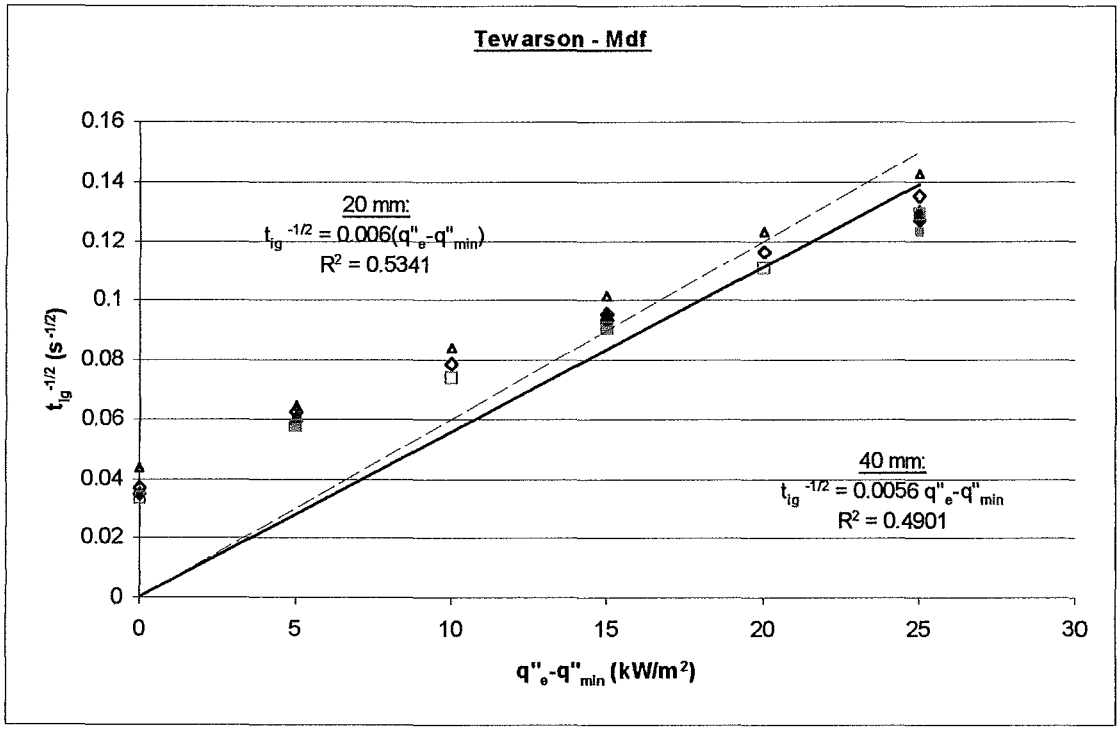

Figure 5.1: Ignition data of mdf plotted by Tewarson (same as Figure E2 in Appendix E)

The Quintiere and Harkleroad method has the worst correlation with the ignition data. The reason is that in this correlation, ignition data must be plotted to pass through the origin. The variation of the ignition time between the high values of $\dot{q}''_{min}/\dot{q}''_e$ (> 0.8) and low values of $\dot{q}''_{min}/\dot{q}''_e$ is so large that one is forced to ignore the values at high $\dot{q}''_{min}/\dot{q}''_e$. (See Figures C3, D3, E3, F3, G3 and H3). For this reason, the values of $\dot{q}''_{min}/\dot{q}''_e > 0.8$ were ignored for Beech, mdf and Plywood. For Macrocarpa, Radiata Pine and Rimu, the ignition times ($t_{ig}^{1/2}$) at $\dot{q}''_{min}/\dot{q}''_e > 0.6$ were ignored to obtain a reasonably well-fit line. Figure 5.2 below, is a good example of a poorly correlated ignition data of Rimu by Quintiere and Harkleroad. All the values of $\dot{q}''_{min}/\dot{q}''_e > 0.6$ were ignored. One can see that the data points ($\dot{q}''_{min}/\dot{q}''_e > 0.6$) are so far from the 2 linear best-fit lines.

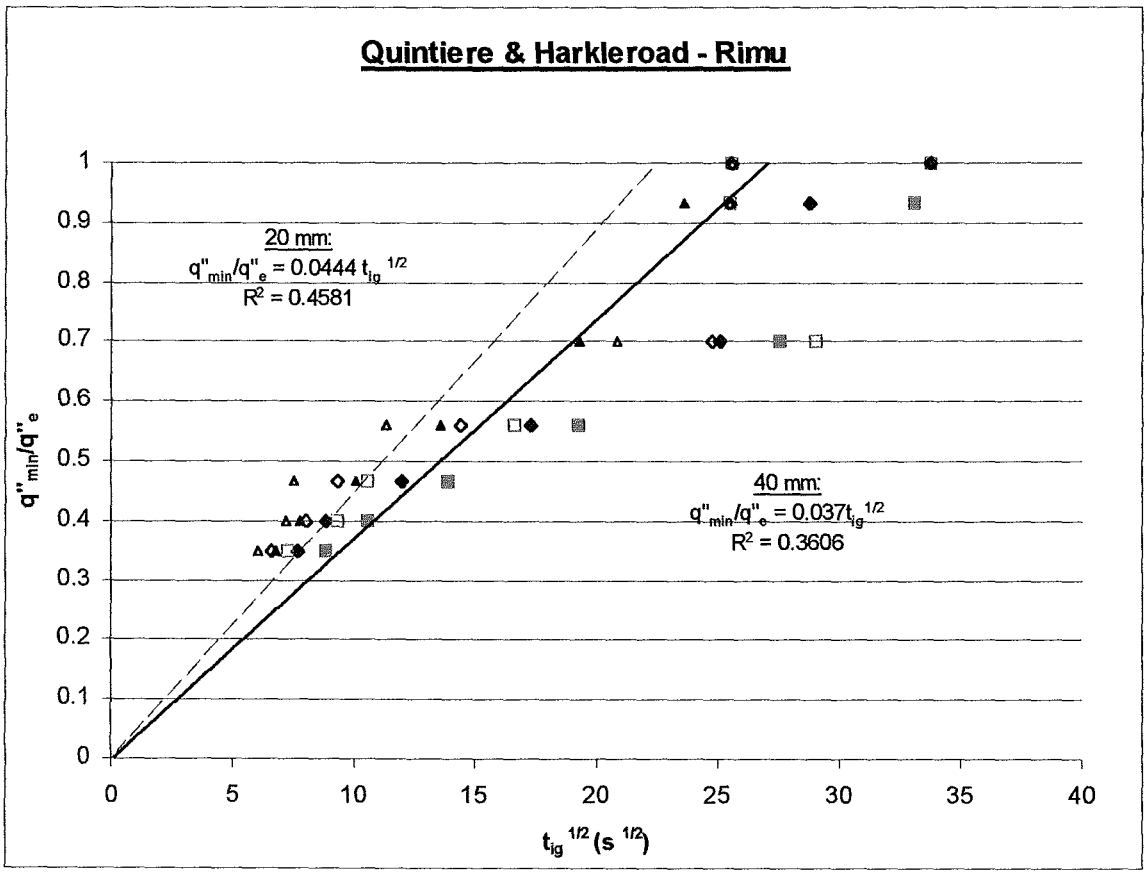

Figure 5.2: Ignition data of Rimu plotted by Quintiere and Harkleroad (same as Figure G3)

From the graphs plotted in Appendix C to H, the error bar (the difference between the extreme values) is very large at high levels of irradiances. Figure 5.3 shows a good example of this phenomena, the rest are shown in Appendix C to H. From Figure 5.3, the error bar at high heat flux (40 kW/m^2) is large, and getting smaller and smaller as heat flux becomes lower. This indicates the inaccuracy of the ignition times, t_{ig} recorded. Although the variance of t_{ig} at high heat fluxes is small, such a small difference will produce a big percentage difference in terms of accuracy, especially when the t_{ig} is very small. However, at low levels of irradiances, this effect will not affect the results significantly. At low heat fluxes, ignition times are very sensitive to minor changes in environmental conditions such as airflow over the sample, and the development of a char layer at the surface. If the char layer formed is too deep, ignition hardly occurred.

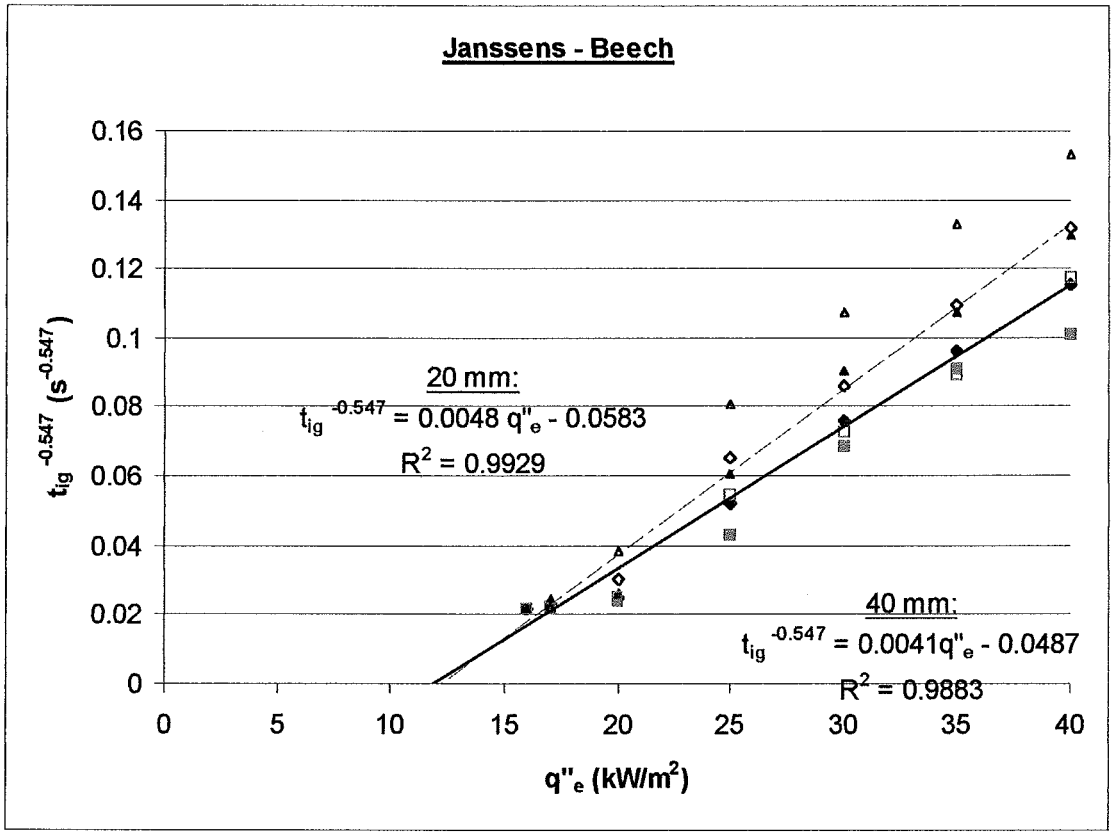

Figure 5.3: Ignition data of Beech plotted by Janssens (same as Figure D4)

It is surprising to see that both the 20-mm and 40-mm samples have a very similar intercept value of incident heat flux, $(\dot{q}_e^{"})_{int}$. This is clearly shown in Figure 5.3 above, that the 20-mm and 40-mm best-fit lines have very close x-intercept values ($(\dot{q}_e^{"})_{int}$). This is also clearly shown in the graphs plotted by correlations: Mikkola and Wichman; Janssens; Toal et al.; Delichatsios et al.; and Spearpoint et al.

According to all the plots, the linear regression best-fit lines drawn through the 20-mm sample ignition data have a higher gradient than the 40-mm ones. Almost all the 40-mm ignition data is better correlated than the 20-mm samples, especially for the correlations which are applicable to the thermally thick solids only, as these simple thermal models are derived for thermally thick solids. Although the Quintiere and Harkleroad correlation is only applicable to the thermally thick solids only, it plotted a better correlation of the 20-mm samples. This is clearly shown in Figure 5.2 above, where the 20-mm best-fit line is better correlated (greater R^2 values) than the 40-mm line.

5.4) Thermally Thin or Thermally Thick Behaviour?

From the ignition data plotted by Delichatsios et al.; Spearpoint et al.; Janssens; and Tewarson, all the tested wood species have relatively good thermally thick behaviour. The reason the Quintiere and Harkleroad (QH) method does not give a good correlation from the experimental data has been explained, but from Figure E3, it is apparent that the mdf has a very good linear relationship plotted by QH method for both thicknesses ($R^2 > 0.98$). Mikkola and Wichman's method is applicable to both thermally thin and thick solids; they also say that all the timbers behave as thermally thick solids, as the data is better correlated when the power index, n = 2. Therefore, the limit for thermally thick wood of 15-20 mm recommended by them is reasonable.

The correlation by Toal, Silcock and Shields is usable for thermally thin, thick and intermediate solids, depending on the n values. Such a correlation showed that some 20-mm samples exhibit thermally intermediate behaviour; that is, the n is around 1.5. These samples include Macrocarpa (n = 1.58), Radiata Pine (n = 1.63) and Beech (n = 1.65). Plywood and Rimu behave as thermally thick for both 40-mm and 20-mm samples with n = 1.9 and n = 2 respectively. The Plywood reported in Mikkola and Wichman's paper [11] had a thermally thin behaviour although it was physically thick. This is because of the glue between laminae. Shields, Silcock and Murray [2] also tested Plywood but they did not get similar result. This might be because of the different ways of manufacturing Plywood and the nature of the Plywood itself.

Attempts to correlate the 40-mm mdf ignition data with the thermally thick formula of Toal, Silcock and Shields failed completely. The best correlation, found at n = 1.2, indicates the 40-mm samples behave as thermally thin. The problem arises when the 20-mm mdf behave vice versa, with n = 1.7. This may be related to the change of environmental conditions of the fume cupboard during the early stage of this research when the ISO ignitability apparatus was not put in a specially designed cage to avoid the airflow draughts affecting the occurrence of ignition. The apparatus was just set in the fume cupboard with the extraction fan on. Although the test environment in the fume

cupboard was checked before the tests, the air velocity in the cupboard was later found to exceed 0.02 m/s. The main contributor to this high velocity was the fan, located inside and on top of the cupboard.

Therefore the ignition tests on the 40-mm mdf samples were redone. Figure E7, in Appendix E, shows the results of the repeated test. The correlation improved by using a thermally intermediate formula, with n = 1.5. This is still not a satisfactory result and the reason for this is unknown, but such result leads to another important discovery; that is, how the testing environment affects the ignition result. This is discussed in section 5.7 in this report in terms of repeatability and reproducibility. The calculations and results obtained by all the correlations for the mdf come from this repetition of the ignition test.

5.5) Ignition Temperature and Thermal Inertia

The ignition temperature, T_{ig}, for each species is shown in Tables B1 to B14 in Appendix B. As stated before, the T_{ig} was calculated theoretically by using equation (4) and the selected convective heat transfer coefficient, h_c rather than measured experimentally. Note that from the calculated T_{ig}, the values differ widely between the correlations.

The ranges of the ignition temperature, T_{ig}, of the wood (both the thin and thick samples) are shown in the following table. Tewarson's correlation does not require calculation of the ignition temperature.

	T_{ig}(deg C) range	
	40 mm	20 mm
Macrocarpa	362(MW) – 468(DPK)	361(MW) – 466 (DPK)
Beech	327 (MW) – 423(DPK)	335(MW) – 433(DPK)
mdf	197(MW) – 389(QH)	202(MW) – 389(QH)
Radiata Pine	281(MW) – 376(QH)	275(MW) – 389(QH)
Rimu	275(MW) – 376(QH)	269(MW) – 376(QH)
Plywood	245(MW) – 362(QH)	262(MW) – 362(QH)

Table 5.3: The ranges of ignition temperature, T_{ig}, of each wood

Note:

MW = Mikkola and Wichman

DPK = Delichatsios, Panagiotou and Kiley

QH = Quintiere and Harkleroad

The above Table 5.3 shows the order of the ignition temperature from the highest to the lowest generally. Macrocarpa has the highest ignition temperature and Plywood has the lowest. Such results give a good agreement with the minimum heat flux, $\dot{q}''_{min}$, as the wood species in the above Table 5.3, are arranged in order from the highest to the lowest minimum heat flux. The minimum irradiance is directly proportional to the ignition temperature.

It is worth noticing that the Mikkola and Wichman technique always gives the lowest estimate of T_{ig}. The reason is that the T_{ig} is proportional to the critical heat flux, $\dot{q}''_{cr}$. Therefore, the low values of T_{ig} are due to the low values of $\dot{q}''_{cr}$ estimated by this method. The technique by Delichatsios et al. has the highest ranking of T_{ig} for Macrocarpa and Beech. The reason is the same; that is, the $\dot{q}''_{cr}$ obtained by this method is greater than other correlations. However, Quintiere and Harkleroad's correlation gives the greatest values of T_{ig} for the remaining wood. This is because, unlike the other correlations, the estimate of T_{ig} of this correlation is based on the minimum heat flux, $\dot{q}''_{\min}$ instead of $\dot{q}''_{cr}$ (see equation (19)) and the $\dot{q}''_{\min}$ always greater than the $\dot{q}''_{cr}$. Therefore, one can conclude that Mikkola and Wichman's correlation has a tendency to under-predict the ignition temperature, T_{ig}, whereas the Quintiere et al. correlation and Delichatsios et al. correlation have a tendency to over-predict the T_{ig}.

According to Tables B1 to B14, the values of the evaluated T_{ig} for 20-mm and 40-mm samples in the same correlation are very close to each other. This is also happened for all other values, such as $\dot{q}''_{cr}$, $\dot{q}''_{\min}$, kρc, TRP, FTP, and b.

The values of thermal inertia, kρc, are also shown in Tables B1 to B14 in Appendix B of this report. In section 4.3, it has been explained that only five of the Ignition time/Irradiance correlations estimate the kρc. Table 5.4 below gives the same type of information for the thermal inertia as given by Table 5.3 above.

	kρ c $(kW/m^2K)^2s$	
	40 mm	20 mm
Macrocarpa	0.331(J) - 0.784, 4.435 (DPK)	0.241(J) - 0.555, 6.005(DPK)
Beech	0.461(J) - 0.974, 2.935(DPK)	0.340(J) - 0.700, 4.060(DPK)
mdf	0.551(DPK) - 2.550, 3.100(MW)	0.664(DPK) - 2.143, 2.652(MW)
Radiata Pine	0.573(J) - 0.810, 2.135(DPK)	0.479(J) - 0.725, 2.386(DPK)
Rimu	0.870(J) - 1.342, 1.436(QH)	0.670(J) - 1.016, 1.698(DPK)
Plywood	0.938(J) - 2.271, 1.500(MW)	0.596(J) - 0.918, 1.350(DPK)

Table 5.4: The ranges of thermal inertia, kρc, of each wood

Note:

J = Janssens

MW = Mikkola and Wichman

DPK = Delichatsios, Panagiotou and Kiley

QH = Quintiere and Harkleroad

The first numbers in the columns in the above table are the ranges of the four lowest kρc values for each species. The second number is the single value of the greatest kρc. From the results, it is obvious that the values of kρc are very messy and do not follow any particular orderly trend. The degree of variation is very large for all the wood specimens. Unlike the ignition temperature, T_{ig}, the kρc is influenced by several factors instead of one factor only, which is the critical heat flux in the case of T_{ig} determination. The kρc depends on the gradient of the best-fit line, the h_{ig}, the T_{ig} and so on, depending on the type of the model.

Janssens always give the lowest kρc among the correlations. In estimating the highest values of kρc, Mikkola and Wichman's; Quintiere and Harkleroad's; and Delichatsios et al.'s were important.

The thermal inertia, kρc, of Rimu, mdf and Plywood calculated by all the correlations, except that of Delichatsios et al. correlation, have the greatest kρc values, whereas the thermal inertia of Macrocarpa calculated by most correlations except that Delichatsios et al. correlation, have the lowest values of kρc.

From Table 5.4 above, the kρc calculated by Delichatsios et al. is always the highest. The main reason is that the kρc depends on the T_{ig} and the slope of the best-fit line, and the T_{ig} is dependent on the critical heat flux, $\dot{q}''_{cr}$. This model calculated a very high value of $\dot{q}''_{cr}$. Therefore, the kρc is also high, since it is linearly proportional to the $\dot{q}''_{cr}$. This reason can also be used to explain why the thermal inertia, kρc, of Beech, Radiata Pine, Rimu and Plywood determined by this model are the highest among the other correlations.

Mikkola and Wichman, as shown in Table 5.4, calculated a relatively high value for the kρc (mdf and Plywood) compared to the other correlations. This is because the kρc is inversely proportional to the T_{ig} and the slope (see equation (11)). From Table 5.3, the ignition temperature, T_{ig}, of the mdf is the smallest. This produces a very high kρc value.

5.6) Minimum Heat Flux and Critical Heat Flux

The values of critical heat fluxes, $\dot{q}''_{cr}$, calculated by each method are shown in Table B1 to B14 in Appendix B, as well as minimum heat fluxes, $\dot{q}''_{\min}$. The table below shows the ranges of the four smallest values of $\dot{q}''_{cr}$ and the single greatest value of $\dot{q}''_{cr}$; and minimum heat fluxes for each type of wood.

	40 -mm sample		20-mm sample	
	q" min (kW/m²)	q" cr (kW/m²)	q" min (kW/m²)	q" cr (kW/m²)
Macrocarpa	17	13.0 (MW) - 17.4, 20.3 (DPK)	17	12.9 (MW) - 17.0, 20.1 (DPK)
Beech	16	10.7 (MW) - 14.1, 16.7 (DPK)	16	11.2 (MW) - 14.7, 17.5 (DPK)
mdf	15	4.5 (MW) - 7.0, 9.3 (TSS)	15	4.7 (MW) - 7.4, 7.7 (TSS)
Radiata Pine	14	8.1 (MW) - 10.7, 12.7 (DPK)	15	7.8 (MW) - 11.5, 12.2 (DPK)
Rimu	14	7.8 (MW) - 10.3, 12.2 (DPK)	14	7.5 (MW) – 9.9, 11.7 (DPK)
Plywood	13	6.4 (MW) - 8.4, 10.0 (DPK)	13	7.2 (MW) - 9.5, 11.3 (DPK)

Table 5.5: The ranges of minimum heat flux of each wood

Note:

MW = Mikkola and Wichman

DPK = Delichatsios, Panagiotou and Kiley

TSS = Toal, Silcock and Shields

Macrocarpa has the greatest critical heat flux and minimum heat flux in both 20-mm and 40-mm samples. This is followed by Beech, Radiata Pine, Rimu and Plywood in general. Moderate density fibreboard, mdf, has the lowest values of critical heat fluxes but not in terms of minimum heat fluxes. As a reminder, only 5 correlations by Mikkola and Wichman; Janssens; Toal, Silcock and Shields; Delichatsios, Panagiotou and Kiley; and; Spearpoint and Quintiere allow the determination of critical heat fluxes.

It is surprising to see both the 20-mm and 40-mm samples have the same or very close $\dot{q}''_{cr}$ and $\dot{q}''_{\min}$. Such a result suggests that the values of $\dot{q}''_{\min}$ or $\dot{q}''_{cr}$ are not affected by the thickness of the samples for this range (20-40 mm). According to Mikkola and Wichman [11], there are two possible explanations for this. First, the chemical explanation, which suggests that all woods have very similar composition; that is, they contain very nearly the same percentages of lignin, cellulose and hemicellulose. As a result, the ignition temperatures, T_{ig}, and $\dot{q}''_{cr}$ (or $\dot{q}''_{\min}$) are almost the same for all woods and consequently the heat losses at ignition are always practically identical.

The second physical explanation suggests that the atmosphere in all experiments is quiescent; the different samples all lose heat by radiation and natural convection. In a laboratory the value of h_c may not always be constant for all because of the change in convection heat transfer. This will change the heat loss at ignition. However, if radiation forms the major part of the heat loss, the problem of changes in convection character will not affect the results significantly. Therefore one still can get similar results for $\dot{q}''_{cr}$ or $\dot{q}''_{\min}$. These two explanations can also be used for the same values of $\dot{q}''_{cr}$ or $\dot{q}''_{\min}$ obtained from two different wood species.

When looking at the type of correlations, Delichatsios et al.'s method, and Mikkola and Wichman's method always give the highest and lowest values of $\dot{q}''_{cr}$ respectively. Mikkola and Wichman's method gives a small $\dot{q}''_{cr}$ because the critical heat fluxes were found from the intercept of the $\dot{q}''_{e}$ without being increased by any factor, as Delichatsios, Panagiotou and Kiley did. Delichatsios et al. suggested the obtained $(\dot{q}''_{e})_{int}$ should be increased by a factor of 0.64. This also indicates that the increasing factor of 0.76 recommended by Spearpoint and Quintiere will give an intermediate result, which is more appropriate.

The Toal, Silcock and Shields correlation gives the highest $\dot{q}''_{cr}$ value of 9.3 kW/m^2 for mdf. This is related to the unexplainable results having been obtained for 40-mm mdf, as discussed in Section 5.4 of this report. The 40-mm mdf should behave as thermally thick but it did not. From the ignition data obtained, it was found that the data fit best when n = 1.5, (see Figure E7). However, in theory, if the 40-mm mdf behaves as thermally thick with n = 2, one will get a flatter best-fit line, hence a smaller $\dot{q}''_{cr}$. Therefore if the value (9.3 kW/m^2) obtained by this correlation is not taken into account, again the correlation by Delichatsios et al. will dominate the highest value of $\dot{q}''_{cr}$. Overall the $\dot{q}''_{\min}$ is greater than the $\dot{q}''_{cr}$ ($\dot{q}''_{\min} > \dot{q}''_{cr}$).

From the literature, the $\dot{q}''_{cr}$ for Radiata Pine given by Mikkola and Wichman [11] is10 kW/m^2 in their research. The values reported by Bluhme [19] and Janssens [18] are 13 kW/m^2 and 12.9 kW/m^2. All these fell in the range of the $\dot{q}''_{cr}$ obtained for Radiata Pine in this research. The difference might be due to the different methodology used and different thicknesses of the tested samples.

Toal, Silcock and Shields obtained a value of 8.3 kW/m^2 for the critical heat flux of fibreboard. The type and thickness of fibreboard tested by them is unknown. Since they used the same methodology, it is worth comparing their results with the results obtained in this research. Their value compares well with 7.7 kW/m^2 obtained for 20-mm mdf obtained in this research by their method. Although the accuracy of the data for 40-mm sample is questionable, its $\dot{q}''_{cr}$ of 9.3 kW/m^2 is still comparable with the value (8.3 kW/m^2) given by Toal et al.

Another critical irradiance value reported for fibreboard is 4 kW/m^2. Similarly this value is very close to the value obtained in this research using their correlation. The $\dot{q}''_{cr}$ values obtained in this research by using their method are 4.5 and 4.7 kW/m^2 for 40-mm and 20-mm samples respectively.

Toal, Silcock and Shields [1] found that the critical irradiance for Plywood is 10.6 kW/m^2. Mikkola and Wichman [11] give a value of 13 kW/m^2 for Plywood. These values are located in the high range of the values determined in Table 5.5 above. However, the value reported by Shields, Silcock and Murray [2] for horizontal mounted Plywood with an ignition mode of Spark is 8.5 kW/m^2. Since the thickness of the Plywood samples tested by them is 12 mm, such a value (8.5 kW/m^2) is compared very well with the range of $\dot{q}''_{cr}$ for 20-mm Plywood (see Table 5.5). In conclusion, the data from the literature and this study demonstrate that there is a reasonable degree of variability in the critical heat fluxes of wood.

5.7) Repeatability and Reproducibility

Table J1 to Table J11 show the absolute differences (Δ) between the extreme values and the average values – that is, between maximum ignition time and average ignition time (Upper extreme); and between average ignition time and minimum ignition time (Lower extreme). Among the 5 replications at each level of irradiance, there are always one or two results outside the range. This outlying data will produce a very high value of Δ, as Δ is derived from the absolute difference between the extremes and the averages. Therefore, these outlying data were removed to improve the Δ. By doing this, the average values were not changed significantly but the Δ were. Where the outlying data was removed is highlighted in bold as shown in Appendix I: Raw Data, and Appendix J.

According to Table 1 in Annex A BS 476, Part 13:1987 [14], the limits of repeatability for chipboard and hardboard are 20-29% and 15-25% respectively. The greatest r value in Tables J1 to J11 is 29%, which is reasonable compared to those limits, although some of them are beyond the limits. These limits for chipboard and hardboard can be used only as a reference comparison, since both the thicknesses of these boards and the type of the wood are different from those tested in this study..

The average r and R calculated for mdf are 32 seconds and 40 seconds (see Appendix J). The limits suggested for chipboard and hardboard at each level of irradiance are shown in Table 5.6 below. When the calculated values and the limits are compared, the r and R are within the limits. The relationship between the mean of ignition time, m, and r and R is shown in Figure 5.1. Obviously, the r and R curves are not linearly related to the m. They behave more like an exponential relationship. What is certain is that the higher the m, the higher the r and R. The exact relationship needs to be discussed further.

Level (kW/m^2)	m_{2lab}	r	R	r (%)	R (%)	r_{lim} (%)	R_{lim} (%)
40	67	17	25	24.8	37.0	21^1, 25^2	41^1, 34^2
30	116.6	16	17	13.8	14.8	23^1, 15^2	33^1, 39^2
20	294.9	64	77	21.8	26.2	20^1, 19^2	49^1, 54^2

Table 5.6: Comparison between the calculated r (and R) and the limits

Where, m_{2lab} = mean ignition time of the batches of products tested between the 2 labs

r_{lim} = limit of r found in Table 1 in reference [14]

R_{lim} = limit of R found in Table 1 in reference [14]

Note 1 = limits for chipboard

Note 2 = limits for hardboard

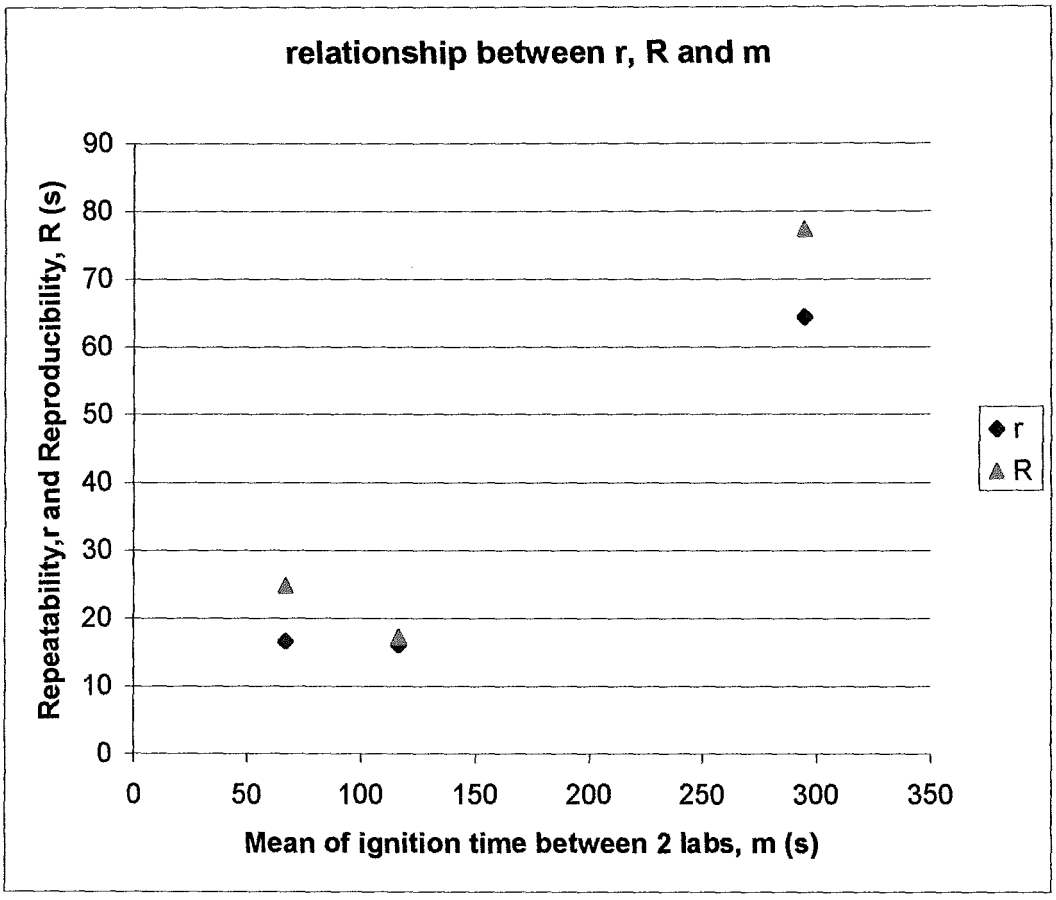

Figure 5.4: Relationship between r, R and m

The differences between lab 1 and lab 2 are the environmental conditions and the calibration scale. One can see from this, how sensitive the results of ignition time, t_{ig}, are to the environmental conditions. This explains why the results obtained from different equipment, such as Cone Calorimeter, ISO Ignitability Apparatus and so on, varied significantly at identical levels of irradiance. This also explains why repeatability, r is smaller than reproducibility, R. This is because different equipment have different designs, and hence different geometries that result in different environmental conditions, for example, the airflow pattern on the surface of the sample. In their paper, Barbrauskas and William J. Parker [21] compared the results obtained from different equipment.

Since, all the calculated repeatability, r and reproducibility, R are within the limits recommended in Table 1 in reference [14] (also shown in Table 5.6 above), the results obtained in this research are acceptable and hence accurate enough to be used.

5.8) Which is the Best Method?

In order to know which method is the best among the seven correlations, comparative plots of the measured ignition time versus the predicted are plotted. These plots are shown in Appendix K, Figures K1 to K12. From these figures (K1 to K12), notice that the results show relative good comparison at high heat fluxes; that is, at heat fluxes exceed 20 kW/m^2 and at time to ignition less than 200 seconds. The comparison is very poor at low heat fluxes (less than 20 kW/m^2) when approaching minimum heat flux, $\dot{q}''_{\min}$. Figure 5.5 below shows a particular case for Beech. According to Figure 5.5, Quintiere and Harkleroad (QH), and Tewarson (T) are the worst method to be used. Although, in general, all the methods do not give good comparison at low heat fluxes, due to some reason these two methods are the worst. As said before, the reason is that both methods require the best-fit line to be drawn to pass through the origin. This gives a poor correlation at low heat fluxes. Tewarson's method also causes significant over prediction of time to ignition as the incident heat flux, $\dot{q}''_e$, approaching minimum heat flux, $\dot{q}''_{\min}$.

Quintiere and Harkleroad is recommended to be the worst method to be used because of the requirement of making the judgement by the researchers when drawing the best-fit line through the ignition data. As said before, one has to ignore the high values of $\dot{q}''_{\min}/\dot{q}''_e$ to obtain a reasonable fit line through the data. Therefore it depends on the decision of researcher. This can be very subjective. The way it estimates the T_{ig} and kρc based on $\dot{q}''_{\min}$ obtained experimentally is not a good idea. This is because the $\dot{q}''_{\min}$ always much greater than $\dot{q}''_{cr}$.

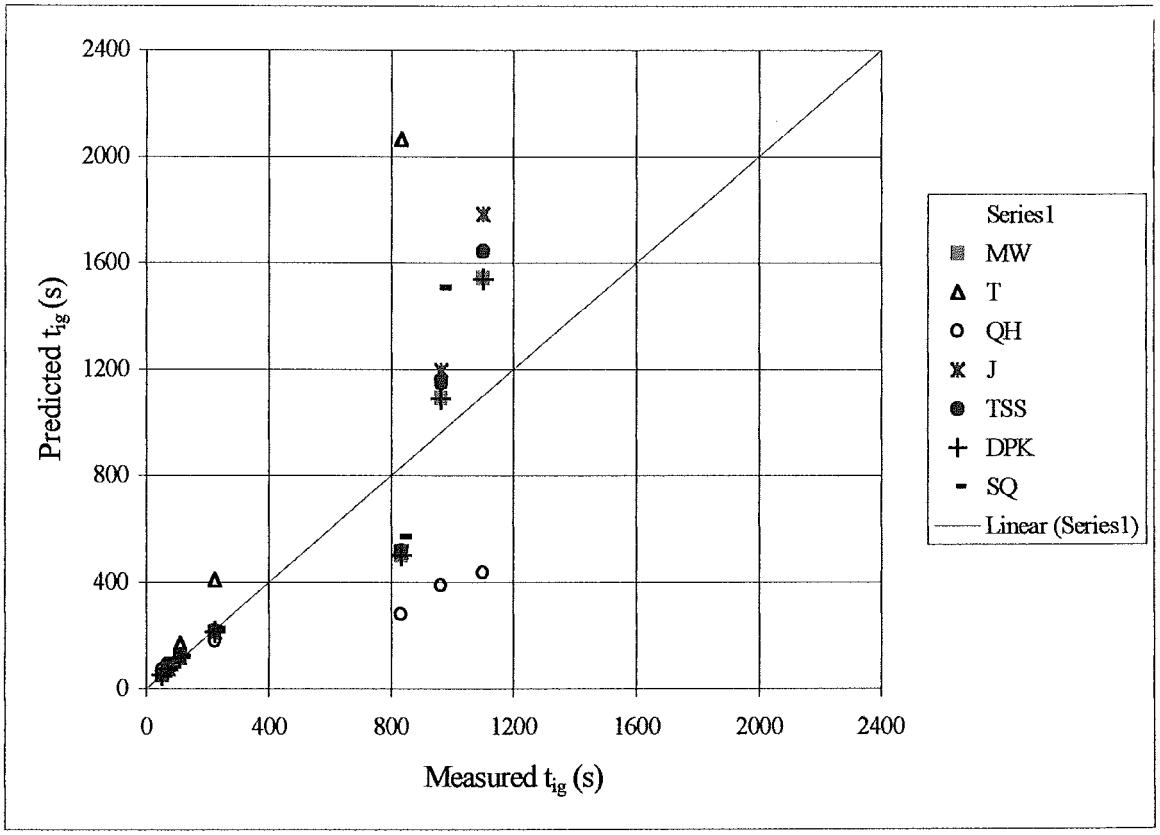

Figure 5.5: Predicted ignition time versus Measured ignition time for Beech (same as Figure K5)

Note:

MW	= Mikkola and Wichman	TSS	= Toal, Silcock and Shields
T	= Tewarson	DPK	= Delichatsios, Panagiotou and Kiley
QH	= Quintiere and Harkleroad	SQ	= Spearpoint and Quintiere
J	= Janssens		

The remaining five correlations always give a fairly good comparison between the predicted and measured t_{ig}. At high heat fluxes (> 20 kW/m^2) and t_{ig} < 200 s, these five correlations are so good in estimating the ignition time. This can be seen in Figure 5.6, a closer look of Figure 5.5 at high heat fluxes. From Figure 5.6, one can see that, even at high heat fluxes, Tewarson (T) and Quintiere and Harkleroad (QH) method, do not give good comparison of the results.

Therefore, the decision of the best methods has to be made based on their performances at low heat fluxes. By looking at Figures K1 to K12, MW method and DPK method have a better performance in comparing the measured and predicted time to ignition, although MW and DPK always give lowest and highest values of $\dot{q}''_{cr}$ and T_{ig}. The other correlations are intermediate between these selected best and worst methods.

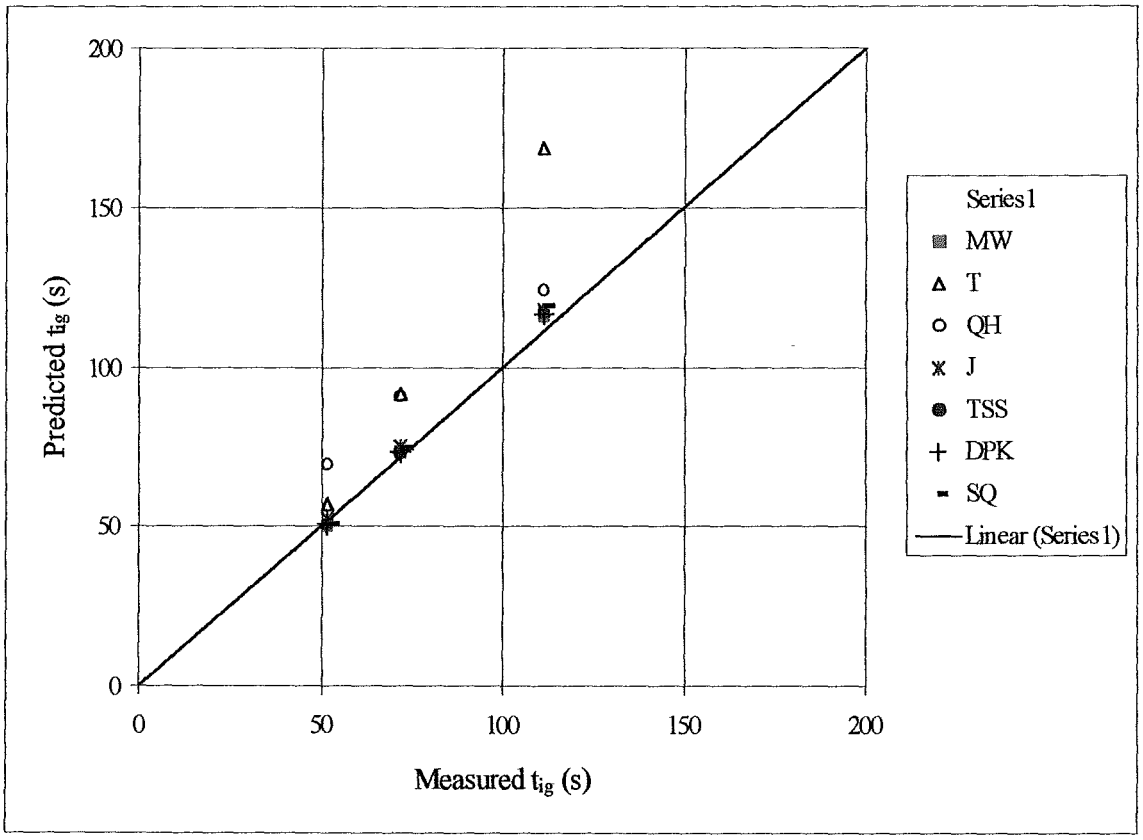

Figure 5.6: Predicted ignition time versus Measured ignition time at t_{ig} < 200 s for Beech

CHAPTER 6: SOURCES OF ERROR

Every experiment will have a number of errors. In this research, there are two major possible errors, which may significantly affect the ignition results. The first one, as discussed before, is the change of calibration scale. Two calibrations had been done on the apparatus, one on 5 December 2000 and one on 20 December 2000. According to Figure 4.1, the temperatures were dropped slightly over the period of 15 days. The reasons for this, has been explained above, are briefly as follows.

- The radiator cone heater gave a poor heat distribution in terms of uniformity. As a result, the highest temperature point was found to be not at the center point of the cone heater and hence produced two different calibration scales. The probability of this is low.
- The radiometer gave the wrong readings. This may due to the backing board used to hold the radiometer.
- The difficulty in determining the centre point when calibrating the apparatus and checking the level of irradiance released at a certain temperature.

The second major possible error is the absence of a quiescent environment in the early stage of the experiments; that is, when the 40-mm samples were tested. The air draught in the fume cupboard, where the apparatus is placed, exceeded 0.02 m/s. Such a airflow will affect the natural convective heat transfer at the surface of the sample.

Even though the accuracy of the 40-mm samples is questionable because of the air draught problem, from the results of the calculated repeatability, r, and reproducibility, R in Section 5.7, it suggests that this problem does not significantly affect the results. This is because the r and R values lie within the limits. Therefore, the results of 40-mm samples tested in the early stage of this research based on calibration scale 5 December 2000, are usable and accurate.

CHAPTER 7: CONCLUSION

- There is no perfect method of estimating the ignition properties of the New Zealand Timbers, but one can know which methods will give a higher or lower results from this research.

- Although there is no perfect method, the recommendation of the best and worst methods is shown in the table below:

Correlation	Best to Worst
Mikkola & Wichman and Delichatsios, Panagiotou & Kiley	Best
Toal, Silcock & Shields, Janssens and Spearpoint & Quintiere	Intermediate
Quintiere & Harkleroad and Tewarson	Worst

Table 7.1: Recommendation of Best and Worst Correlations

- The minimum heat flux, $\dot{q}''_{min}$ for each type of wood, in the order of highest to the lowest are: Macrocarpa, Beech, moderate density fibreboard (mdf), Radiata Pine, Rimu and Plywood.

- The correlation: (1) Delichatsios et al.; and (2) Quintiere and Harkleroad dominate the high-ranged results of ignition temperature, T_{ig}, of the woods. The correlation by Mikkola and Wichman gives a lower T_{ig} values. Other methods give intermediate values between these correlations.

- The correlation: (1) Mikkola and Wichman; (2) Quintiere and Harkleroad; and (3) Delichatsios et al. always gives the highest values of kρc. The correlation by Janssens always gives the lowest kρc. Other methods give intermediate values between these correlations.

- The correlation: (1) Delichatsios et al.; and (2) Mikkola and Wichman always give the highest and lowest values of $\dot{q}''_{cr}$ respectively. Other methods give intermediate values between these correlations.

- The values of T_{ig}, $\dot{q}''_{cr}$, and kρc for each wood are as follows:

	q" cr (kW/m^2)	T_{ig} (deg C)	kρ c $(kW/m^2K)^2s$
Macrocarpa	13 – 17, 20	360 – 470	0.25 – 0.75, 6.0
Beech	11 – 15, 17	330 – 430	0.35 – 0.95, 4.0
mdf	5 – 7, 8	200 – 390	0.55 – 2.55, 3.1
Radiata Pine	8 – 11, 13	280 – 390	0.50 – 0.80, 2.4
Rimu	8 – 10, 12	270 – 380	0.70 – 1.30, 1.7
Plywood	6 – 9, 11	250 – 360	0.60 – 2.27, 1.5

Table 7.2: Values of thermal inertia, critical heat flux and ignition temperature

- The results T_{ig}, $\dot{q}''_{cr}$, $\dot{q}''_{min}$, FTP, b, kρc, TRP and n, obtained for 20-mm and 40-mm samples of the same wood species, are very close to each other.

- The data from literature and this study demonstrate that there is a reasonable degree of variability in the critical heat fluxes of wood.

- Both 20-mm and 40-mm samples behaved as thermally thick or thermally intermediate solids, except the medium density fiberboard, mdf, which is due to possible experimental error, as explained above.

- Repeatability, r (Δ), and Reproducibility, R, from this research lie within the limits suggested by Table 1 in reference [14], after some of the outlying data has been removed.

- The effect of environmental conditions during the test, especially on the surface of the specimen, will have a significant effect on the results. This is why different equipment will give different results for the same materials. (This is why the reproducibility, R, is usually greater than repeatability, r)

NOMENCLATURE

A_s = exposed surface area of the sample

b = a constant related to kρc

c = specific heat of the material

F(t) = a function of time and thermal properties of the solid

FTP = Flux Time Product

h_c = convection heat transfer coefficient

h_{ig} = heat transfer coefficient which incorporates both the radiative and convective components

k = thermal conductivity of material

L_0 = specimen thickness

m = mean of ignition time

mdf = moderate density fibreboard

m_{2lab} = mean ignition time between the 2 labs

n_i = number of replicates per level

P = perimeter

p = number of laboratories

$\dot{q}_e^{"}$ = external or incident heat flux

$\dot{q}_{cr}^{"}$ = critical heat flux

$(\dot{q}_e^{"})_{int}$ = external or incident heat flux that intercept along the x-axis (abscissa)

$\dot{q}_{min}^{"}$ = minimum heat flux

r = repeatability

R = reproducibility

s_i = intra-cell standard deviation

s_r^2 = repeatability variance

s_L^2 = between-lab variance

s_R^2 = reproducibility variance

T_{ig} = ignition temperature of surface

T_s = surface temperature

T_∞ = ambient temperature

T_f = hot gas temperature

TRP = Thermal Response Parameter

t_{ig} = ignition time

$t_{ig\,min}$ = minimum t_{ig} of the five tested specimens at certain irradiance level

$t_{ig\,max}$ = maximum t_{ig} of the five tested specimens at certain irradiance level

t_m = a characteristic time indicative of the time to reach thermal equilibrium

V = volume

y_i = any one of the results (ignition time, t_{ig})

yi bar = average ignition times of the n replicates

ρ = density of the material

ρ_d = dried density of the material

ρ_{avg} = average dried density of the material

ε = emissivity or absorptivity of the surface

σ = Stefan Boltzmann constant (5.67×10^{-11} kW/m^{2}K^4)

α = thermal diffusivity (evaluated at ignition)

ν = viscosity (m^2/s)

Δ_{up} = absolute difference between maximum t_{ig} and mean t_{ig}

Δ_{low} = absolute difference between minimum t_{ig} and mean t_{ig}

m = mean t_{ig} of the five specimens at certain irradiance level

SUBSCRIPT

cr	= critical
∞	= ambient (infinity)
min	= minimum
e	= external or incident
f	= hot gas (fire)
ig	= at ignition
s	= surface
c	= convective heat transfer
int	= intercept
d	= dry
avg	= average

REFERENCES

[1]Toal, B.R., Silcock,, G.W.H., & Shields, T.J., "An Examination of Piloted Ignition Characteristics of Cellulosic Materials Using the ISO Ignitability Test", *Fire and Materials*, Vol. 14, 97-106, 1989.

[2]Shields, T.J., Silcock, G.W.H., & Murray, J.J., "Evaluating Ignition Data Using the Flux Time Product", *Fire and Materials*, Vol. 18, 243-254, 1994.

[3]Silcock, G.W.H., & Shields, T.J., "A Protocol for Analysis of Time-to-Ignition Data From Bench Scale Tests", *Fire Safety Journal*, Vol. 24, 75-95, 1995.

[4]Janssens, M., "A Thermal Model for Piloted Ignition of Wood Including Variable Thermophysical Properties", *Fire Safety Science-Proceeding of the 3rd International Symposium*, 167-176, 1991.

[5]Quintiere, J.G. and Hakleroad, M., "New Concepts for Measuring Flame Spread Properties," *Fire Safety: Science and Engineering, ASTM STP 882*, T.Z. Harmathy, Ed., American Society for Testing and Materials, Philadephia, 239-267, 1985.

[6]Kanury, A.M., in "Fire Research Abstracts and Reviews", *Factory Mutual Research Corporation*, Norwood, MA, Vol.14, No.1, 24-72, 1972.

[7]Simms, D.L., Combustion and Flame, Vol. 7, 253-261, Sept. 1963.

[8]Atreya, A., Carpentier, C., and Harkleroad, M., "Effect of Sample Orientation on Piloted Ignition and Flame Spread", *Fire Safety Science – Proceeding of the 1st International Symposium*, 91-109, 1986.

[9]Janssens, M.L., "Fundamental Thermophysical Characteristics of Wood and their role in Enclosure Fire Growth", PhD Dissertation, University of Gent, Belgium, 1991.

[10]Tewarson, A., "Generation of Heat and Chemical Compounds in Fires", *The SFPE Handbook of Fire Protection Engineering*, Section 3/Chapter 4, 1995.

[11]Mikkola, E. and Wichman I.S., "On the Thermal Ignition of Combustible Materials", *Fire and Materials*, Vol. 14, 87-96, 1989.

[12]Wesson, H., "The Piloted of Wood under Radiant Heat", Ph.D Thesis, University of Oklahoma, Norman, OK, USA, 1971.

[13]Delichatsios, M.A., Panagiotou, TH., and Kiley, F., "The Use of Time to Ignition Data for Characterizing the Thermal Inertia and the Minimum (Critical) Heat Flux for Ignition or Pyrolysis", *Combustion and Flame*, Vol. 84, 323-332, 1991.

[14]"Fire Tests on Building Materials and Structures, Part 13: Method of measuring the ignitability of products subjected to thermal irradiance", *British Standard BS 476*, 1987.

[15]Spearpoint, M.J and Quintiere, J.G., "Predicting The Piloted Ignition of Wood in the Cone Calorimeter using an Integral Model – Effect of Species, Grain Orientation and Heat Flux", Department of Fire Protection Engineering, University of Maryland (in print).

[16]Quintiere, J.G., "A Semi-Quantitative Model for the Burning Rate of Solid Materials", NISTIR 4840, National Institute of Standards and Technology, Gaithersburg, MD, 1992.

[17]Arvind Atreya, "Convective Heat Transfer", *The SFPE Handbook of Fire Protection Engineering*, Section 1/Chapter 3, 1995.

[18]Janssens, M., "Mathematical Model to Predict the Contribution of Wood under Radiant Heat", Ph.D Thesis, University of Gent, Gent, Belgium, 1991

[19]D.A. Bluhme, "ISO Ignitability Test and Proposed Ignition Criteria", *Fire and Materials*, Vol. 11, 195-9, 1987.

[20]"Precision of Test Methods, Part 1: Guide for the determination of repeatability and reproducibility for a standard test method by inter-laboratory tests", *British Standard BS 5497*, 1987.

[21]V. Barbrauskas and William J. Parker, "Ignitability Measurements with the Cone Calorimeter", *Fire and Materials*, Vol. 11, 31-43, 1987.

Appendix A

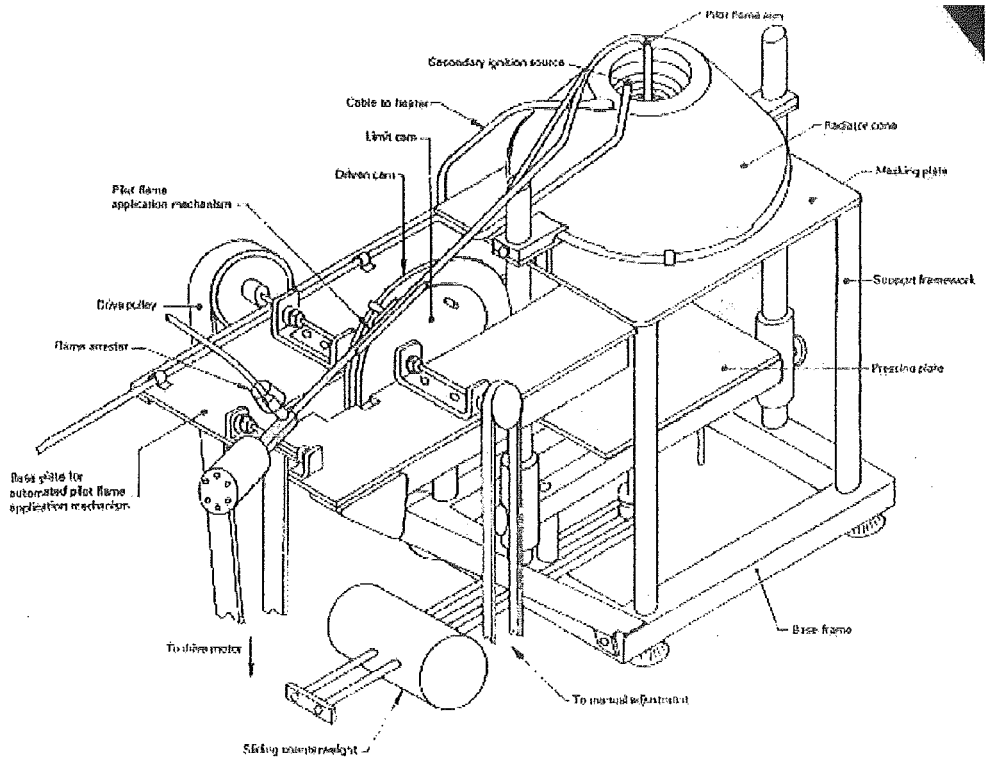

Figure A1: ISO Ignitability test apparatus

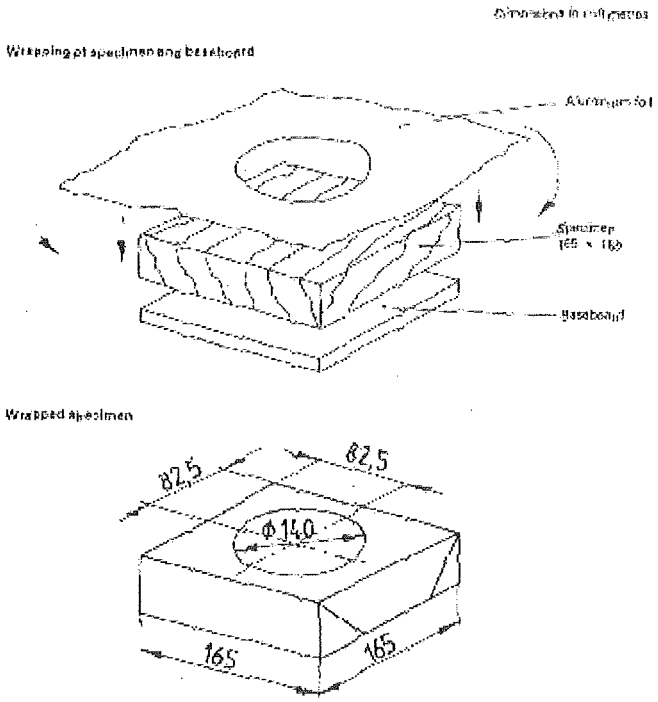

Figure A2: Wrapping of the specimen

Appendix B: Results for each correlation

Thickness = 40 mm

1) Mikkola and Wichman

	q''_{min} (kW/m^2)	q''_{cr} (kW/m^2)	kρ c (kW/m^{2}K)^{2}s	T_{ig} (deg C)
Macrocarpa	17	13.0	0.387	362
Beech	16	10.7	0.585	327
mdf	15	4.5	3.1	197
Radiata Pine	14	8.1	0.81	281
Rimu	14	7.8	1.29	275
Plywood	13	6.4	1.50	245

Table B1: Results of 40-mm wood from Mikkola & Wichman

Thickness = 20 mm

	q''_{min} (kW/m^2)	q''_{cr} (kW/m^2)	kρ c (kW/m^{2}K)^{2}s	T_{ig} (deg C)
Macrocarpa	17	12.9	0.285	361
Beech	16	11.2	0.423	335
mdf	15	4.7	2.652	202
Radiata Pine	15	7.8	0.725	275
Rimu	14	7.5	1.016	269
Plywood	13	7.2	0.902	262

Table B2: Results of 20-mm wood from Mikkola & Wichman

2) Tewarson

	q''_{min} (kW/m^2)	TRP kWs$^{1/2}$/m^2
Macrocarpa	17	196
Beech	16	205
mdf	15	227
Radiata Pine	14	202
Rimu	14	245
Plywood	13	231

Table B3: Results of 40-mm wood from Tewarson

	q''_{min} (kW/m^2)	TRP kWs$^{1/2}$/m^2
Macrocarpa	17	165
Beech	16	179
mdf	15	212
Radiata Pine	15	174
Rimu	14	212
Plywood	13	199

Table B4: Results of 20-mm wood from Tewarson

3) Quintiere and Harkleroad

Thickness = 40 mm

	q''_{min} (kW/m^2)	b ($s^{-1/2}$)	h_{ig} kW/m^{2}K	t_m (s)	kρ c (kW/m^{2}K)^{2}s	T_{ig} (deg C)
Macrocarpa	17	0.0550	0.0432	331	0.784	414
Beech	16	0.0479	0.0419	433	0.974	402
mdf	15	0.0455	0.0438	506	1.014	389
Radiata Pine	14	0.0445	0.0393	502	0.993	376
Rimu	14	0.0370	0.0393	729	1.436	376
Plywood	13	0.0380	0.0380	702	1.271	362

Table B5: Results of 40-mm wood from Quintiere & Harkleroad

Thickness = 20 mm

	q''_{min} (kW/m^2)	b ($s^{-1/2}$)	h_{ig} kW/m^{2}K	t_m (s)	kρ c (kW/m^{2}K)^{2}s	T_{ig} (deg C)
Macrocarpa	17	0.0654	0.0432	234	0.555	414
Beech	16	0.0565	0.0419	313	0.700	402
mdf	15	0.0476	0.0406	437	0.927	389
Radiata Pine	15	0.0589	0.0406	289	0.605	389
Rimu	14	0.0444	0.0393	511	0.997	376
Plywood	13	0.0447	0.0380	497	0.918	362

Table B6: Results of 20-mm wood from Quintiere & Harkleroad

Thickness = 40 mm

4) Janssens

	q''_{min} (kW/m^2)	q''_{cr} (kW/m^2)	h_{ig} kW/m^{2}K	kρ c (kW/m^{2}K)^{2}s	T_{ig} (deg C)
Macrocarpa	17	14.2	0.0349	0.331	379
Beech	16	11.9	0.0320	0.461	346
mdf	15	6.2	0.0246	1.509	240
Radiata Pine	14	9.5	0.0292	0.573	307
Rimu	14	9.3	0.0288	0.870	303
Plywood	13	7.8	0.0268	0.938	275

Table B7: Results of 40-mm wood from Janssens

Thickness = 20 mm

	q''_{min} (kW/m^2)	q''_{cr} (kW/m^2)	h_{ig} kW/m^{2}K	kρ c (kW/m^{2}K)^{2}s	T_{ig} (deg C)
Macrocarpa	17	13.9	0.0344	0.241	375
Beech	16	12.1	0.0325	0.340	349
mdf	15	6.4	0.0251	1.300	245
Radiata Pine	15	9.2	0.0286	0.479	302
Rimu	14	8.9	0.0283	0.670	296
Plywood	13	8.4	0.0279	0.596	287

Table B8: Results of 20-mm wood from Janssens

Thickness = 40 mm

5) Toal, Silcock and Shields

	q''_{min} (kW/m^2)	q''_{cr} (kW/m^2)	FTP (kW s/m^2)^n	n	T_{ig} (deg C)
Macrocarpa	17	13.4	34,592	2.0	368
Beech	16	10.9	42,750	2.0	331
mdf	15	9.3	10,599	1.5	303
Radiata Pine	14	8.6351	41,209	2.0	291
Rimu	14	8.3	61,474	2.0	285
Plywood	13	7.3	39,663	1.9	265

Table B9: Results of 40-mm wood from Toal, Silcock & Shields

Thickness = 20 mm

	q''_{min} (kW/m^2)	q''_{cr} (kW/m^2)	FTP (kW s/m^2)^n	n	T_{ig} (deg C)
Macrocarpa	17	15.4	5,791	1.6	394
Beech	16	13.3	9,094	1.7	367
mdf	15	7.7	20,423	1.7	273
Radiata Pine	15	11.5	8,317	1.6	340
Rimu	14	8.2	45,595	2.0	283
Plywood	13	8.1	27,314	1.9	281

Table B10: Results of 20-mm wood from Toal, Silcock & Shields

Thickness = 40 mm

6) Delichatsios, Panagiotou and Kiley

	q''_{min} (kW/m^2)	q''_{cr} (kW/m^2)	kρ c (kW/m^{2}K)^{2}s	T_{ig} (deg C)
Macrocarpa	17	20.3	4.435	468
Beech	16	16.7	2.935	423
mdf	15	7.0	0.551	253
Radiata Pine	14	12.7	2.135	363
Rimu	14	12.2	1.342	355
Plywood	13	10.0	1.157	316

Table B11: Results of 40-mm wood from Delichatsios et. al.

Thickness = 20 mm

	q''_{min} (kW/m^2)	q''_{cr} (kW/m^2)	kρ c (kW/m^{2}K)^{2}s	T_{ig} (deg C)
Macrocarpa	17	20.1	6.005	466
Beech	16	17.5	4.060	433
mdf	15	7.4	0.664	262
Radiata Pine	15	12.2	2.386	355
Rimu	14	11.7	1.698	347
Plywood	13	11.3	1.350	340

Table B12: Results of 20-mm wood from Delichatsios et. al.

Thickness = 40 mm

7) Spearpoint and Quintiere

	q''_{min} (kW/m^2)	q''_{cr} (kW/m^2)	kρ c (kW/m^{2}K)^{2}s	T_{ig} (deg C)
Macrocarpa	17	17.4	0.336	418
Beech	16	14.1	0.509	378
mdf	15	5.9	2.550	233
Radiata Pine	14	10.7	0.689	327
Rimu	14	10.3	1.090	321
Plywood	13	8.4	1.254	287

Table B13: Results of 40-mm wood from Spearpoint & Quintiere

Thickness = 20 mm

	q''_{min} (kW/m^2)	q''_{cr} (kW/m^2)	kρ c (kW/m^{2}K)^{2}s	T_{ig} (deg C)
Macrocarpa	17	17.0	0.252	414
Beech	16	14.7	0.487	385
mdf	15	6.2	2.143	240
Radiata Pine	15	10.3	0.613	321
Rimu	14	9.9	0.857	314
Plywood	13	9.5	0.758	307

Table B14: Results of 20-mm wood from Spearpoint & Quintiere

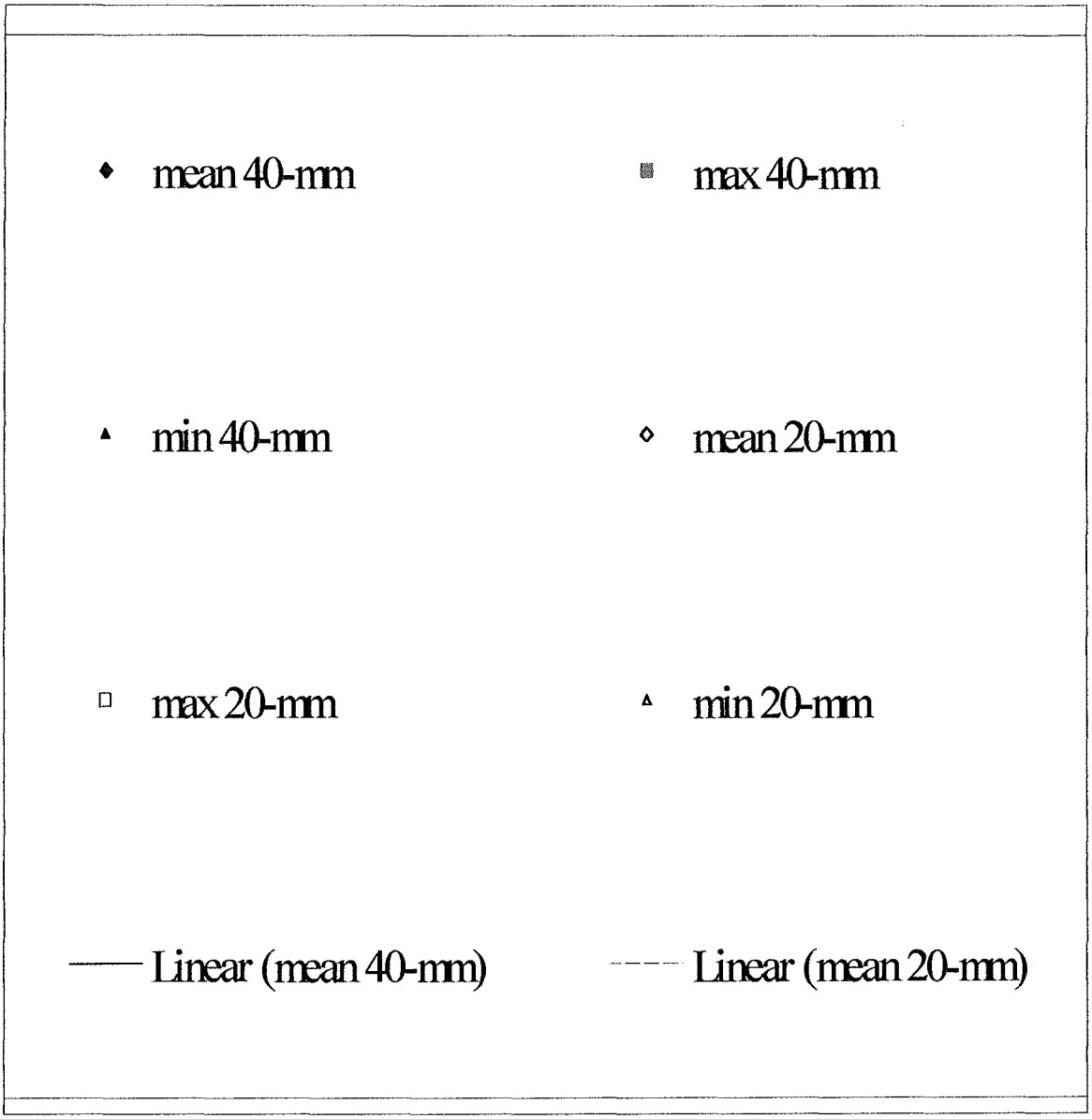

The above is the legend that can be applied to all the following graphs (Appendix C to Appendix H) except for the graphs that have legends with them.

Appendix C: Macrocarpa

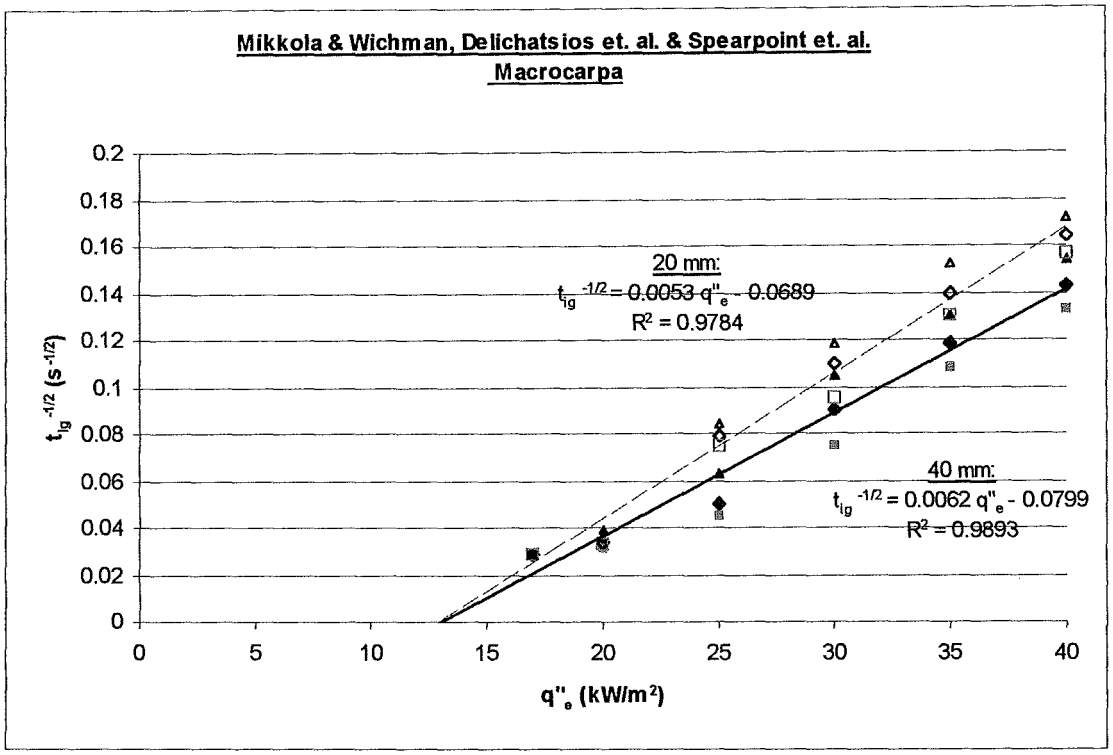

Figure C1: Ignition data of Macrocarpa plotted by Mikkola & Wichman, Delichatsios et. al. and Spearpoint et. al.

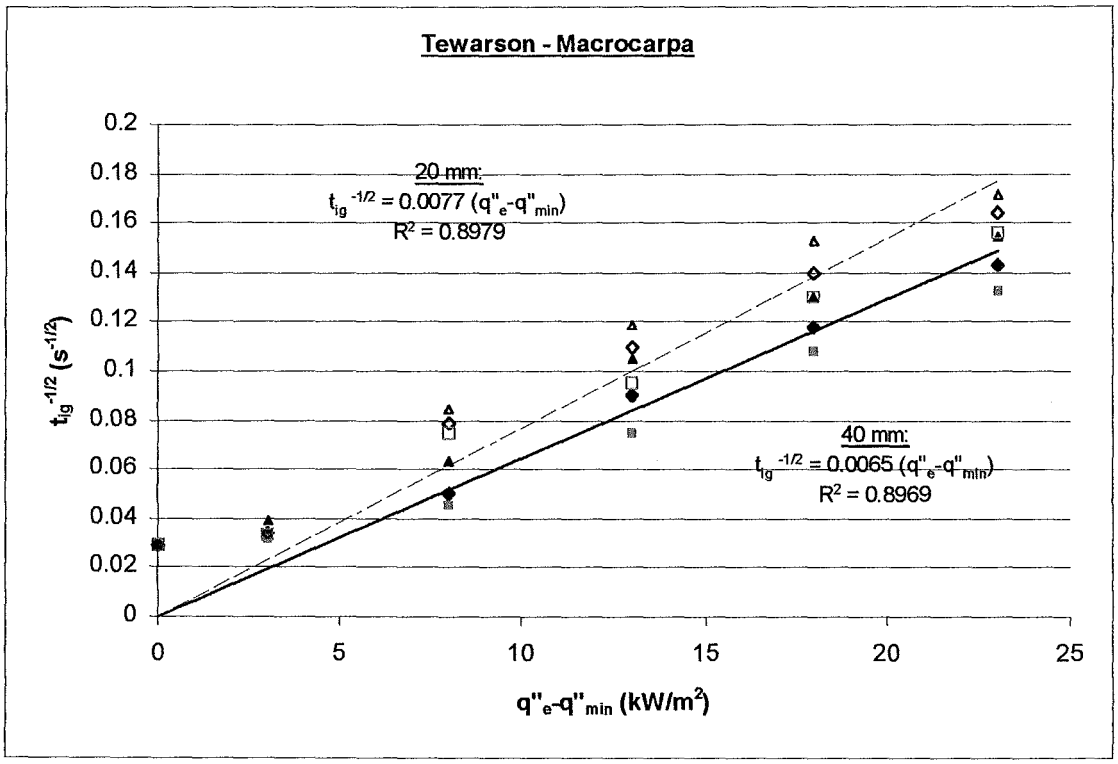

Figure C2: Ignition data of Macrocarpa plotted by Tewarson

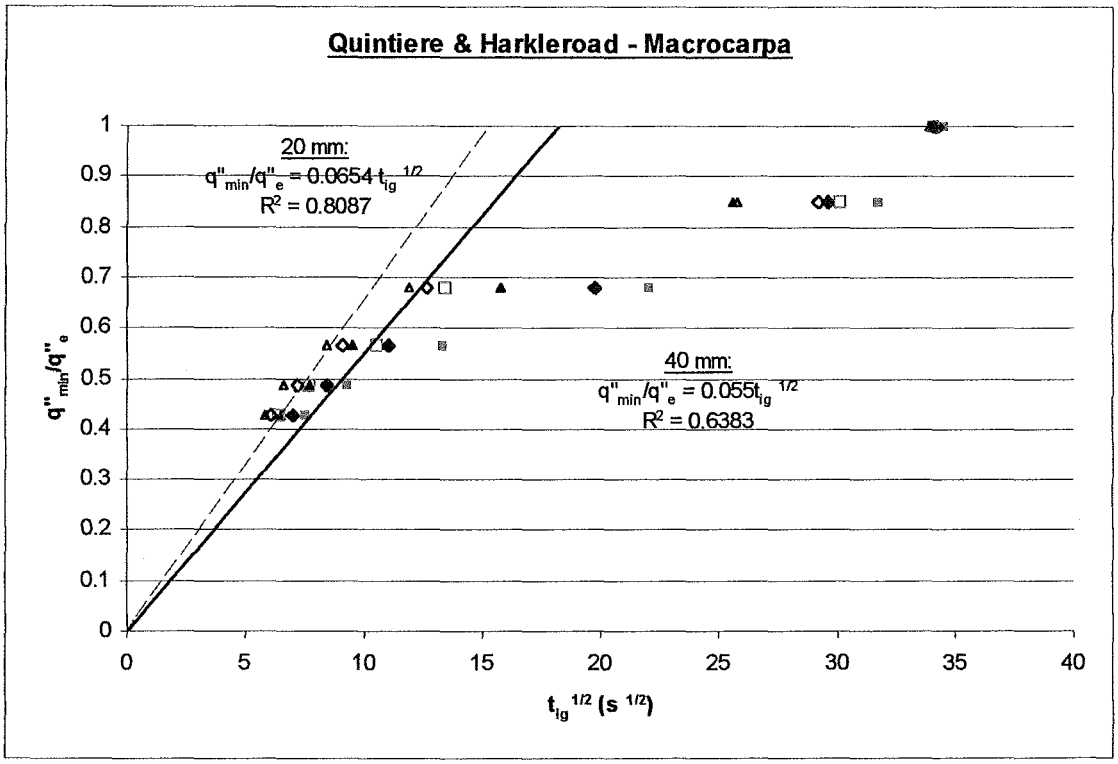

Figure C3: Ignition data of Macrocarpa plotted by Quintere and Harkleroad

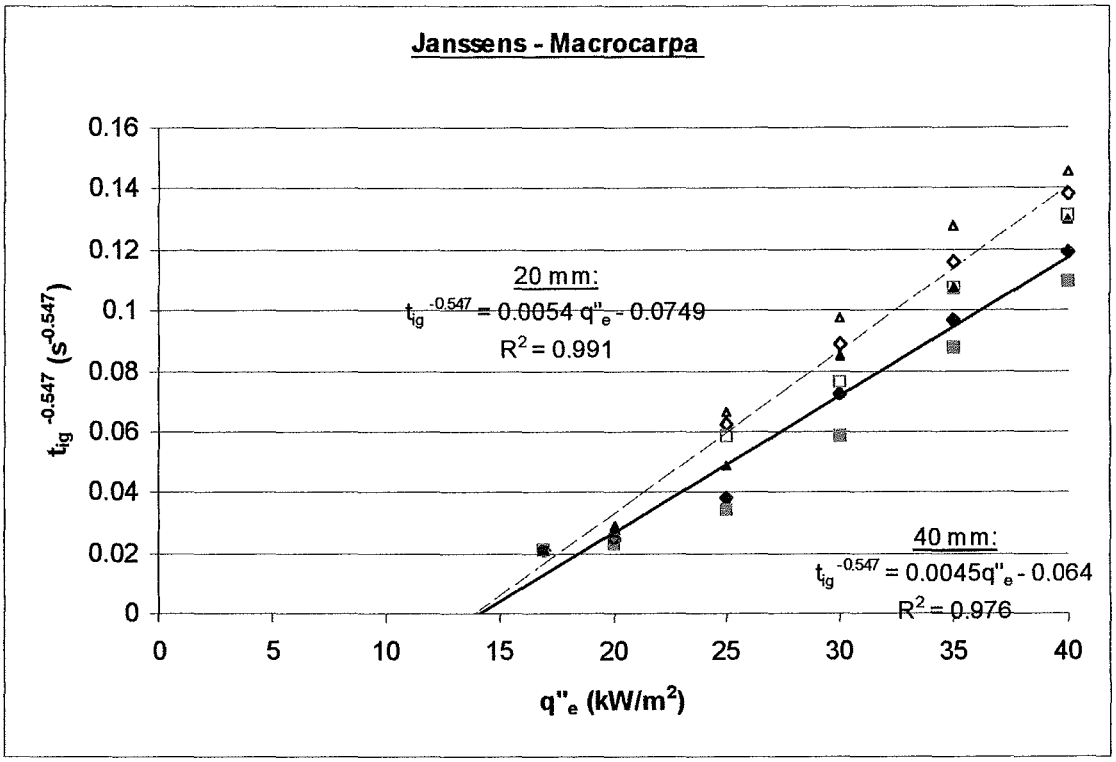

Figure C4: Ignition data of Macrocarpa plotted by Janssens

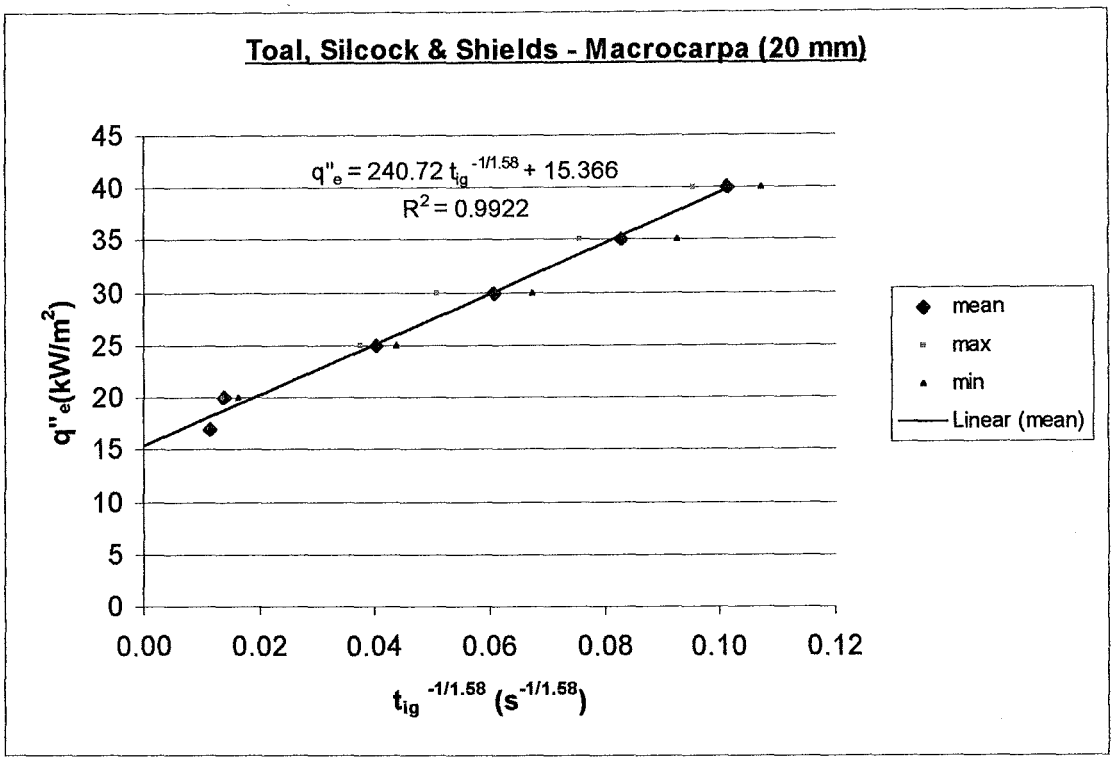

Figure C5: Ignition data of 20-mm Macrocarpa plotted by Toal, Silcock & Shields

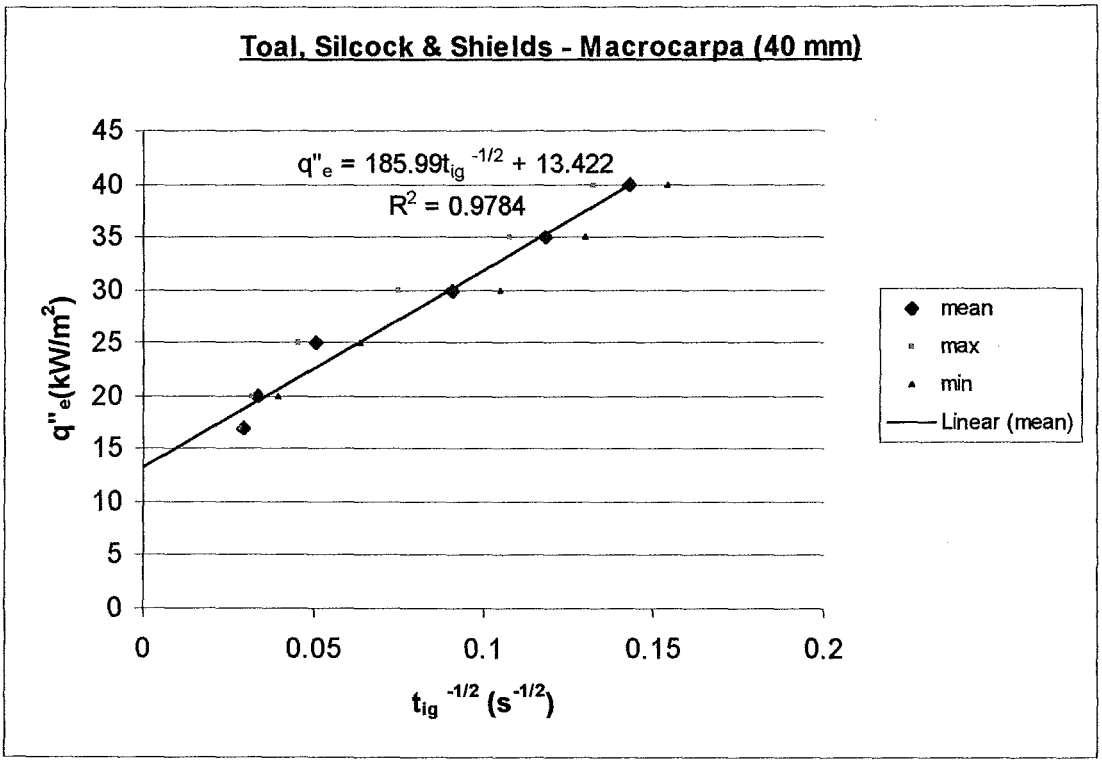

Figure C6: Ignition data of 40-mm Macrocarpa plotted by Toal, Silcock & Shields

Appendix D: Beech

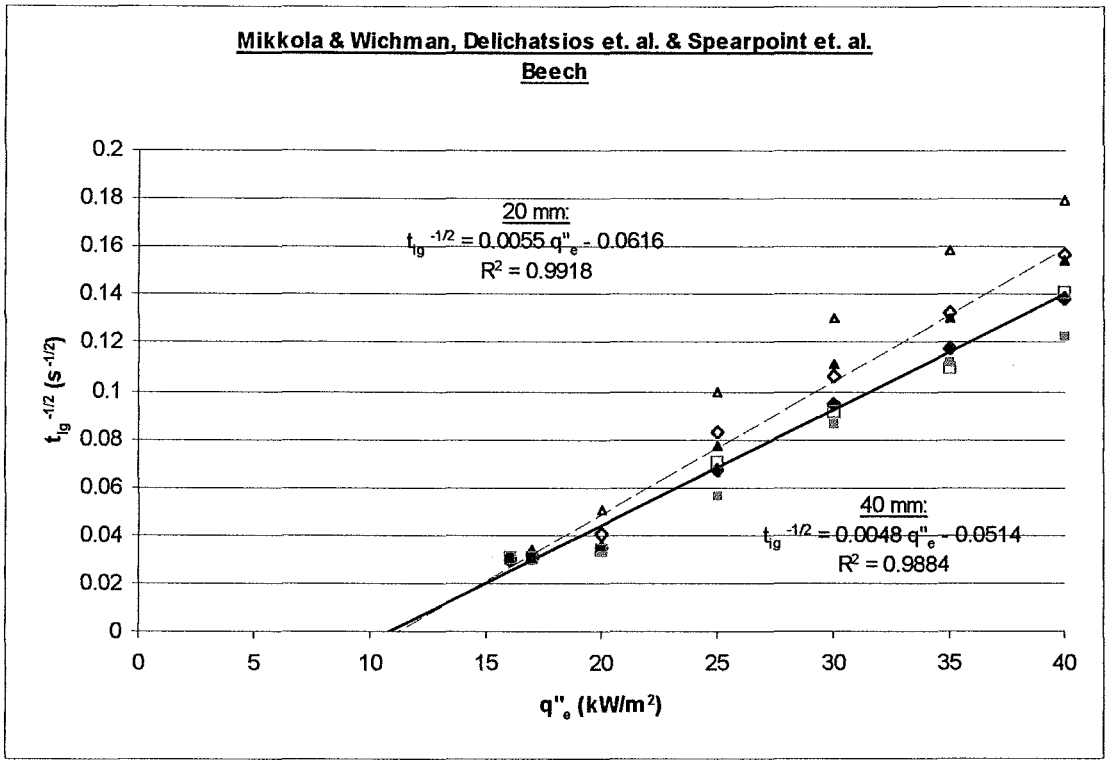

Figure D1: Ignition data of Beech plotted by Mikkola & Wichman, Delichatsios et. al. and Spearpoint et. al.

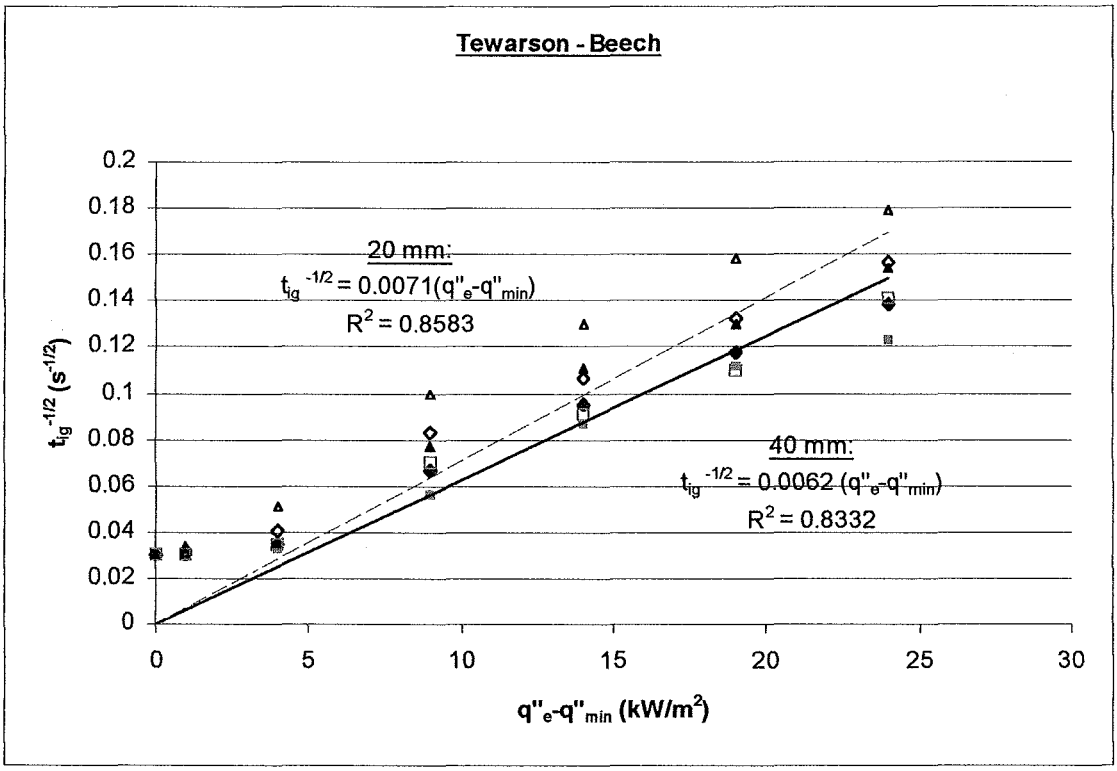

Figure D2: Ignition data of Beech plotted by Tewarson

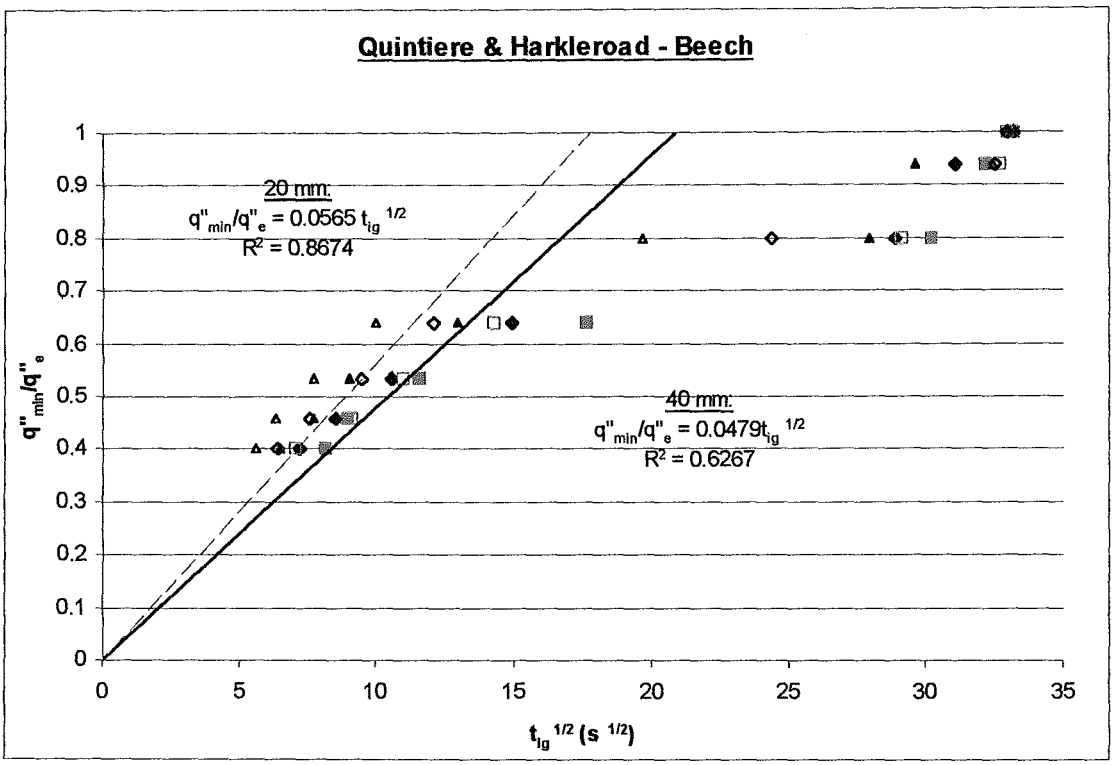

Figure D3: Ignition data of Beech plotted by Quintiere and Harkleroad

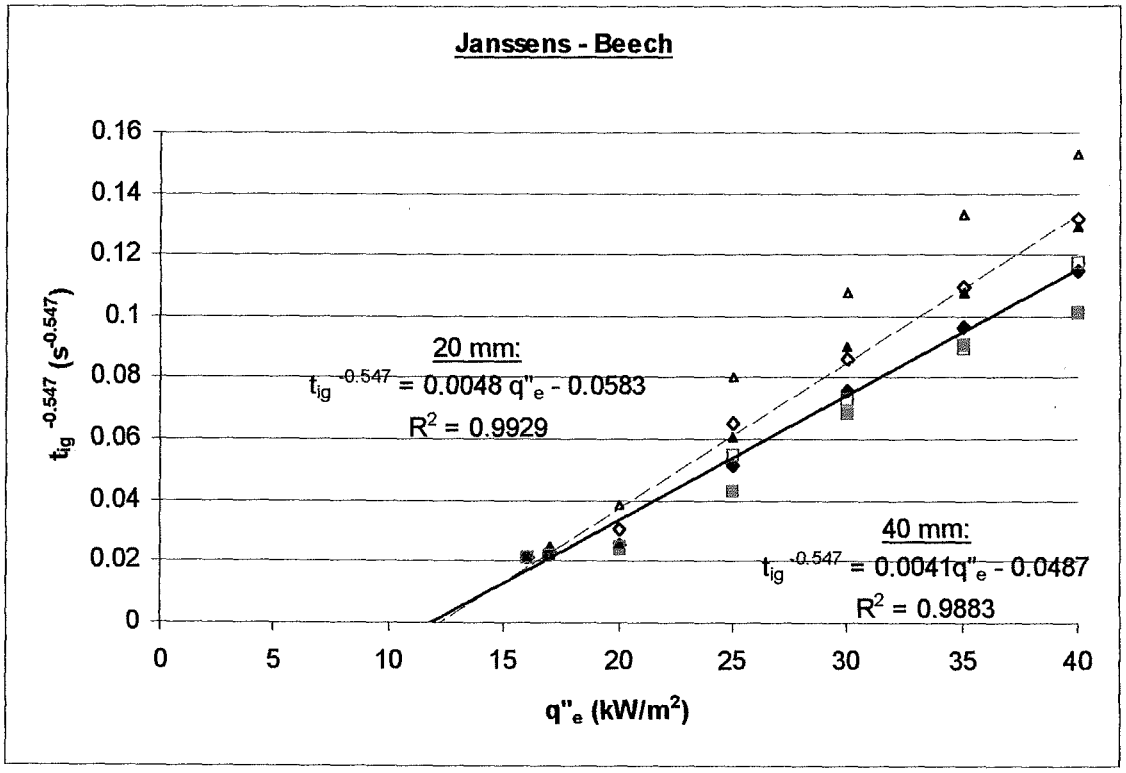

Figure D4: Ignition data of Beech plotted by Janssens

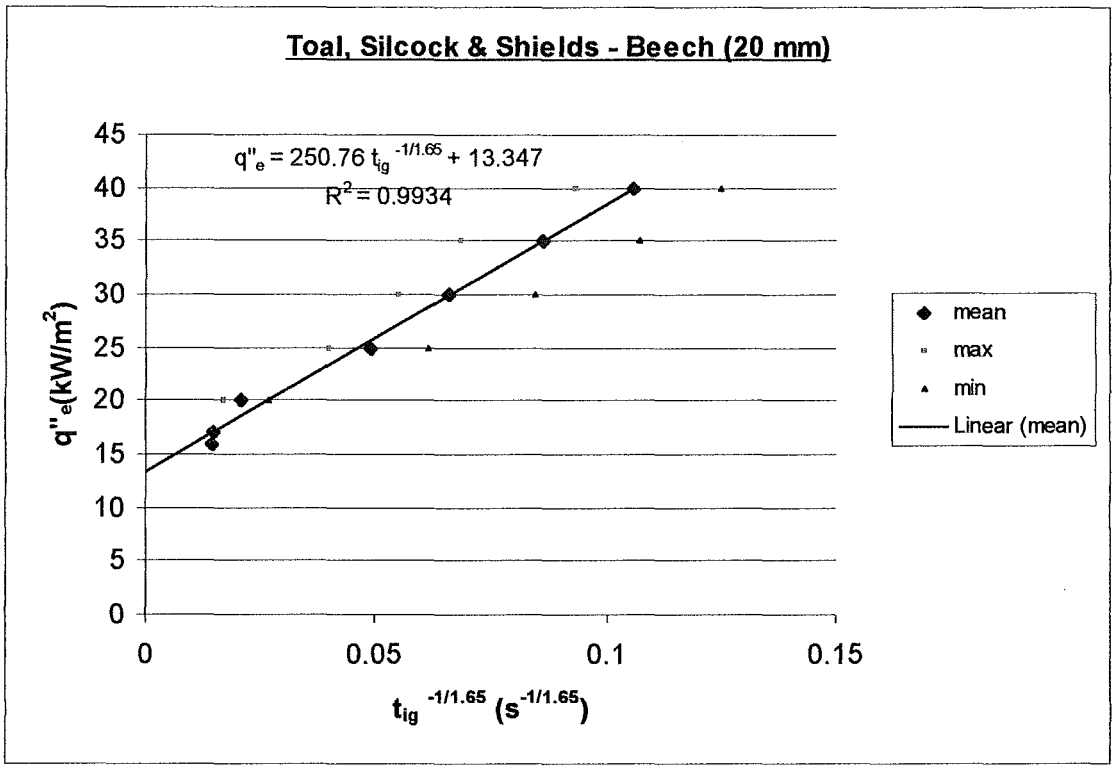

Figure D5: Ignition data of 20-mm Beech plotted by Toal, Silcock and Shields

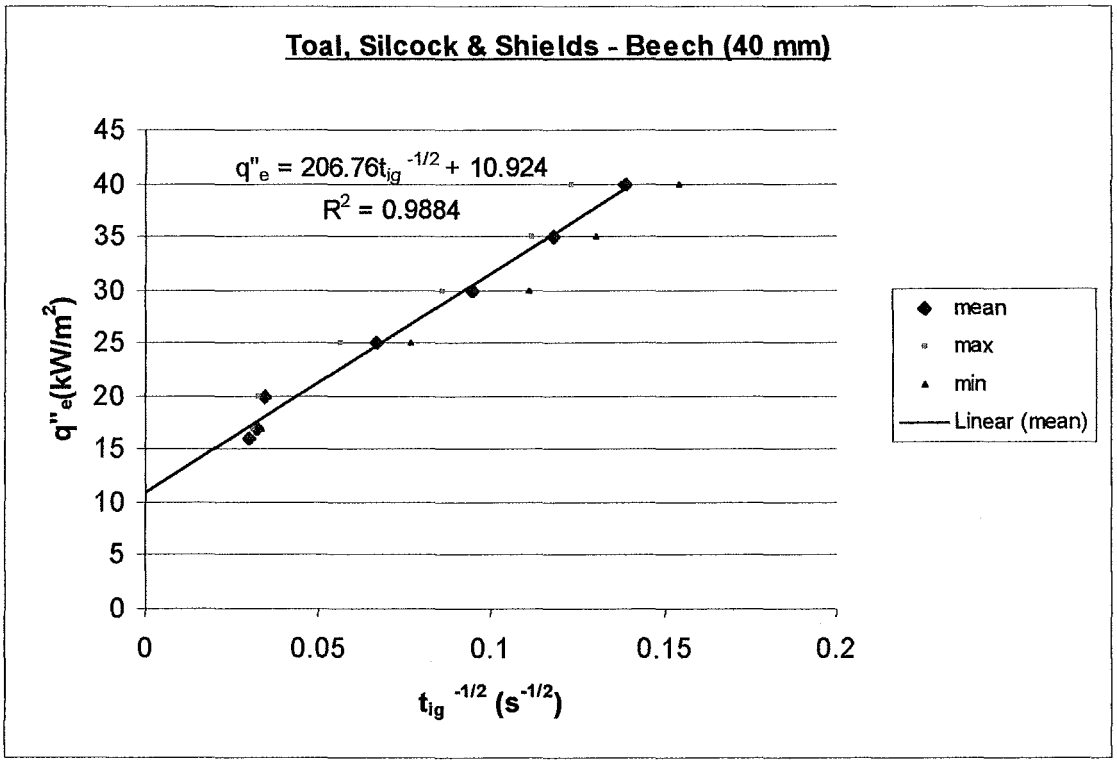

Figure D6: Ignition data of 40-mm Beech plotted by Toal, Silcock and Shields

Appendix E: Medium density fibreboard (mdf)

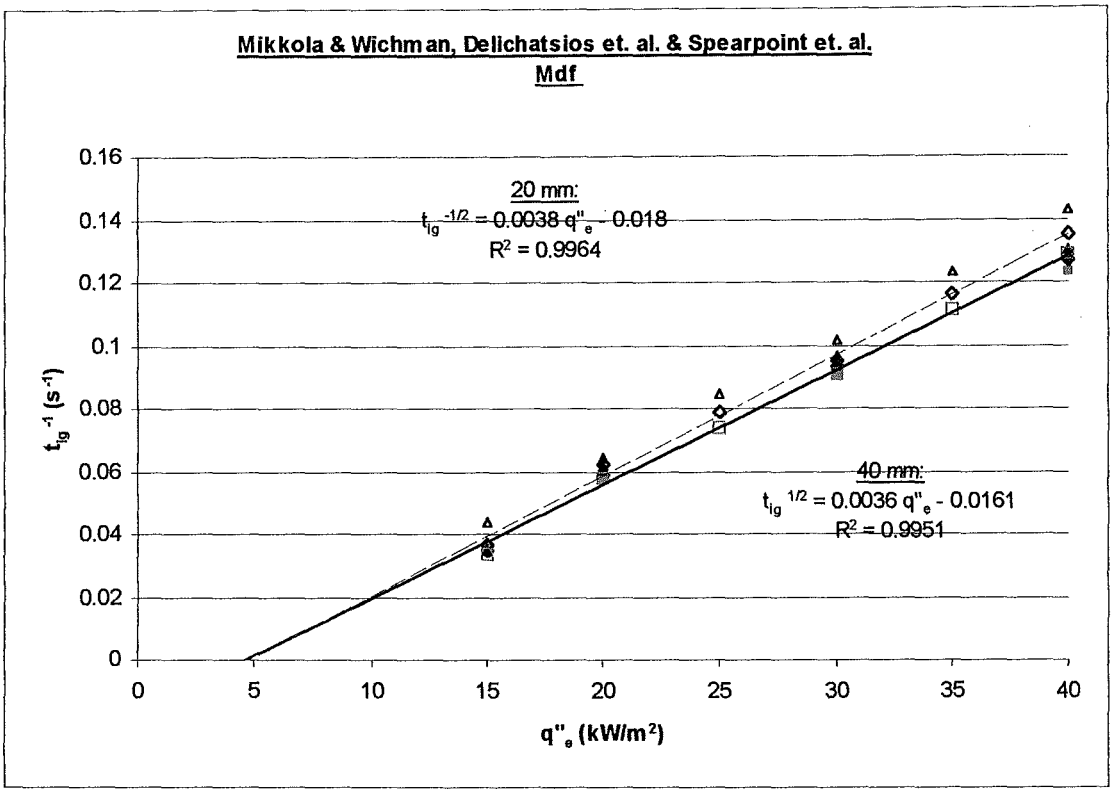

Figure E1: Ignition data of mdf plotted by Mikkola & Wichman, Delichatsios et. al. and Spearpoint et. al.

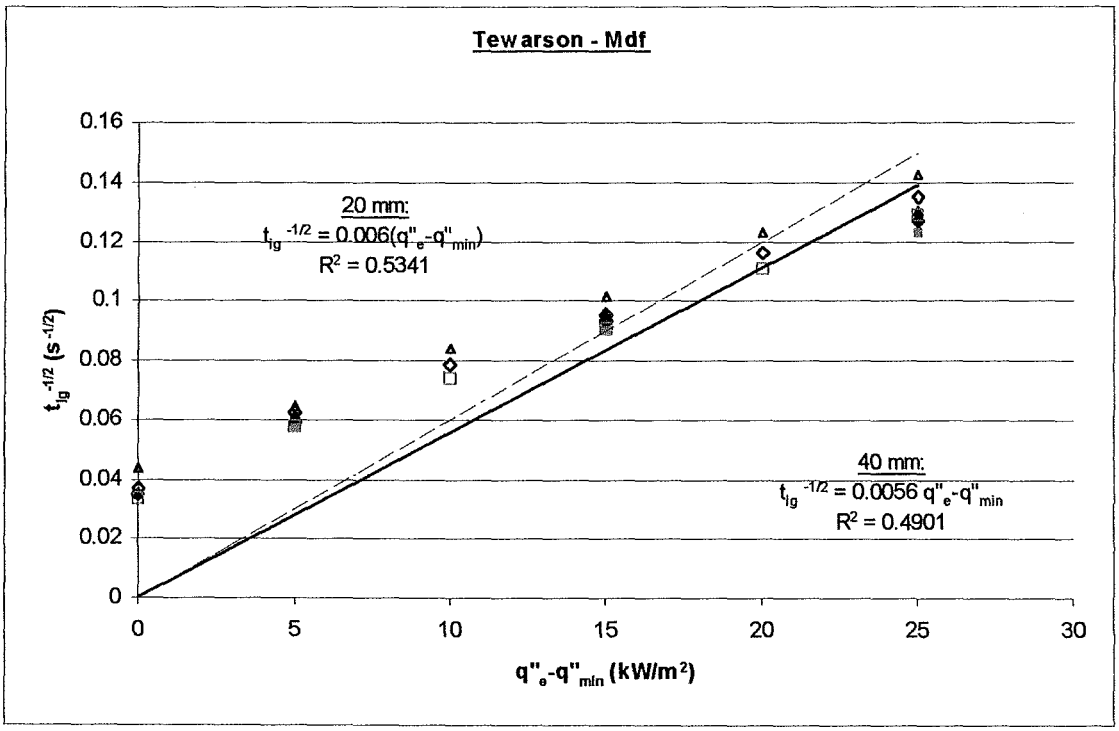

Figure E2: Ignition data of mdf plotted by Tewarson

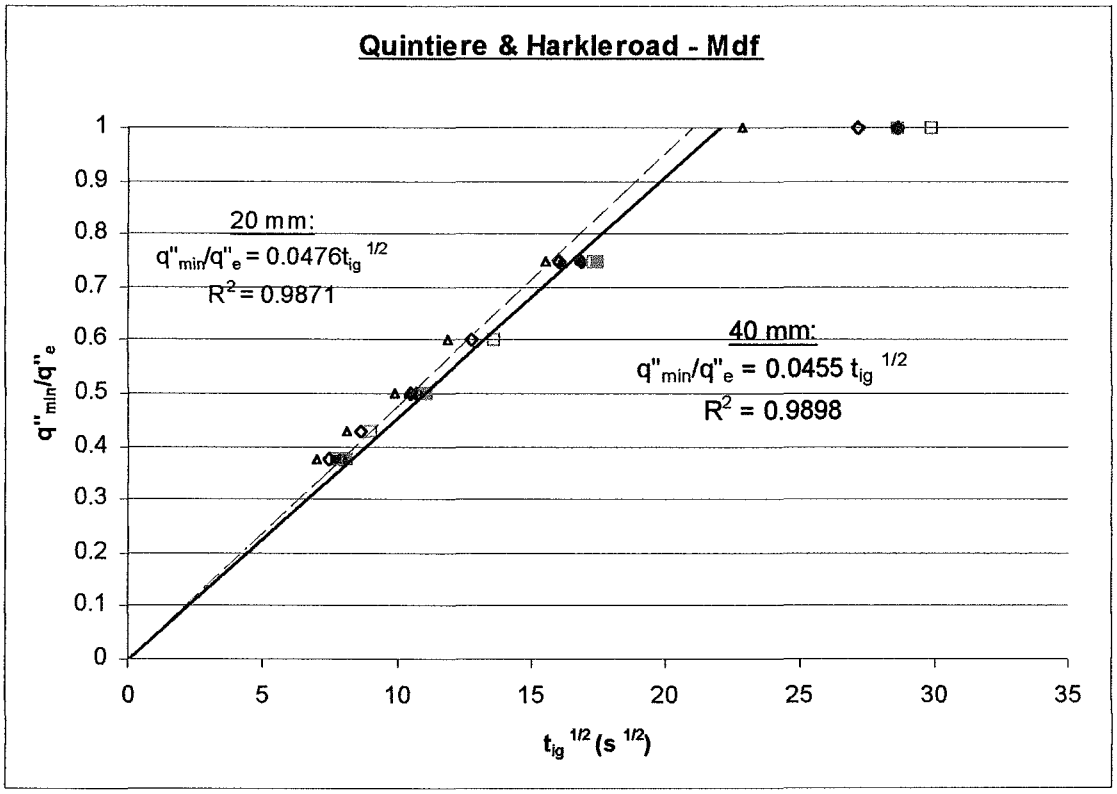

Figure E3: Ignition data of mdf plotted by Quintiere and Harkleroad

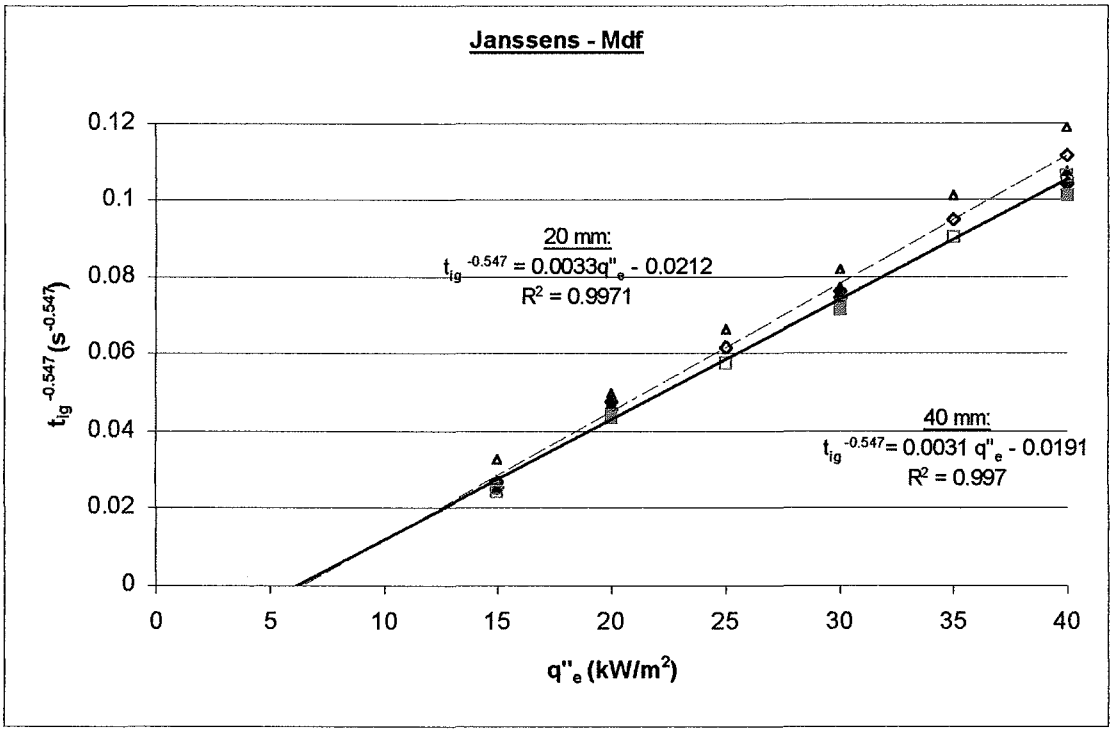

Figure E4: Ignition data of mdf plotted by Janssens

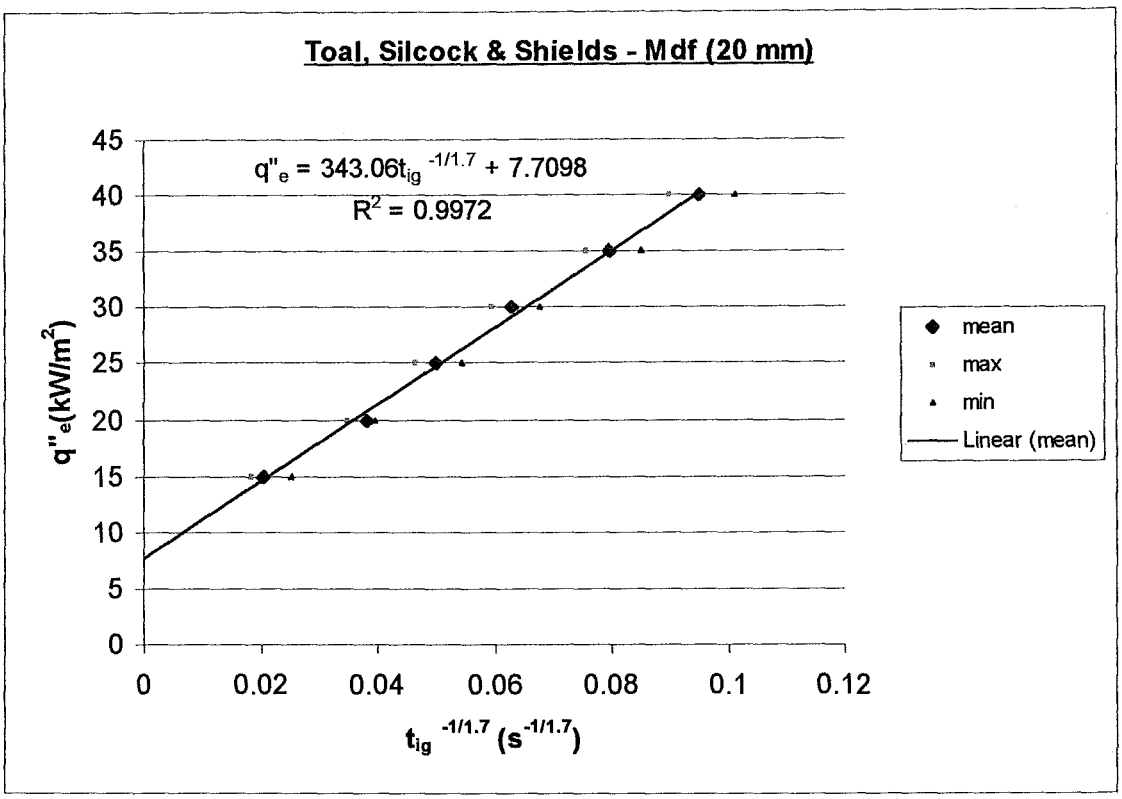

Figure E5: Ignition data of 20-mm mdf plotted by Toal, Silcock and Shields

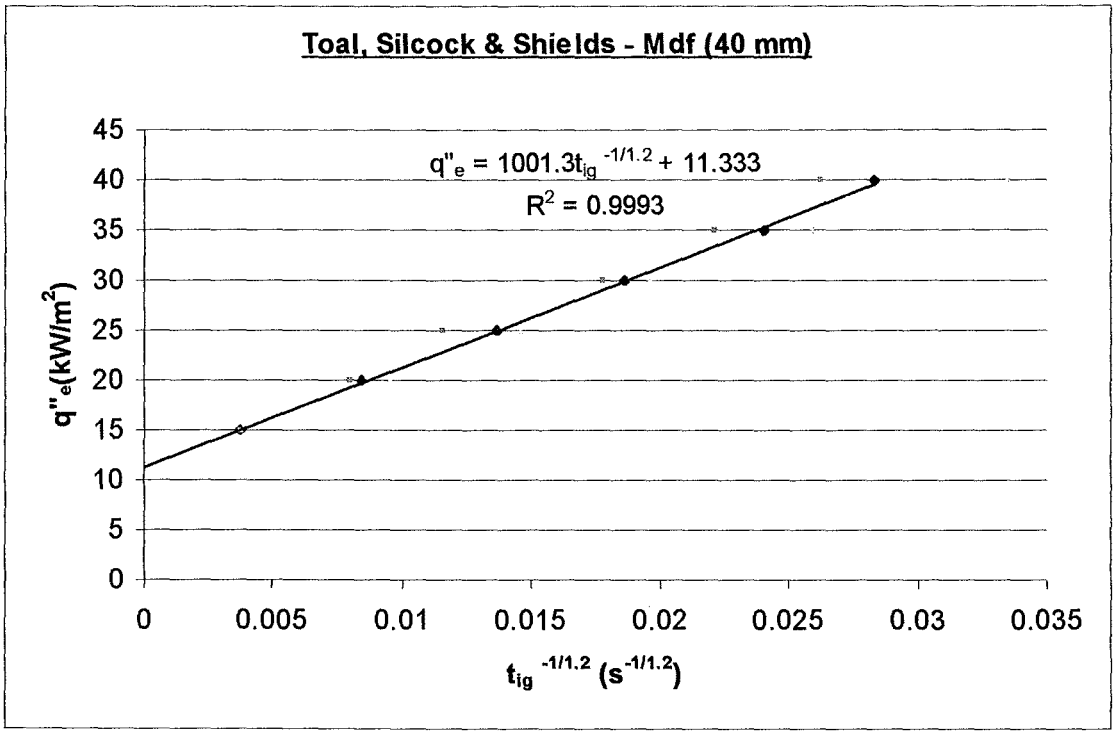

Figure E6: 40-mm mdf plotted by Toal, Silcock and Shields, earlier done based on calibration scale on 5/12/2000

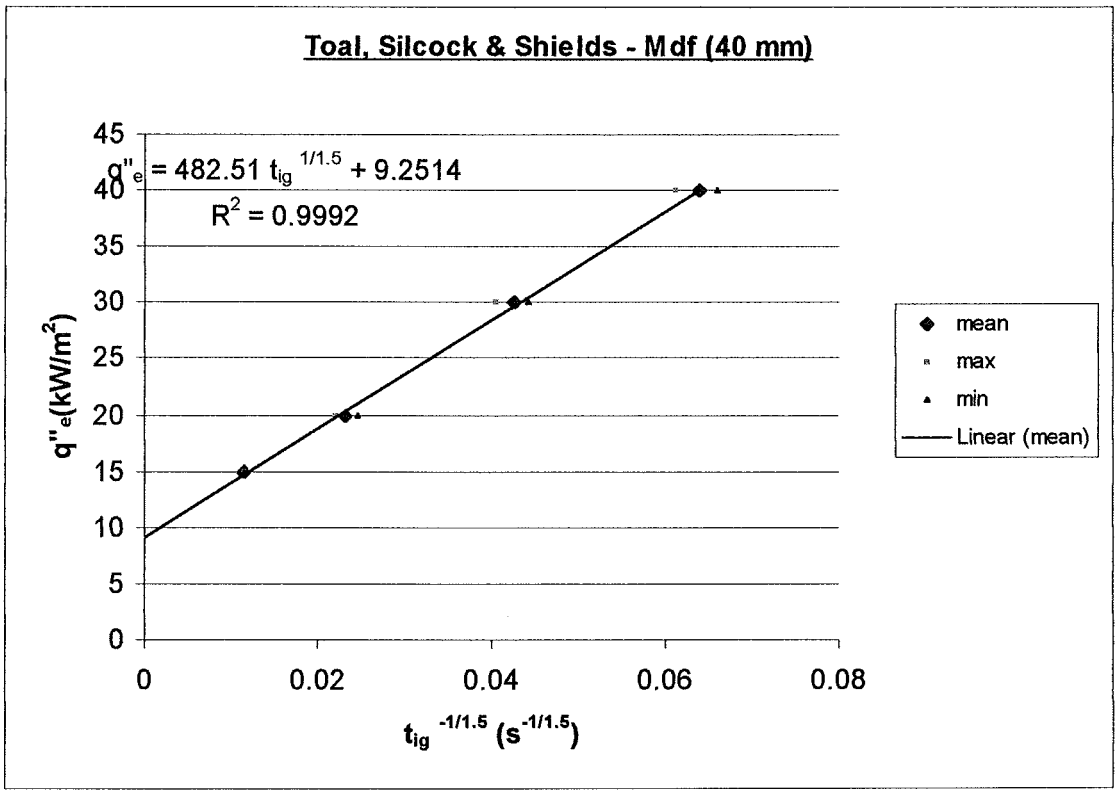

Figure E7: 40-mm mdf plotted by Toal, Silcock and Shields, redone based on calibration scale on 20/12/2000

Appendix F: Radiata Pine

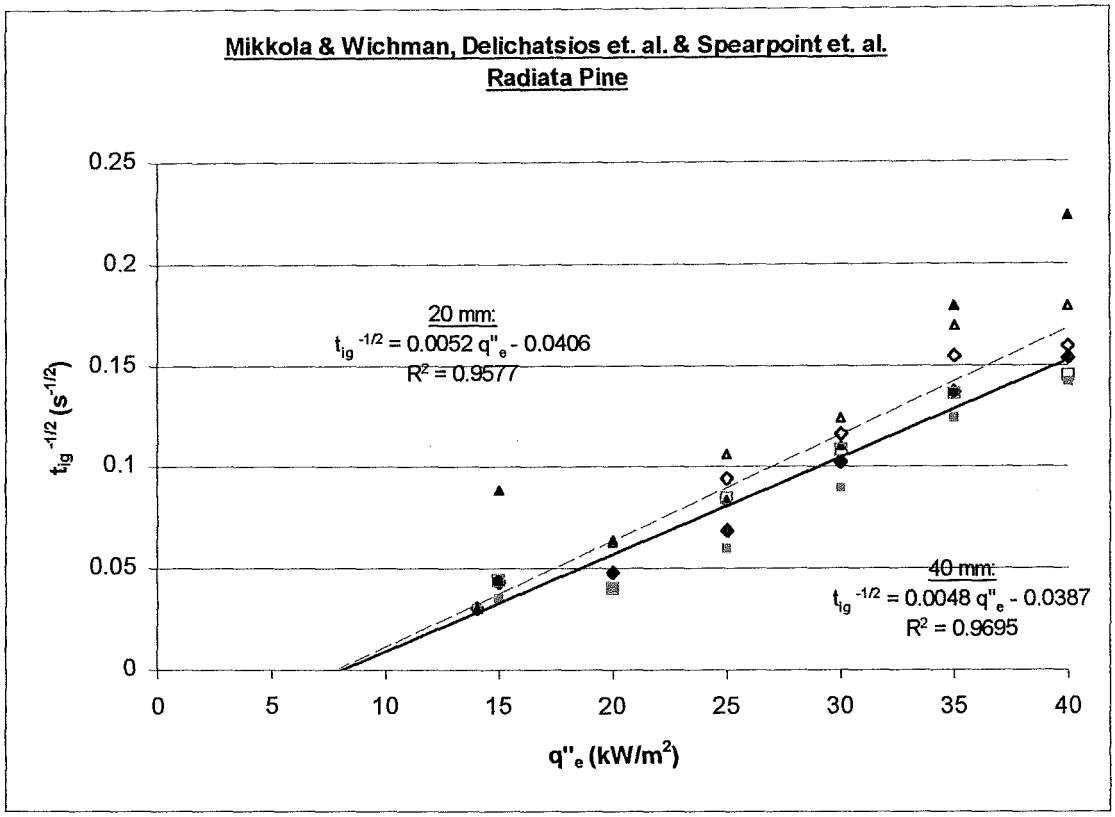

Figure F1: Ignition data of Radiata Pine plotted by Mikkola et. al., Delichatsios et. al. & Spearpoint

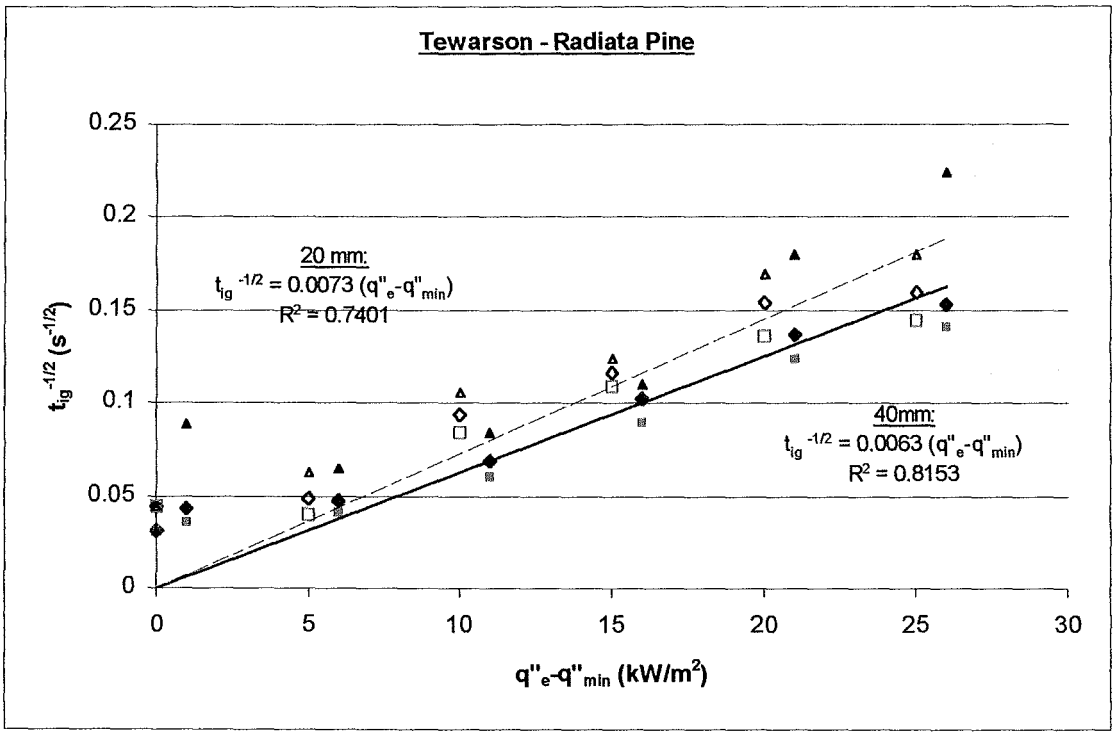

Figure F2: Ignition data of Radiata Pine plotted by Tewarson

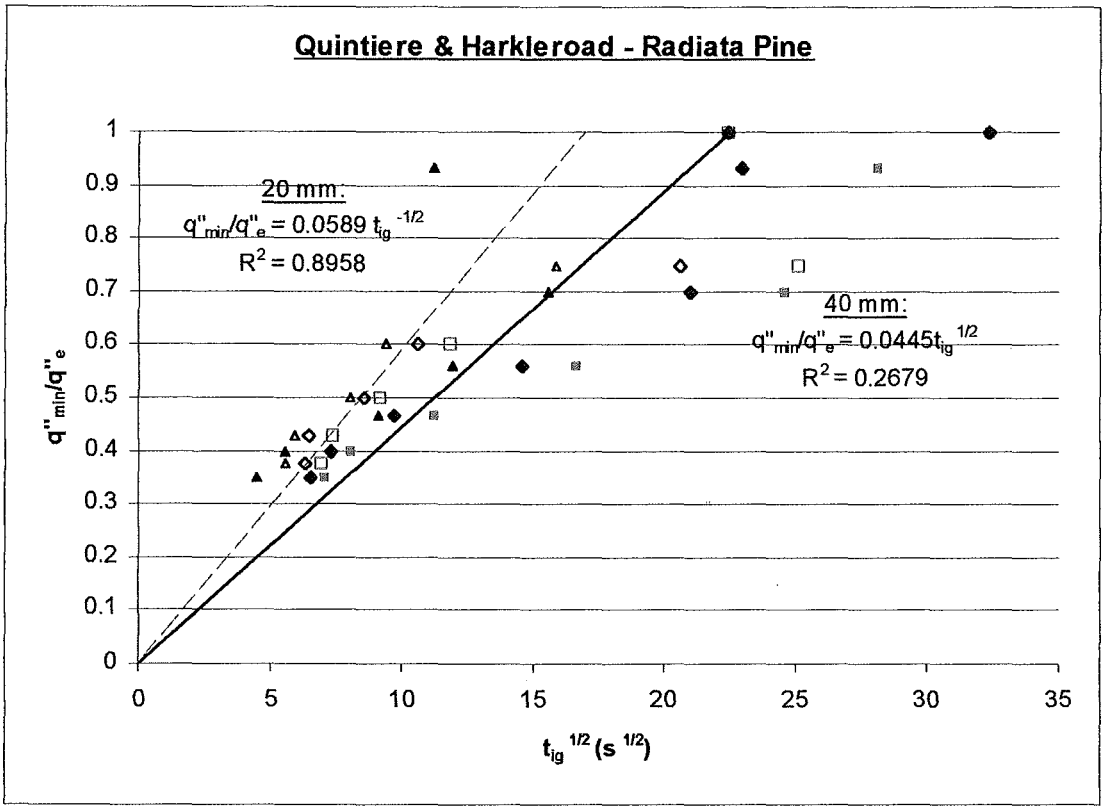

Figure F3: Ignition data of Radiata Pine plotted by Quintiere and Harkleroad

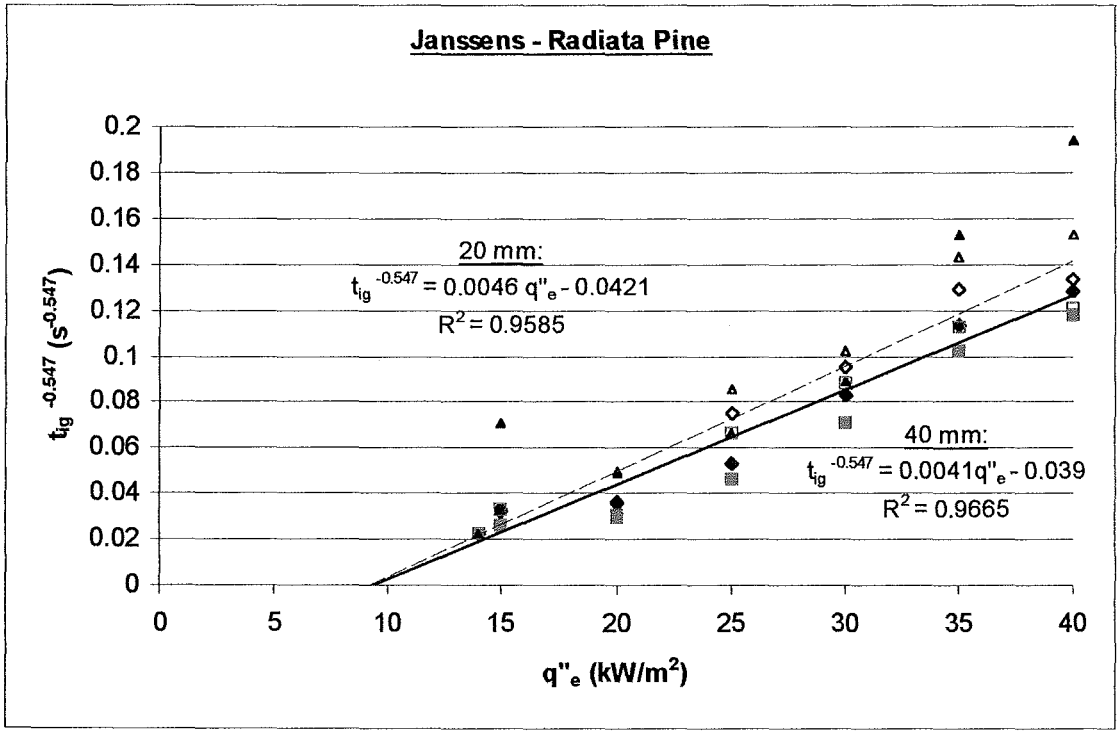

Figure F4: Ignition data of Radiata Pine plotted by Janssens

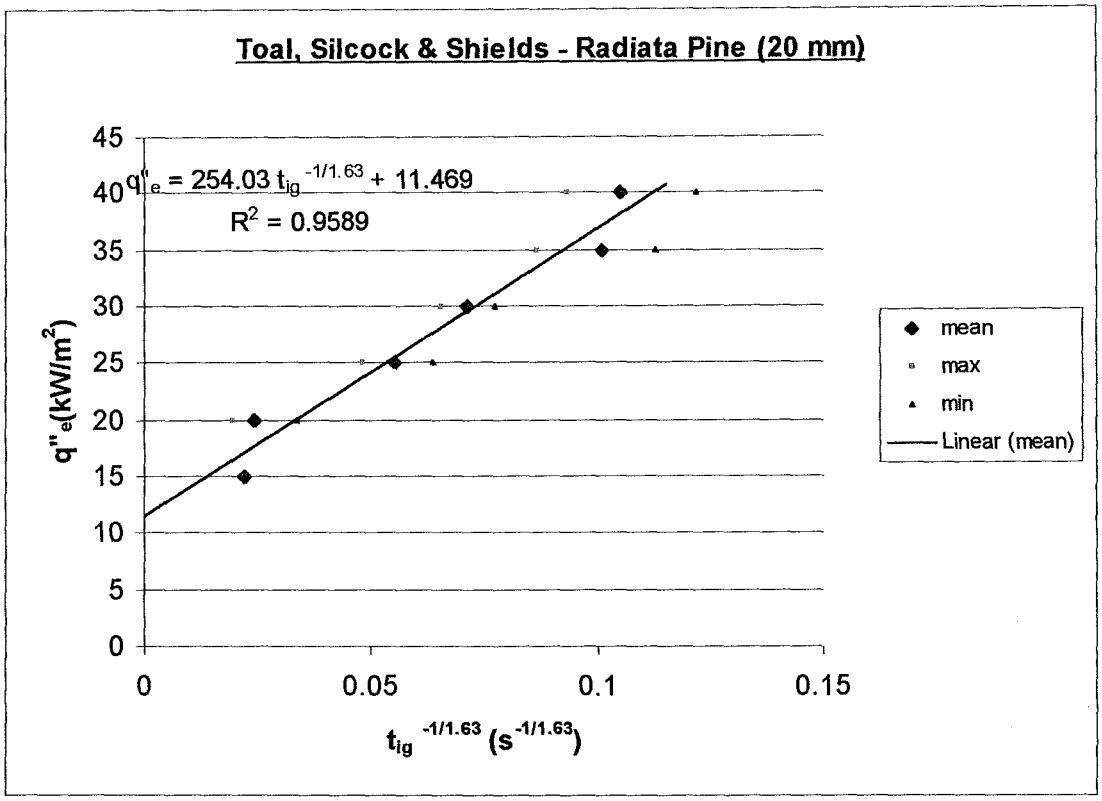

Figure F5: Ignition data of 20-mm Radiata Pine plotted by Toal, Silcock and Shields

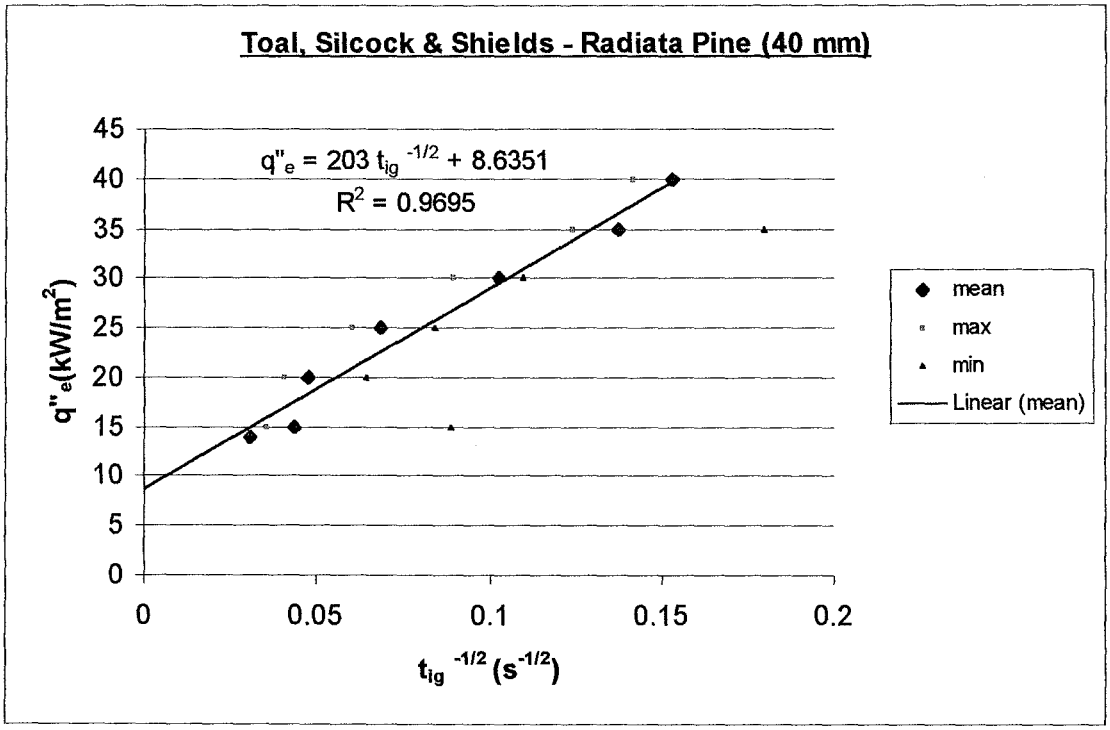

Figure F6: Ignition data of 40-mm Radiata Pine plotted by Toal, Silcock and Shields

Appendix G: Rimu

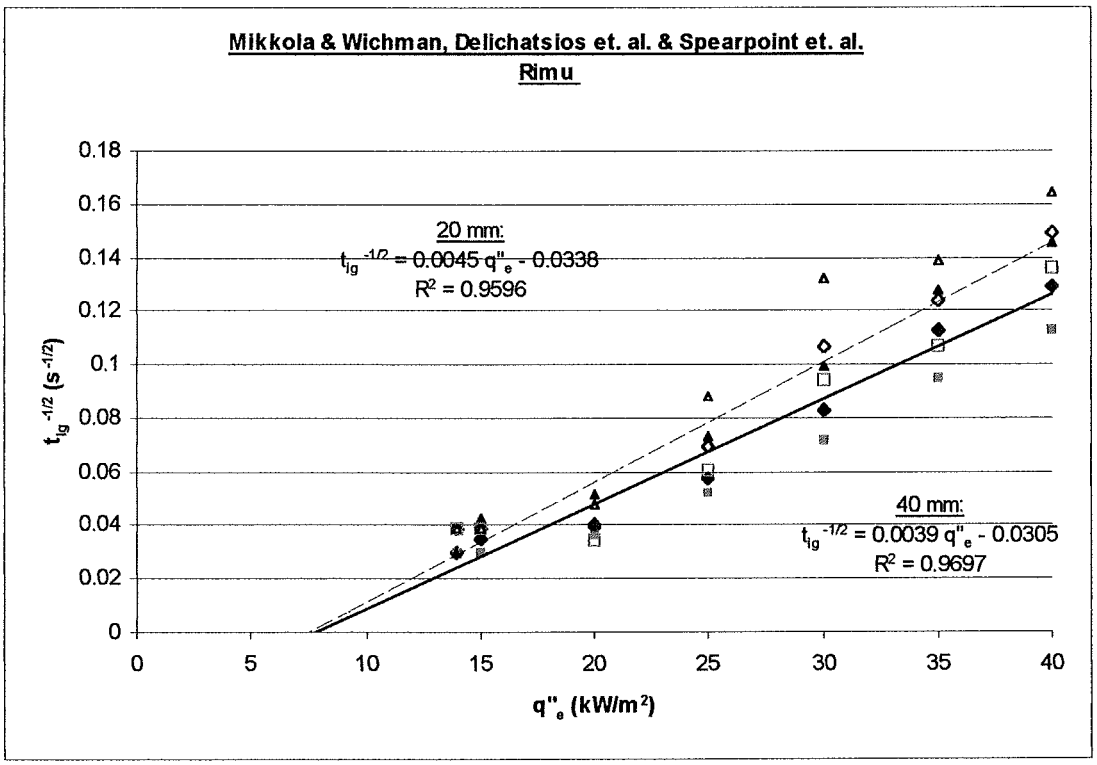

Figure G1: Ignition data of Rimu plotted by Mikkola & Wichman, Delichatsios et. al. and Spearpoint et. al.

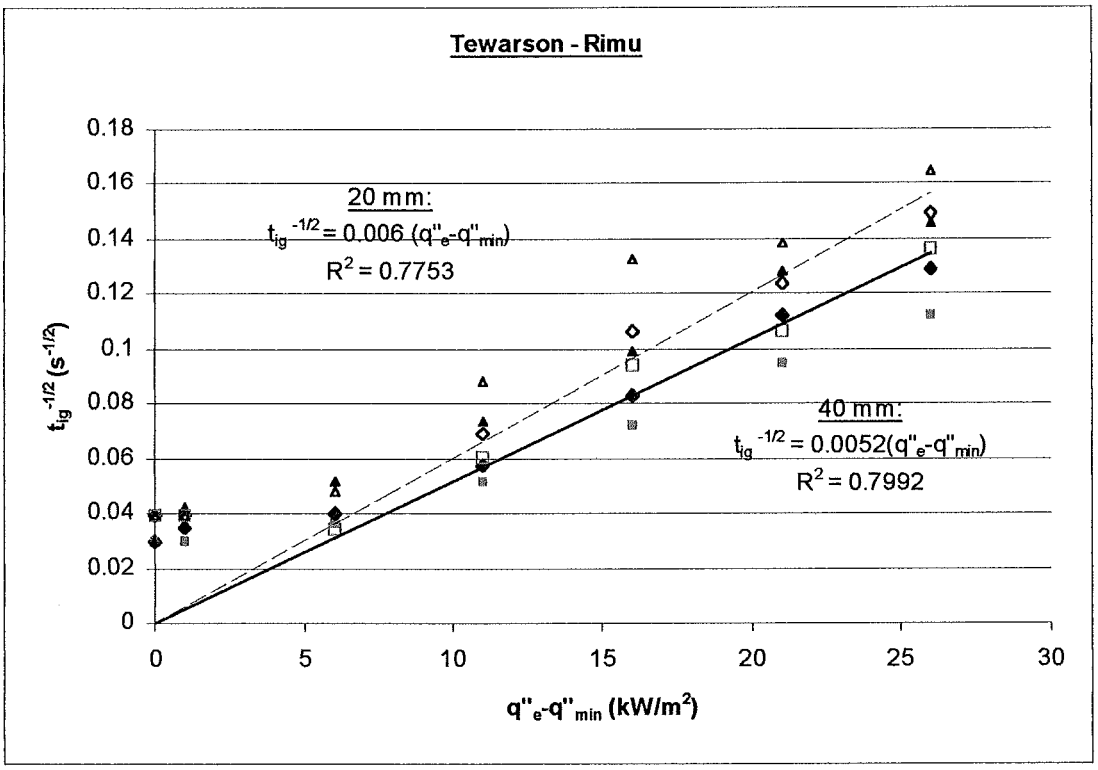

Figure G2: Ignition data of Rimu plotted by Tewarson

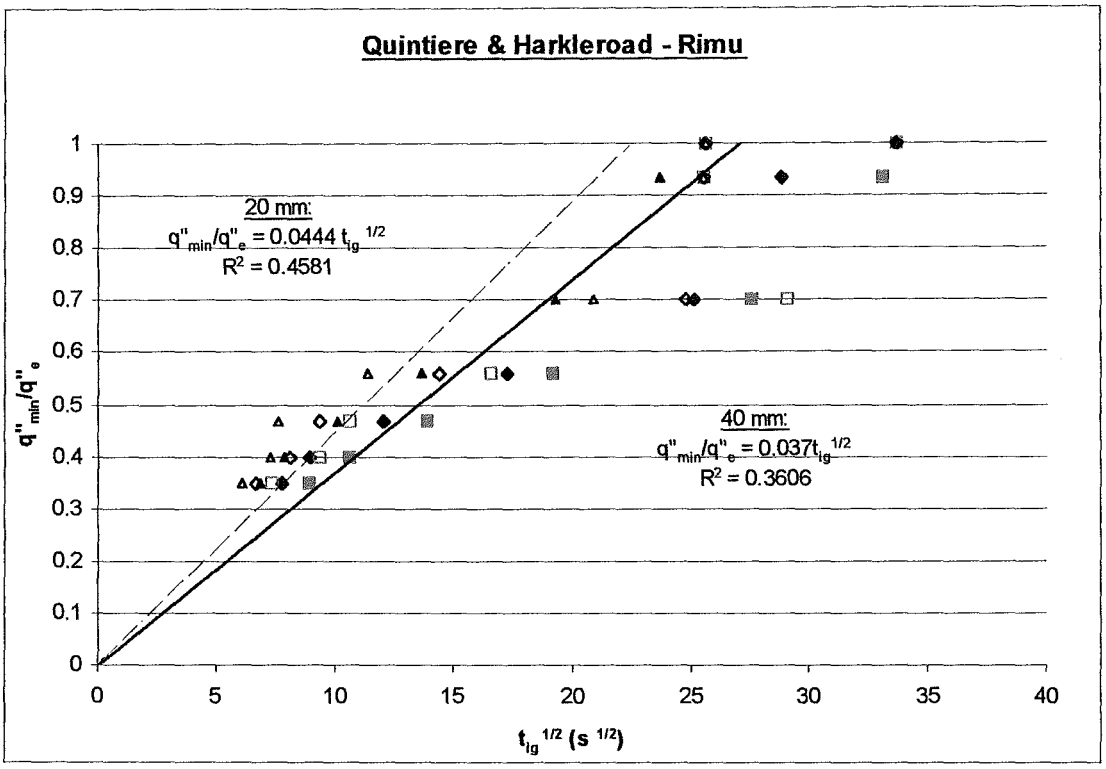

Figure G3: Ignition data of Rimu plotted by Quintiere and Harkleroad

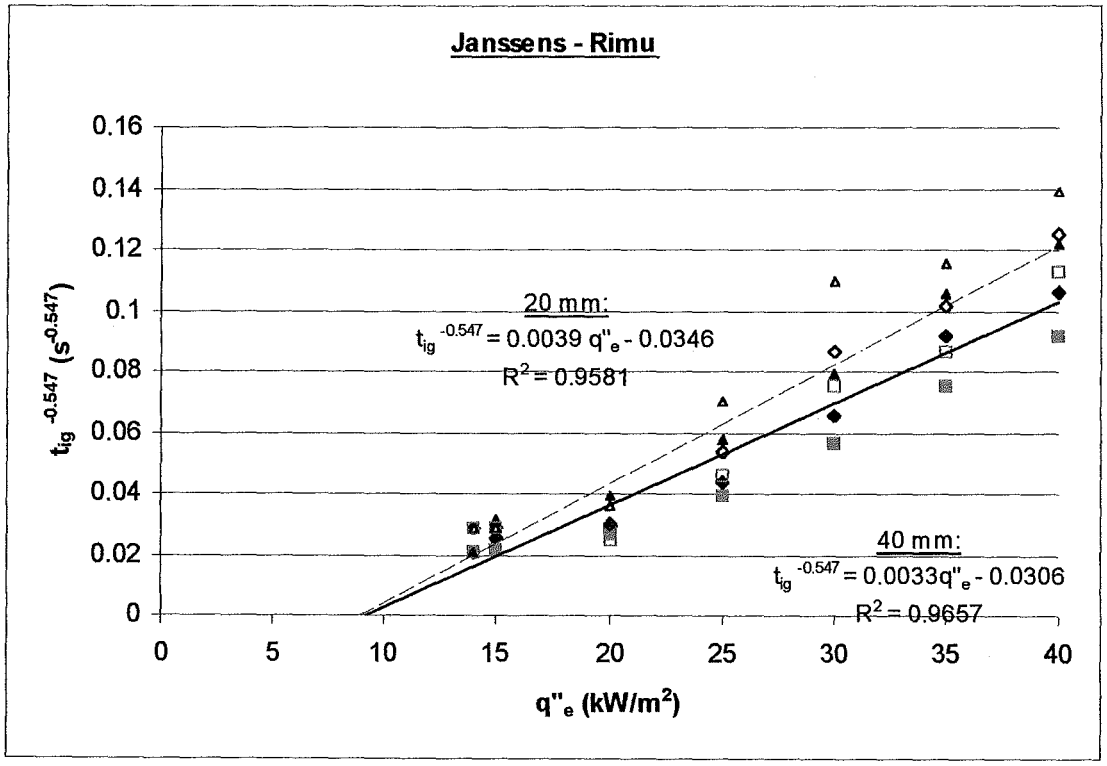

Figure G4: Ignition data of Rimu plotted by Janssens

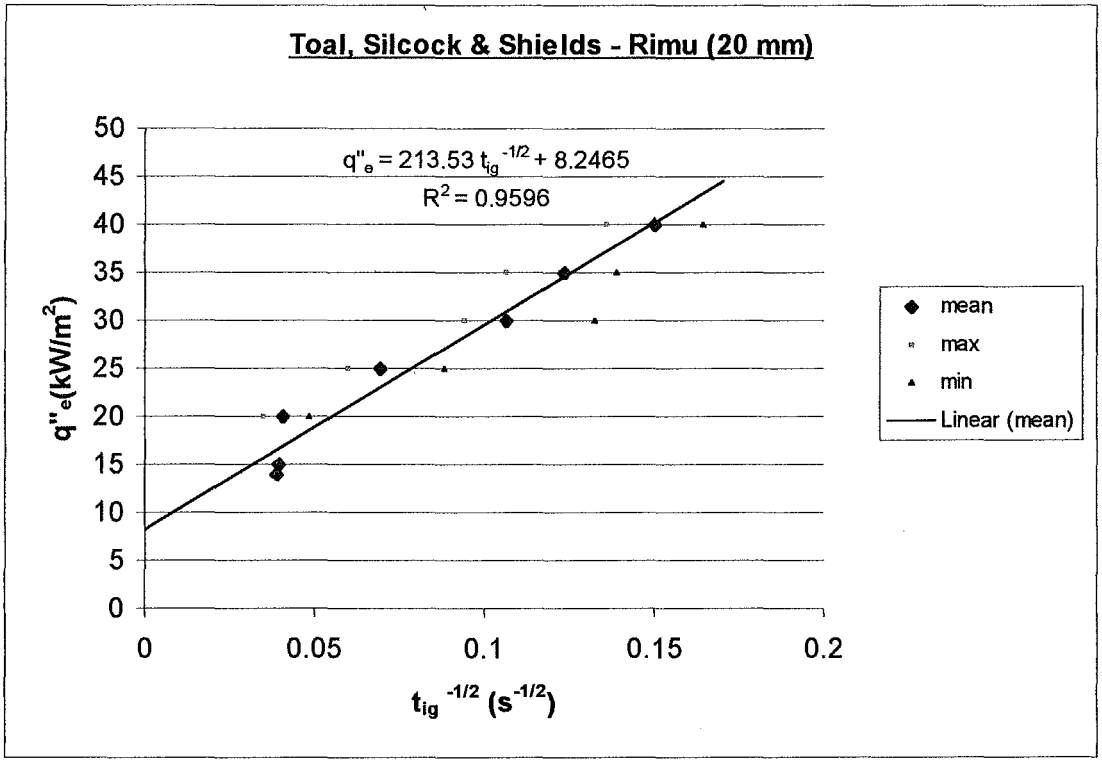

Figure G5: Ignition data of 20-mm Rimu plotted by Toal, Silcock and Shields

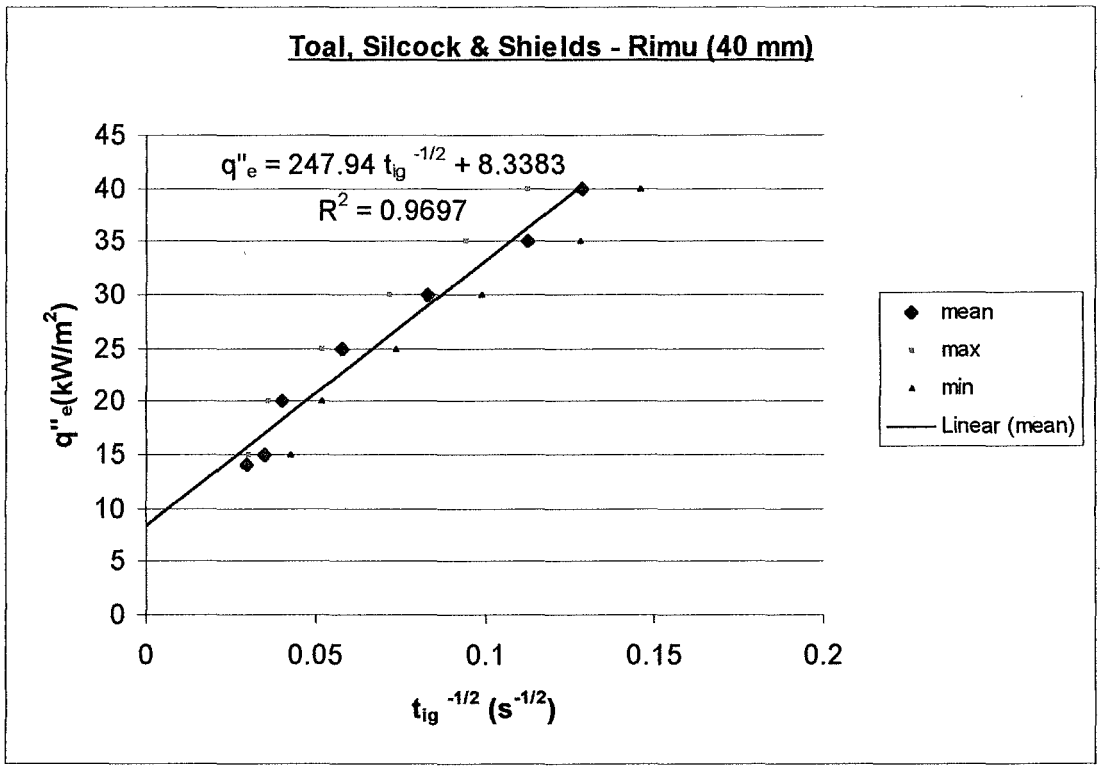

Figure G6 : Ignition data of 20-mm Rimu plotted by Toal, Silcock and Shields

Appendix H: Plywood

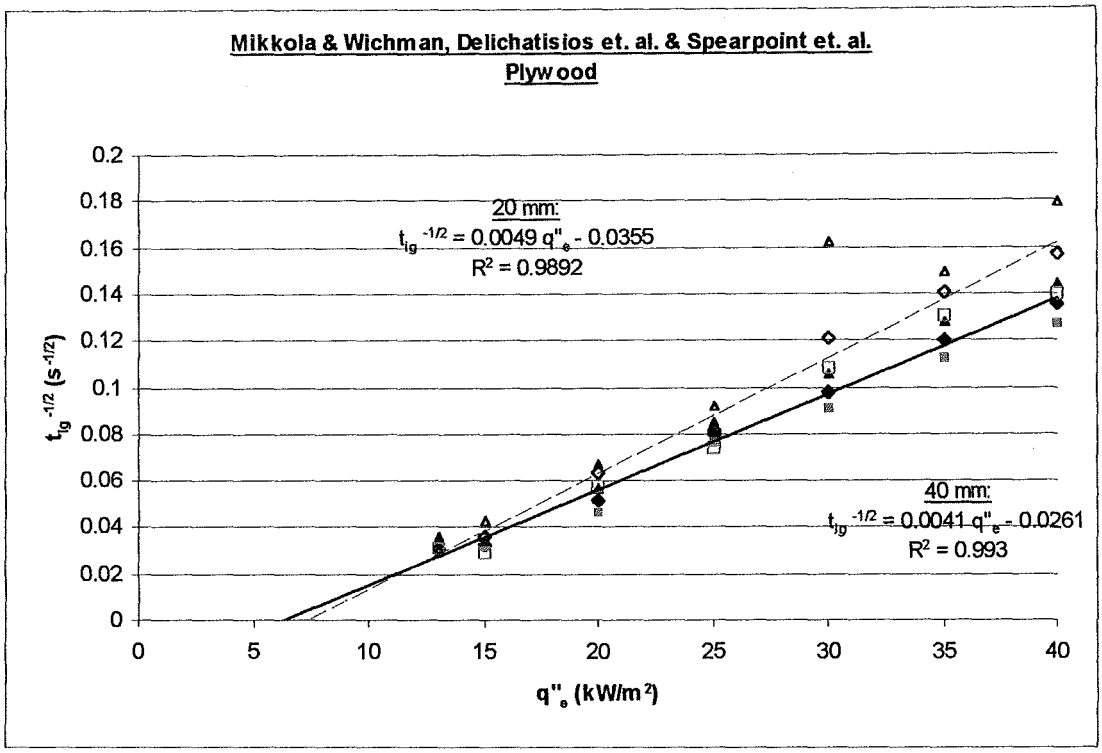

Figure H1: Ignition data of Plywood plotted by Mikkola & Wichman, Delichatsios et. al. and Spearpoint et. al.

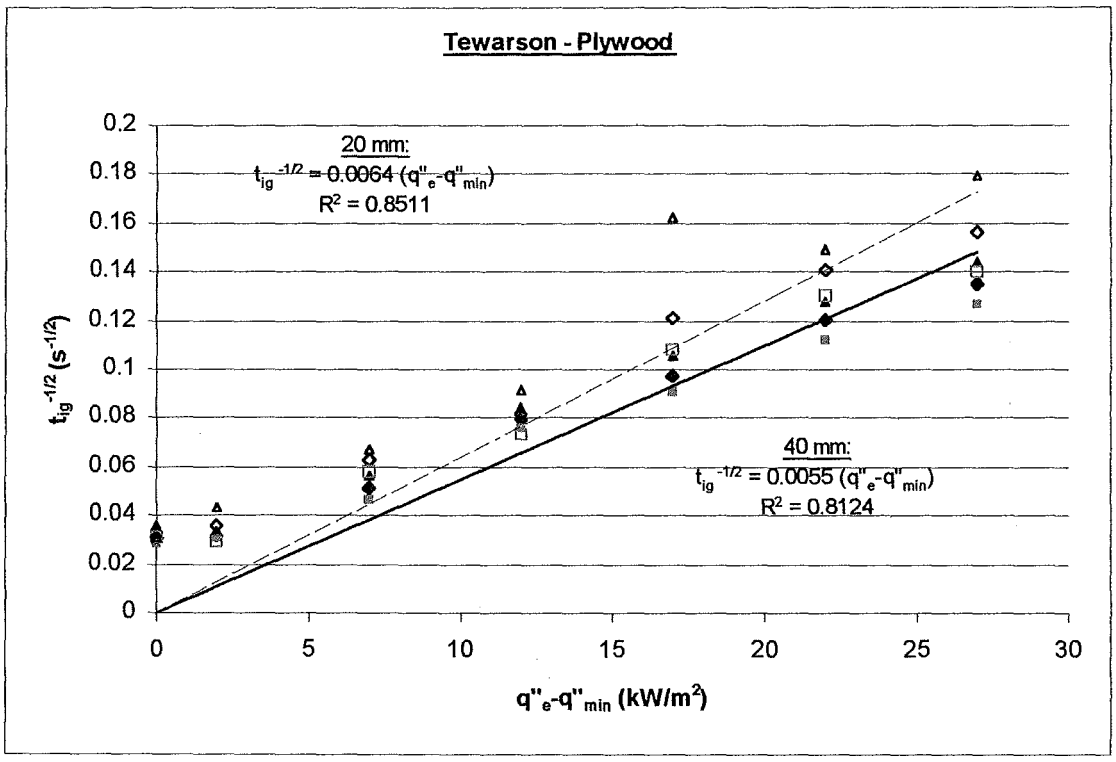

Figure H2: Ignition data of Plywood plotted by Tewarson

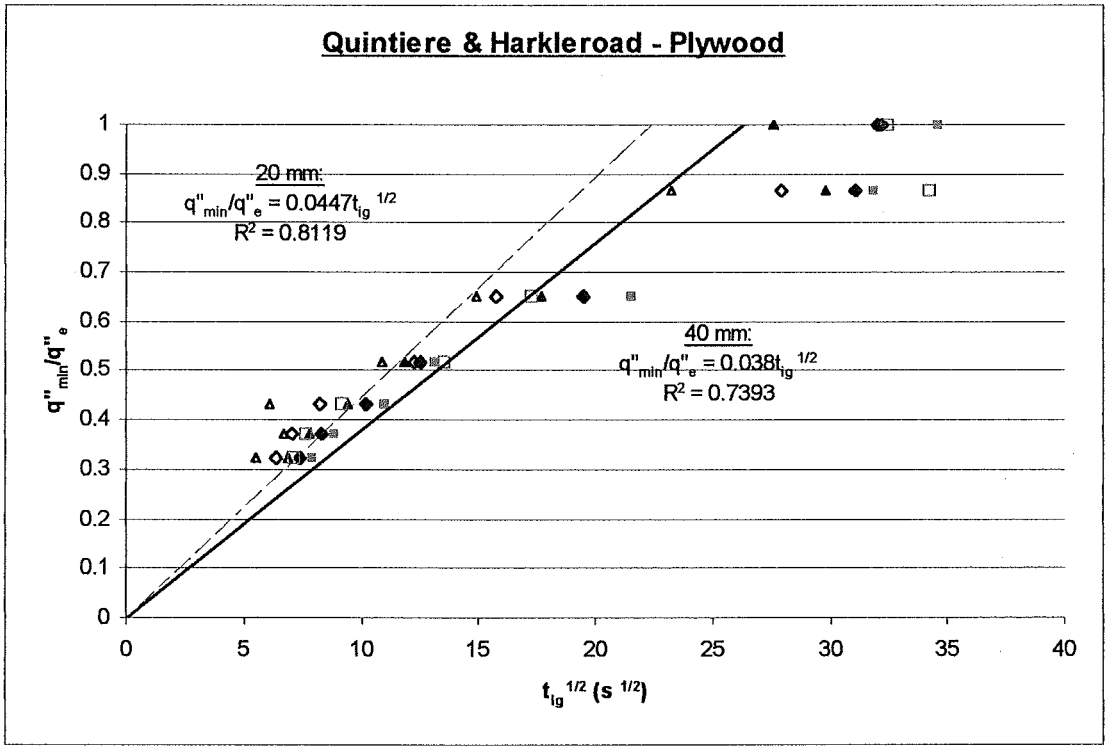

Figure H3: Ignition data of Plywood plotted by Quintiere and Harkleroad

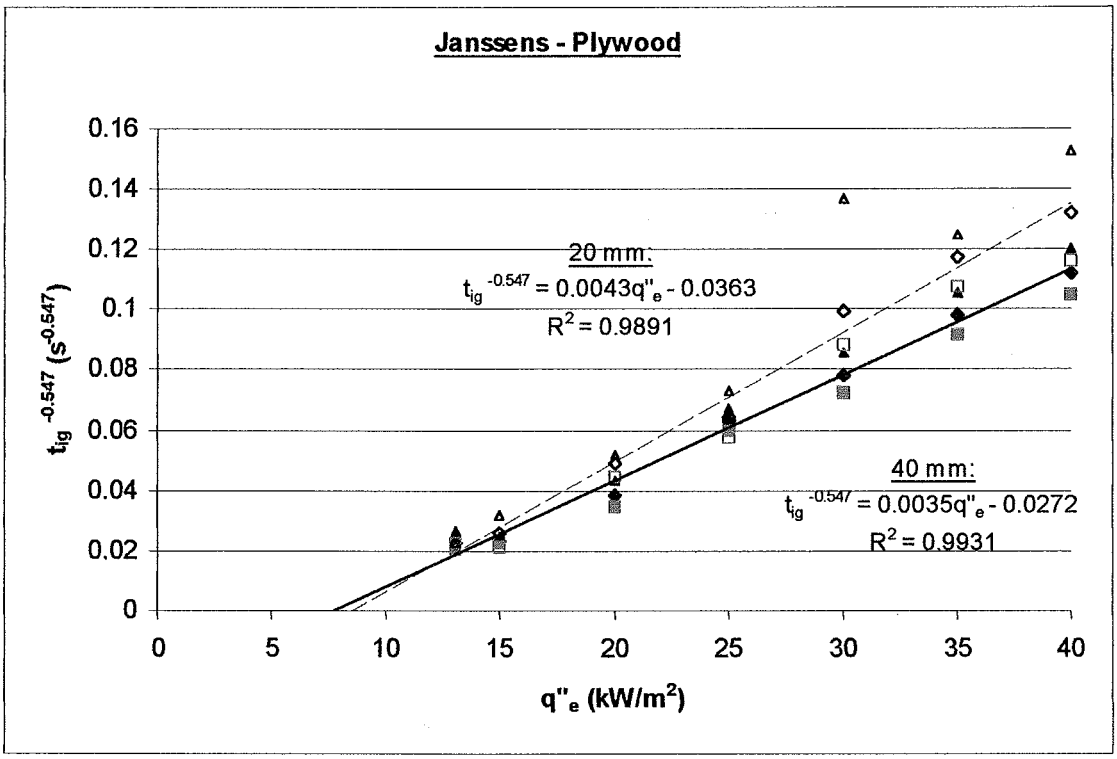

Figure H4: Ignition data of Plywood plotted by Janssens

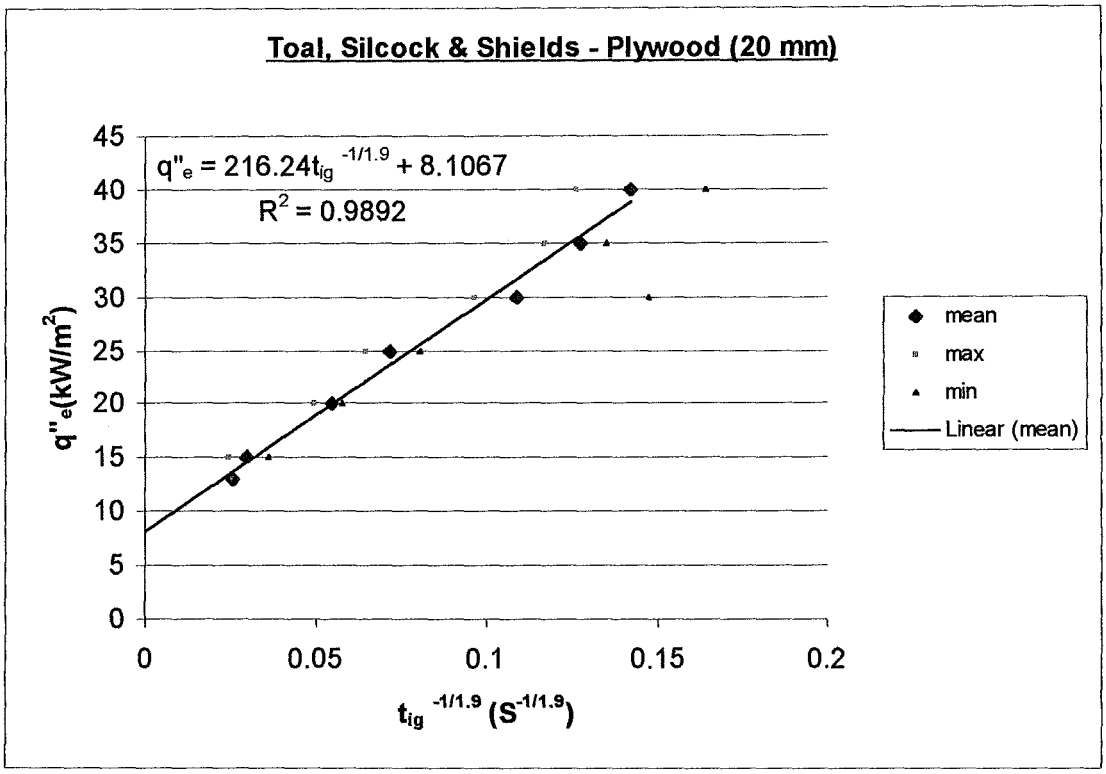

Figure H5: Ignition data of 20-mm Plywood plotted by Toal, Silcock and Shields

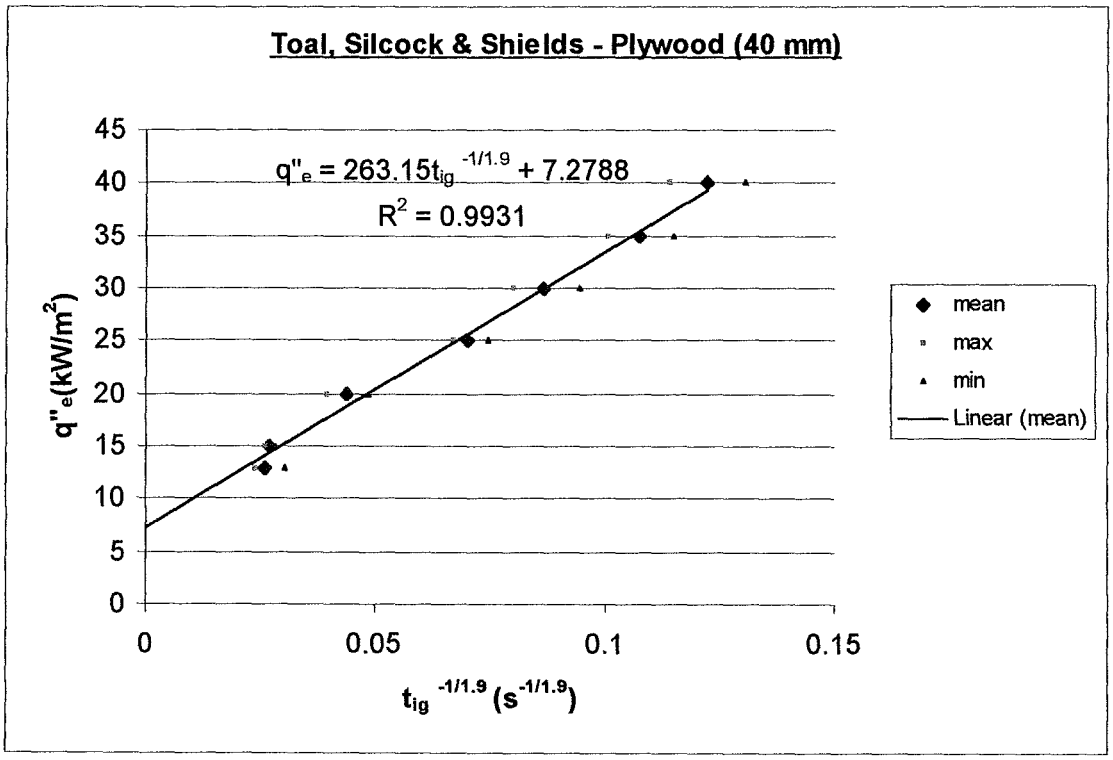

Figure H6: Ignition data of 40-mm Plywood plotted by Toal, Silcock and Shields

Appendix I: Raw Data

Thickness = 40 mm

									previous done		redo			
Timber Type	Radiata Pine		Rimu		Beech		Macrocarpa		mdf		mdf		Plywood	
Incident flux	t_{ig} (s)		t_{ig} (s)		t_{ig} (s)		t_{ig} (s)		t_{ig} (s)		t_{ig} (s)		t_{ig} (s)	
40	48	**20**	57	**47**	66	51	57	46	78	59	59	63	48	57
(kW/m^2)	49	50	79	54	51	50	47	42	72	79	66	61	51	54
	46	42.6	64	60.2	42	52	53	49	72	72	61	62	62	54.4
35	55	64	78	61	80	71	69	83	97	92	NT	NT	68	72
(kW/m^2)	65	31	**112**	70	76	59	62	86	80	82	NT	NT	61	66
	51	53.2	74	79	74	72	59	71.8	87	87.6	NT	NT	79	69.2
30	**126**	85	144	**112**	134	127	130	96	112	120	108	123	106	113
(kW/m^2)	92	87	193	**102**	100	114	91	115	116	126	109	114	89	121
	83	94.6	175	145.2	81	111.2	**178**	122	121	119	117	114.2	93	104.4
25	277	142	354	315	311	266	440	**250**	211	161	NT	NT	157	171
(kW/m^2)	**185**	197	271	**185**	**168**	200	349	486	166	160	NT	NT	159	139
	259	212	370	299	**171**	223.2	431	391.2	168	173.2	NT	NT	160	157.2
20	435	477	678	760	789	881	988	1009	327	266	303	306	313	464
(kW/m^2)	437	603	679	**372**	914	807	652	905	319	324	274	261	341	446
	242	438.8	652	628.2	781	834.4	831	877	294	306	275	283.8	339	380.6
17	NT	NT	NT	NT	879	1034	NI	NI	NT	NT	NT	NT	NT	NT
(kW/m^2)	NT	NT	NT	NT	NI	1006	1193	NI	NT	NT	NT	NT	NT	NT
	NT	NT	NT	NT	937	964	1153	1173	NT	NT	NT	NT	NT	NT
16	NT	NT	NT	NT	NI	NI	NI	NI	NT	NT	NT	NT	NT	NT
(kW/m^2)	NT	NT	NT	NT	NI	NI	NI	NI	NT	NT	NT	NT	NT	NT
	NT	NT	NT	NT	1102	1102	NI	NI	NT	NT	NT	NT	NT	NT
15	663	NI	NI	NI	NI	NI	NI	NI	NI	NI	NI	NI	NI	NI
(kW/m^2)	NI	**127**	1097	**558**	NI	NI	NI	NI	817	NI	817	NI	888	1013
	791	527	NI	827.5	NI	NI	NI	NI	NI	817	NI	817	991	964
14	1048	NI	NI	NI					NI	NI	NI	NI	NT	NT
(kW/m^2)	NI	NI	NI	1137					NI	NI	NI	NI	NT	NT
	NI	1048	NI	1137					NI	NI	NI	NI	NT	NT
13	NI	NI	NI	NI					NI	NI	NI	NI	1192	1093
(kW/m^2)	NI	NI	NI	NI					NI	NI	NI	NI	1148	913
	NI	NI	NI	NI					NI	NI	NI	NI	761	1021.4
12													NI	NI
(kW/m^2)													NI	NI
													NI	NI

Table I1: Ignition Data of 40-mm samples

Note:
NI = No ignition
NT = No tested
The gray-labeled cells are the average values of the 5 recorded ignition time, t_{ig}.
The data in bold is the values considered outside the range and were removed when calculating Δ.

Appendix I: Raw Data

Thickness = 20 mm

Timber Type	Radiata Pine		Rimu		Beech		Macrocarpa		mdf		Plywood	
Incident flux	t_{ig} (s)		t_{ig} (s)		t_{ig} (s)		t_{ig} (s)		t_{ig} (s)		t_{ig} (s)	
40	47	34	54	49	31	42	40	41	53	60	37	51
(kW/m^2)	37	48	43	40	43	37	35	36	53	59	39	45
	31	39.4	37	44.6	50	40.6	34	37.2	49	54.8	31	40.6
35	54	37	88	76	42	56	57	59	74	79	59	45
(kW/m^2)	35	39	57	54	63	40	43	50	70	81	51	50
	45	42	52	65.4	**83**	56.8	47	51.2	66	74	46	50.2
30	73	72	113	113	**59**	87	83	**111**	99	114	77	**38**
(kW/m^2)	65	85	57	84	99	79	71	78	97	119	74	85
	76	74.2	73	**88**	120	**88.8**	74	**83.4**	121	110	66	68
25	121	105	180	218	100	140	180	162	149	177	157	182
(kW/m^2)	89	141	276	235	161	123	141	167	184	141	139	119
	109	113	129	207.6	**203**	145.4	151	160.2	162	162.6	149	149.2
20	628	**252**	842	743	**386**	555	899	893	299	247	246	239
(kW/m^2)	539	**275**	435	484	674	512	909	889	241	249	237	223
	427	424.2	561	613	**847**	594.8	664	850.8	254	258	299	248.8
17	NT	NT	NT	NT	NI	1051	NI	NI	NT	NT	NT	NT
(kW/m^2)	NT	NT	NT	NT	NI	1069	NI	NI	NT	NT	NT	NT
	NT	NT	NT	NT	NI	1060	1162	1162	NT	NT	NT	NT
16	NT	NT	NT	NT	NI	NI	NI	NI	NT	NT	NT	NT
(kW/m^2)	NT	NT	NT	NT	NI	1086	NI	NI	NT	NT	NT	NT
	NT	NT	NT	NT	NI	1086	NI	NI	NT	NT	NT	NT
15	NI	NI	NI	NI	NI	NI	NI	NI	867	519	565	**1046**
(kW/m^2)	502	NI	653	NI	NI	NI	NI	NI	606	893	538	**1168**
	NI	502	NI	653	NI	NI	NI	NI	803	737.6	581	779.6
14	NI	NI	NI	NI					NI	NI	NT	NT
(kW/m^2)	NI	NI	NI	NI					NI	NI	NT	NT
	NI	NI	656	656					NI	NI	NT	NT
13	NI	NI	NI	NI					NI	NI	NI	NI
(kW/m^2)	NI	NI	NI	NI					NI	NI	1050	1024
	NI	NI	NI	NI					NI	NI	NI	1037
12											NI	NI
(kW/m^2)											NI	NI
											NI	NI

Table I2: Ignition Data of 20-mm samples

Appendix J: Repeatability and Reproducibility

Repeatability, r, of Rimu, Radiata Pine, Beech, Macrocarpa and Plywood

Δ (s) = absolute difference between single values of extremes and the mean ignition time
m = mean of the ignition time of the five specimens at certain level of irradiance

The highlighted numbers are the values obtained, after taking out the outlying ignition times

40-mm sample

Rimu

	upper extreme			lower extreme		
Level	Δ (s)	m	Δ (% of mean)	Δ (s)	m	Δ (% of mean)
40	15.5	64	**24**	9.5	64	**15**
35	7.25	71	**10**	9.75	71	**14**
30	22	171	**13**	27	171	**16**
25	43	328	**13**	57	328	**17**
20	68	692	**10**	40	692	**6**

Table J1: Δ of 40-mm Rimu

20-mm sample

	upper extreme			lower extreme		
Level	Δ (s)	m	Δ (% of mean)	Δ (s)	m	Δ (% of mean)
40	9.4	54	17	7.6	54	14
35	22.6	88	26	13.4	88	15
30	25	113	22	31	113	27
25	68	276	25	79	276	28
20	229	842	27	178	842	21

Table J2: Δ of 20-mm Rimu

Radiata Pine

	upper extreme			lower extreme		
Level	Δ (s)	m	Δ (% of mean)	Δ (s)	m	Δ (% of mean)
40	1.75	48.3	**4**	2.25	48.3	**5**
35	6.25	58.8	**11**	7.75	58.8	**13**
30	5.25	86.8	**6**	3.75	86.8	**4**
25	48	230	**21**	45	230	**19**
20	115	488	**24**	53	488	**11**

Table J3: Δ of 40-mm Radiata Pine

	upper extreme			lower extreme		
Level	Δ (s)	m	Δ (% of mean)	Δ (s)	m	Δ (% of mean)
40	8.6	39.4	22	8.4	39.4	21
35	12	42	29	7	42	17
30	10.8	74.2	15	9.2	74.2	12
25	28	113	25	24	113	21
20	97	531.3	**18**	104	531	**20**

Table J4: Δ of 20-mm Radiata Pine

40-mm sample

Beech

	upper extreme			lower extreme		
Level	Δ (s)	m	Δ (% of mean)	Δ (s)	m	Δ (% of mean)
40	14	52	27	10	52	19
35	8	72	11	13	72	18
30	23	111	21	30	111.2	27
25	52	259	**20**	59	259	**23**
20	80	834	10	53	834.4	6
17	70	964	7	85	964	9

Table J5: Δ of 40-mm Beech

20-mm sample

	upper extreme			lower extreme		
Level	Δ (s)	m	Δ (% of mean)	Δ (s)	m	Δ (% of mean)
40	9.4	40.6	23	9.6	40.6	24
35	12.8	50.3	**25**	10.25	50.3	**20**
30	23.8	96.3	**25**	17.25	96.3	**18**
25	30	131	**23**	31	131	**24**
20	94	580	**16**	68	580	**12**
17	9	1060	1	9	1060	1

Table J6: Δ of 20-mm Beech

Macrocarpa

	upper extreme			lower extreme		
Level	Δ (s)	m	Δ (% of mean)	Δ (s)	m	Δ (% of mean)
40	8	49	16	7	49	14
35	14.2	71.8	20	12.8	71.8	18
30	22	108	**20**	17	108	**16**
25	60	427	**14**	78	426.5	**18**
20	132	877	15	225	877	26
17	20	1173	2	20	1173	2

Table J7: Δ of 40-mm Macrocarpa

	upper extreme			lower extreme		
Level	Δ (s)	m	Δ (% of mean)	Δ (s)	m	Δ (% of mean)
40	3.8	37.2	10	3.2	37.2	9
35	7.8	51.2	15	8.2	51.2	16
30	6.5	76.5	**8**	5.5	76.5	7
25	20	160.2	12	19	160	12
20	58	850.8	7	187	851	22

Table J8: Δ of 20-mm Macrocarpa

40-mm sample

Plywood

	upper extreme			lower extreme		
Level	Δ (s)	m	Δ (% of mean)	Δ (s)	m	Δ (% of mean)
40	7.6	54.4	14	6.4	54.4	12
35	9.8	69.2	14	8.2	69.2	12
30	17	104	16	15	104.4	15
25	14	157	9	18	157.2	12
20	83.4	381	22	68	380.6	18
15	49	964	5	76	964	8
13	171	1021	17	260	1021.4	25

Table J9: Δ of 40-mm Plywood

20-mm sample

Moderate density fibreboard (mdf)

	upper extreme			lower extreme		
Level	Δ (s)	m	Δ (% of mean)	Δ (s)	m	Δ (% of mean)
40	5.2	54.8	9	5.8	54.8	11
35	7	74	9	8	74	11
30	11	110	10	13	110	12
25	21	163	13	22	162.6	13
20	41	258	16	17	258	7
15	100.7	792	**13**	186.3	792.3	**24**

Table J11: Δ of 20-mm mdf

20-mm sample

	upper extreme			lower extreme		
Level	Δ (s)	m	Δ (% of mean)	Δ (s)	m	Δ (% of mean)
40	10.4	40.6	26	9.6	40.6	24
35	8.8	50.2	18	5.2	50.2	10
30	9.5	75.5	**13**	9.5	75.5	**13**
25	33	149.2	22	30	149	20
20	50	248.8	20	26	249	10
15	19.7	561.3	**4**	23.3	561	**4**
13	13	1037	1	13	1037	1

Table J10: Δ of 20-mm Plywood

Repeatability, r and Reproducibility, R, of mdf

40-mm mdf

Lab 1: redo
based on calibration scale on 20/12/2000

Lab 2: previous done
based on calibration scale on 5/12/2000

original data, y_i

Level $_i$	40	30	20
Lab 1	59	108	303
	66	109	274
	61	117	275
	63	123	306
	61	114	261
sum	310	571	1419
Lab 2	78	112	327
	72	116	319
	72	121	294
	59	120	266
	79	126	324
sum	360	595	1530

Table J12: Original data, y_i

y_i^2

Level $_i$	40	30	20
Lab 1	3481	11664	91809
	4356	11881	75076
	3721	13689	75625
	3969	15129	93636
	3721	12996	68121
sum of y^2	19248	65359	404267
Lab 2	6084	12544	106929
	5184	13456	101761
	5184	14641	86436
	3481	14400	70756
	6241	15876	104976
sum of y^2	26174	70917	470858

Table J13: y_i^2

$(1/n)*(\text{sum of } y_i)^2$

Level $_i$	40	30	20
Lab 1	19220	65208.2	402712.2
Lab 2	25920	70805	468180

Table J14: $(1/n)*(\text{sum of } y_i)^2$

s_i

Level $_i$	40	30	20
Lab 1	2.646	6.140	19.715
si^2	7	37.7	388.7
Lab 2	7.969	5.292	25.875
si^2	63.5	28	669.5
Total	70.5	65.7	1058.2

Table J15: Intra-cell standard deviation, s_i

cell averages, y_i bar

Level $_i$	40	30	20
Lab 1	62	114.2	283.8
Lab 2	72	119	306
sum	134	233.2	589.8

Table J16: Cell averages, y_i bar

y bar bar

Level $_i$	40	30	20
sum of (n_i * y_i bar)	670	1166	2949
sum of n	10	10	10
y bar bar	67	116.6	294.9

Table J17: y bar bar

n bar bar

Level $_i$	40	30	20
sum of (n_i^2)	50	50	50
sum of n	10	10	10
n bar bar	5	5	5

Table J18: n bar bar

s_L^2

Level	40	30	20
s_L^2	43	4.95	234

Table J19: Between-lab variance, s_L^2

Level $_i$	p_i	m_i	s_r^2	r_i	s_R^2	R_i
40	2	67	35	17	78	25
30	2	116.6	33	16	38	17
20	2	294.9	529	64	763	77

Table J20: Calculation of r and R values

Average values:

r = **32**

R = **40**

Appendix K: Plot of Measured t_{ig} versus Predicted t_{ig}

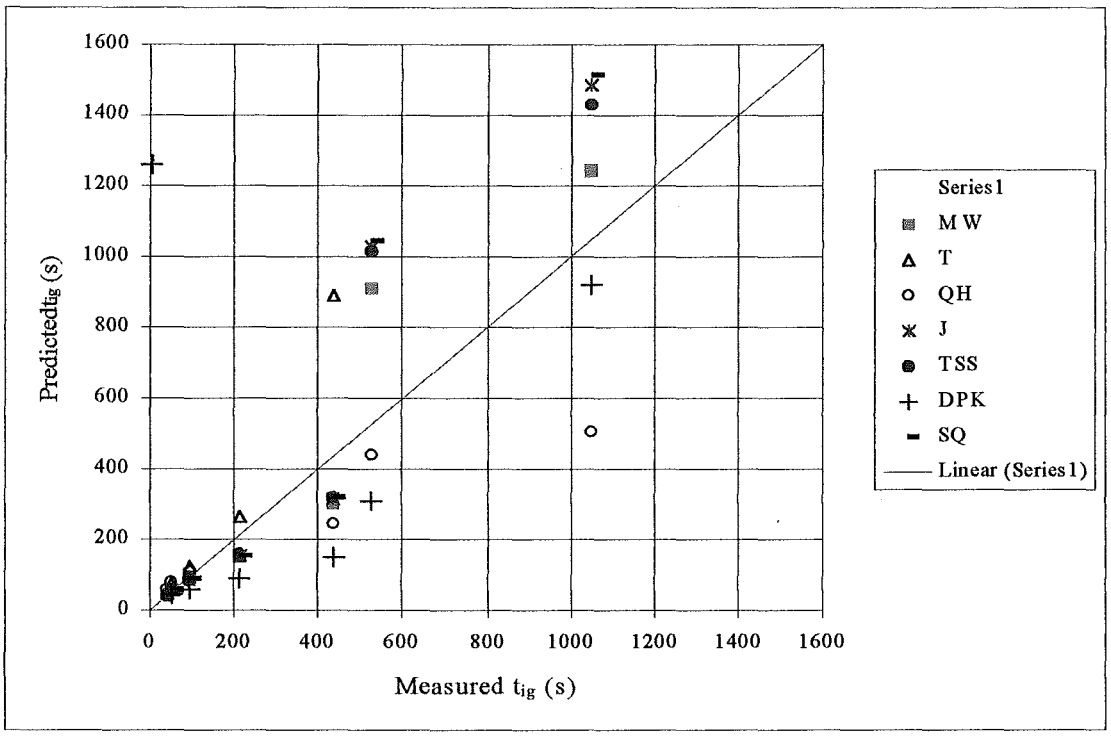

Figure K1: Predicted ignition time versus Measured ignition time for 40-mm Radiata Pine

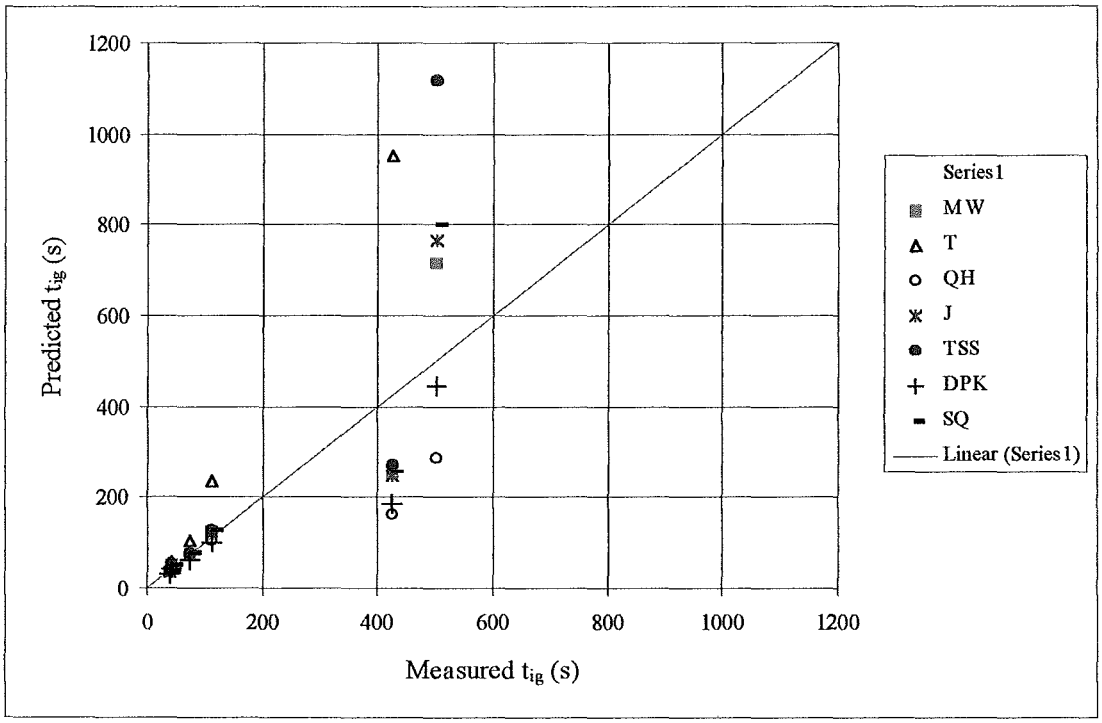

Figure K2: Predicted ignition time versus Measured ignition time for 20-mm Radiata Pine

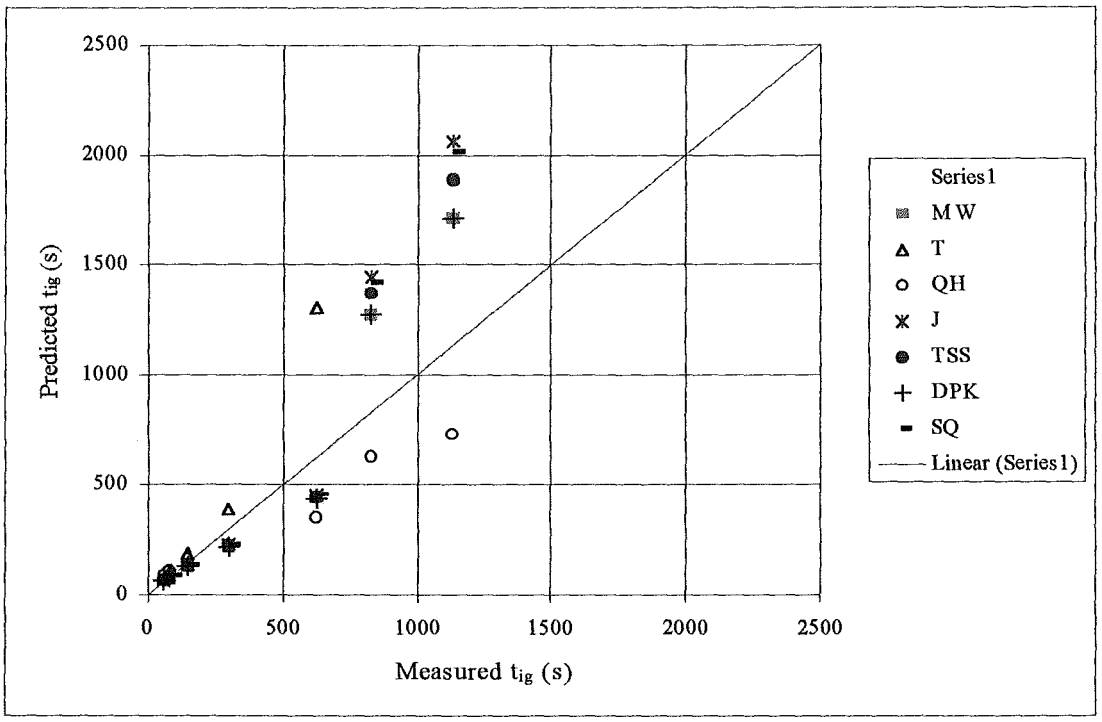

Figure K3: Predicted ignition time versus Measured ignition time for 40-mm Rimu

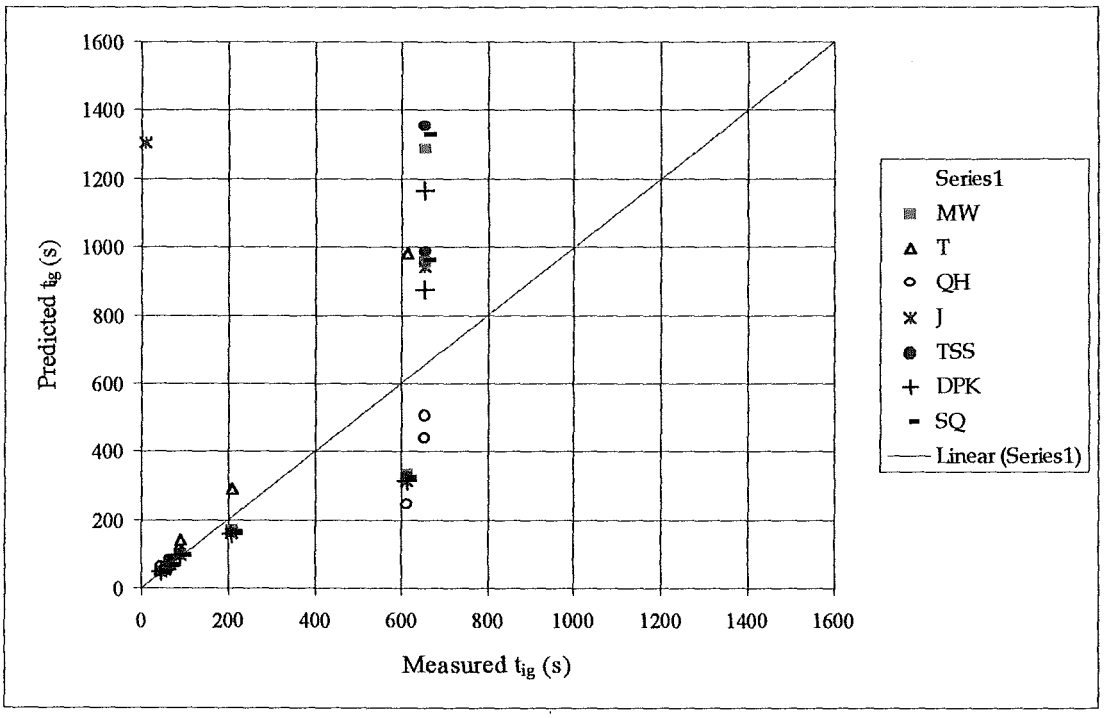

Figure K4: Predicted ignition time versus Measured ignition time for 20-mm Rimu

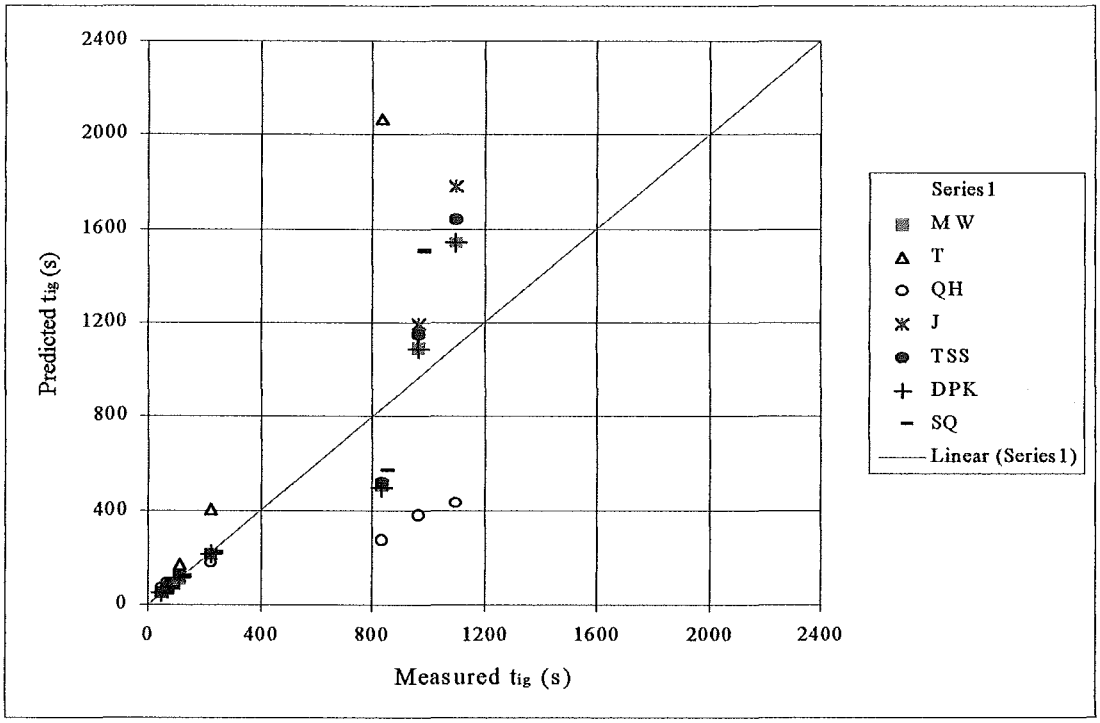

Figure K5: Predicted ignition time versus Measured ignition time for 40-mm Beech

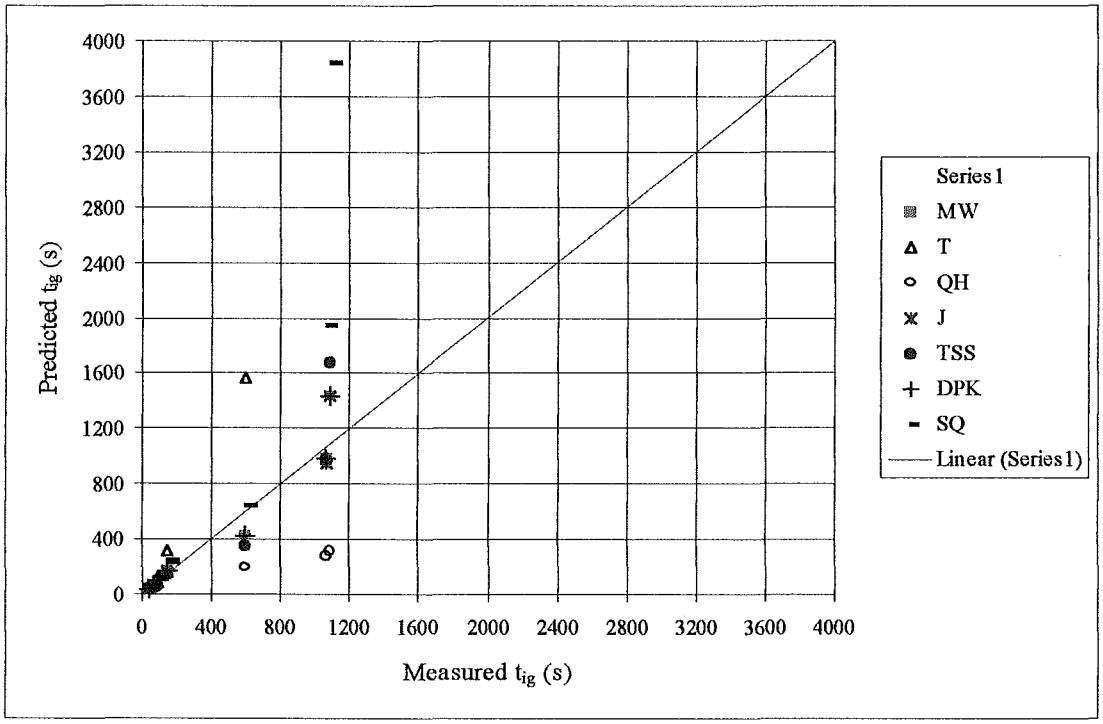

Figure K6: Predicted ignition time versus Measured ignition time for 20-mm Beech

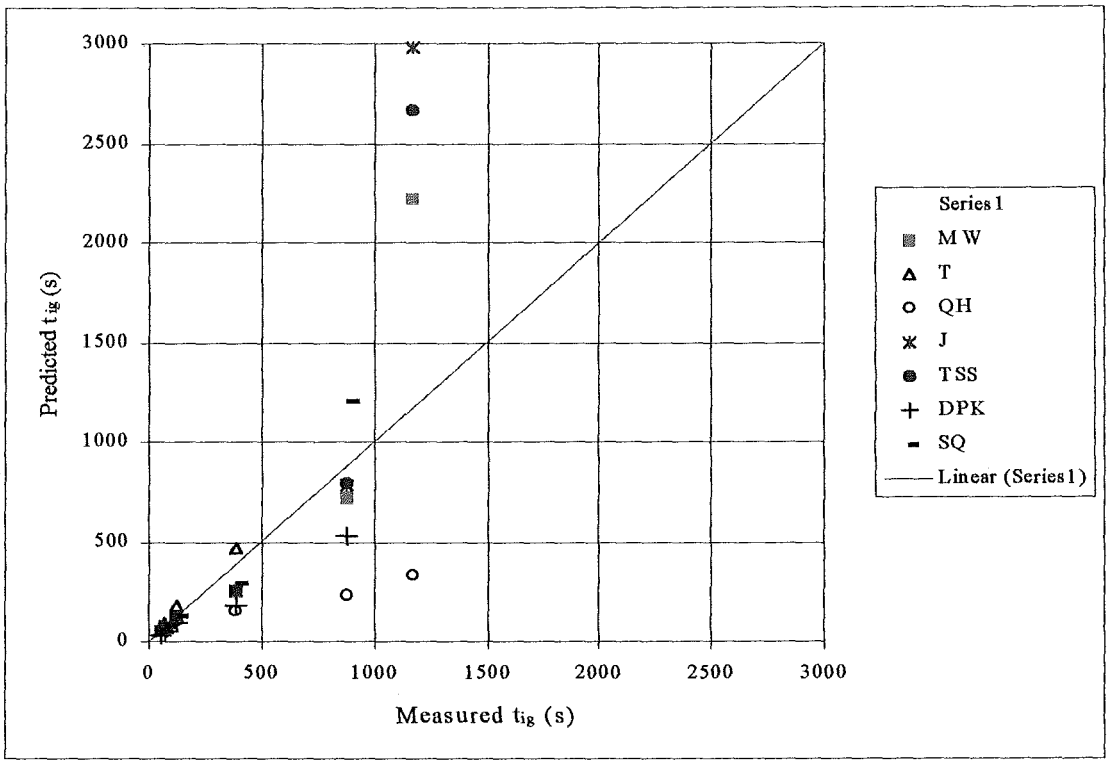

Figure K7: Predicted ignition time versus Measured ignition time for 40-mm Macrocarpa

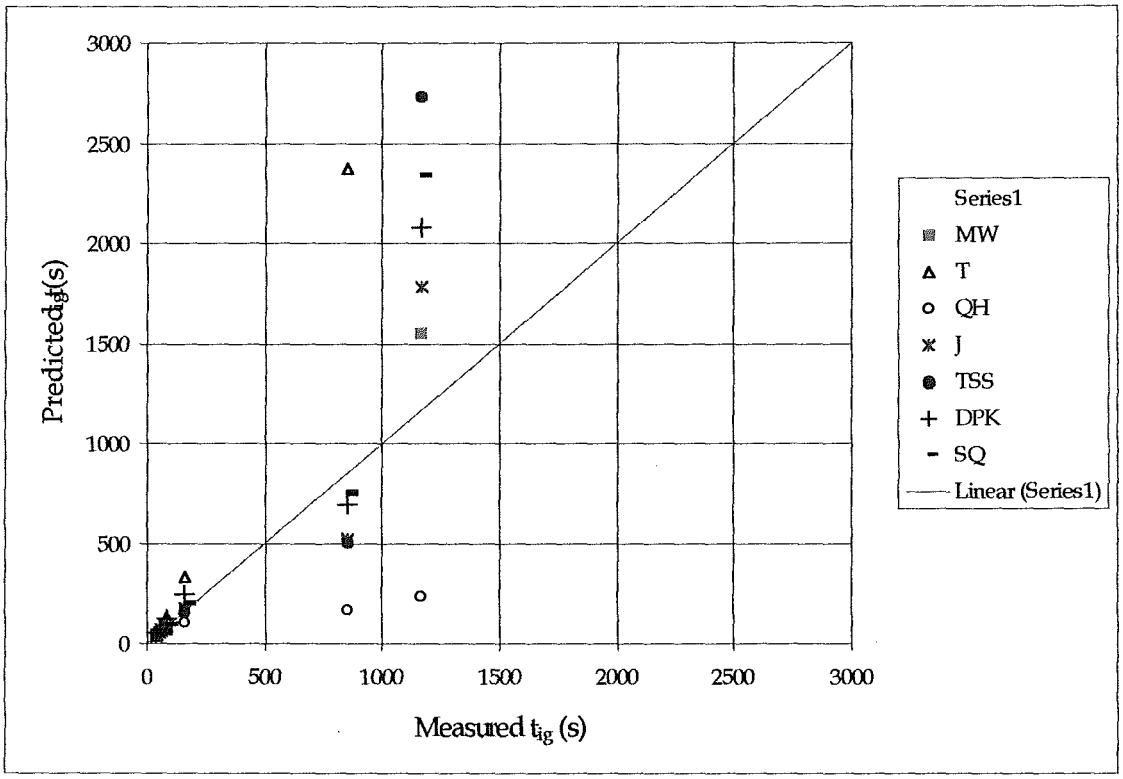

Figure K8: Predicted ignition time versus Measured ignition time for 20-mm Macrocarpa

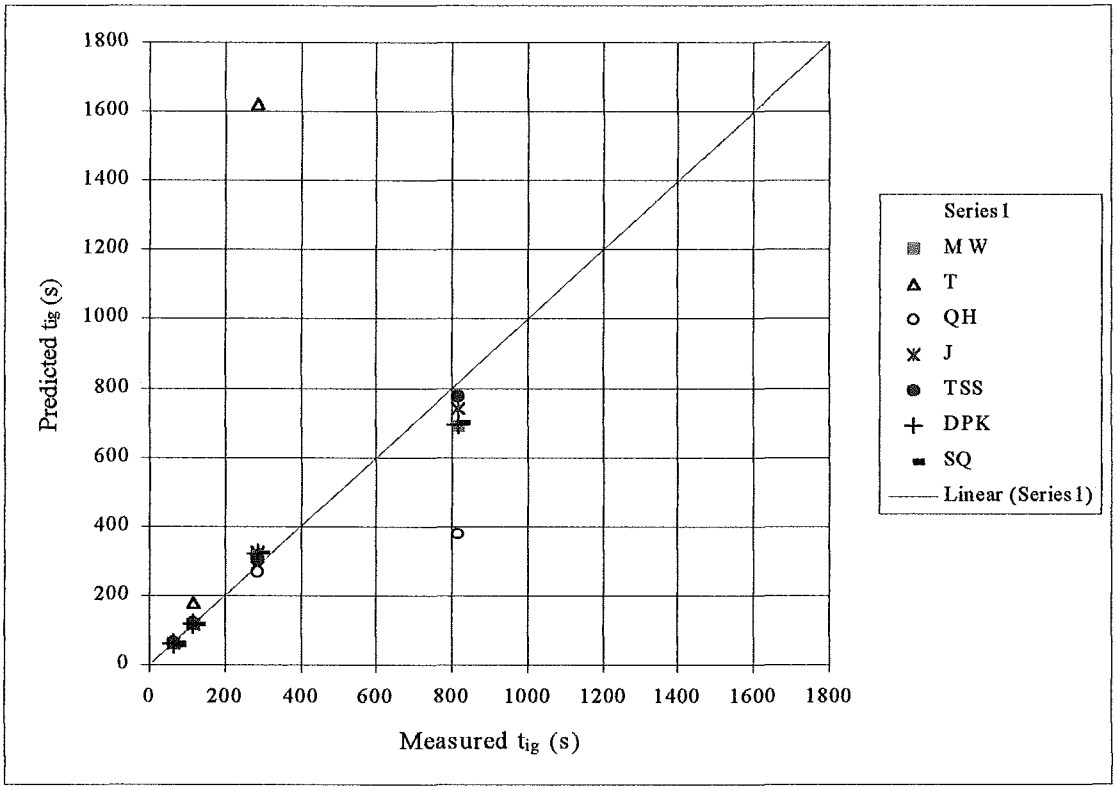

Figure K9: Predicted ignition time versus Measured ignition time for 40-mm mdf

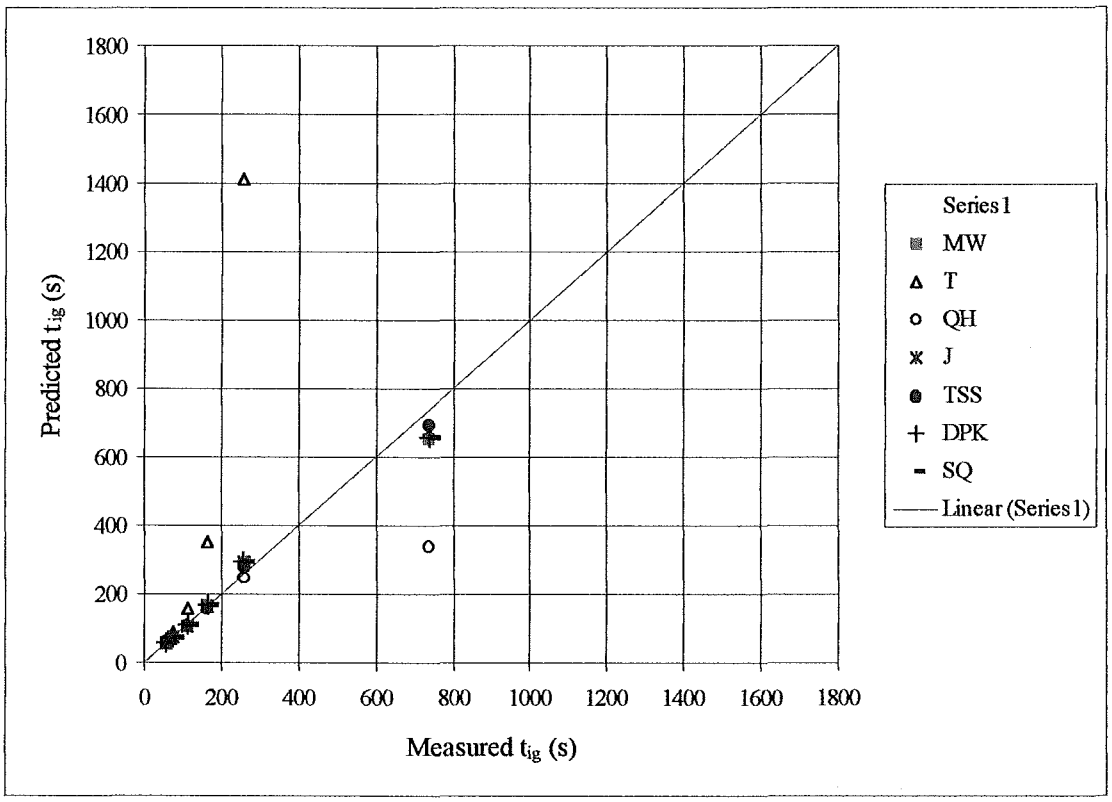

Figure K10: Predicted ignition time versus Measured ignition time for 20-mm mdf

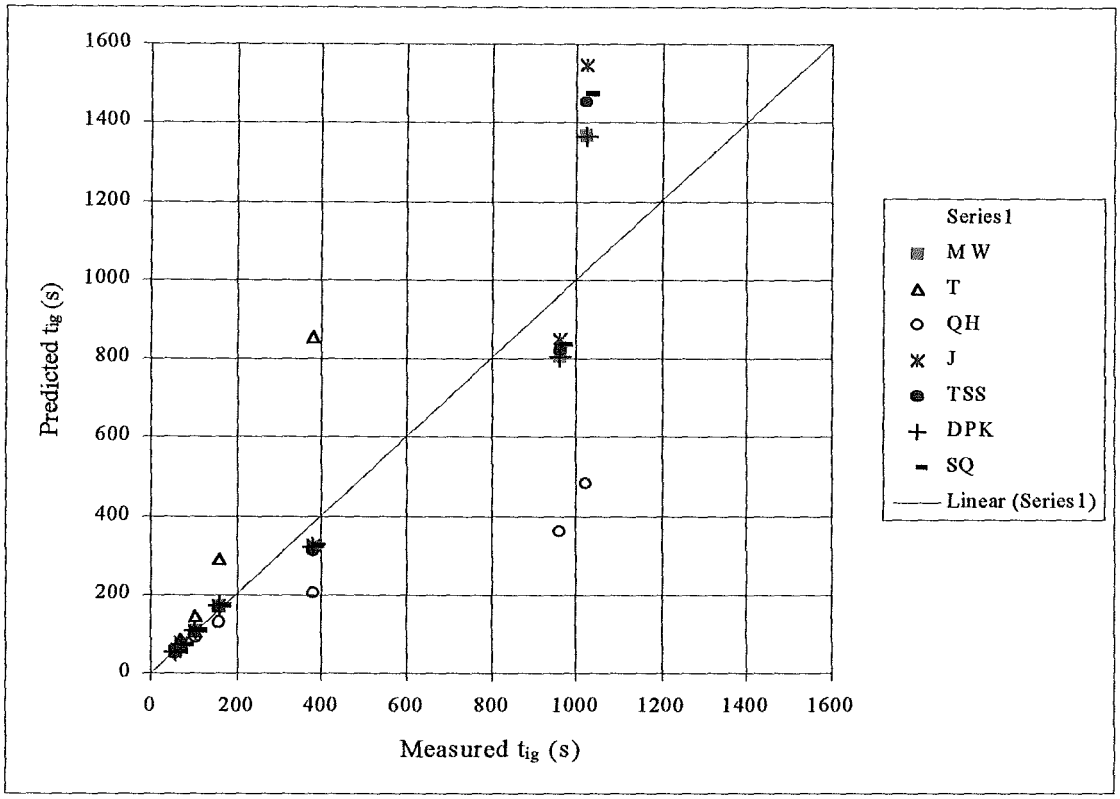

Figure K11: Predicted ignition time versus Measured ignition time for 40-mm Plywood

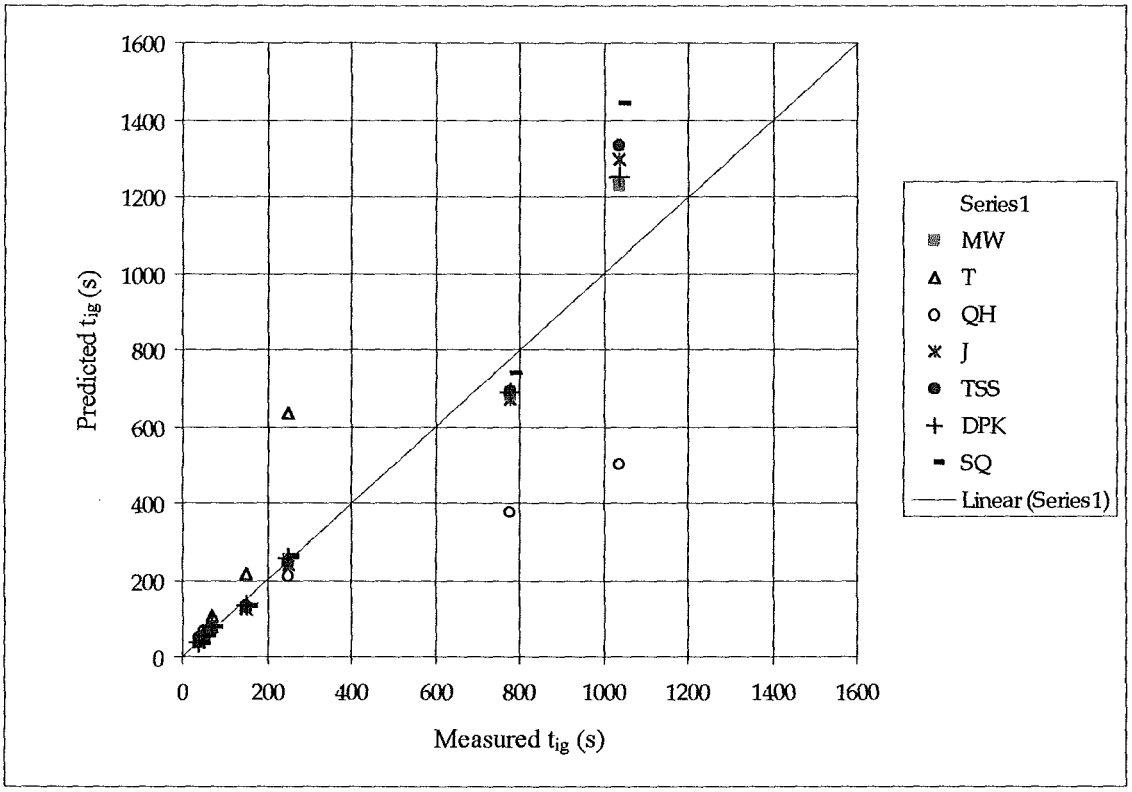

Figure K12: Predicted ignition time versus Measured ignition time for 20-mm Plywood

FIRE ENGINEERING RESEARCH REPORTS

95/1	Full Residential Scale Backdraft	I B Bolliger
95/2	A Study of Full Scale Room Fire Experiments	P A Enright
95/3	Design of Load-bearing Light Steel Frame Walls for Fire Resistance	J T Gerlich
95/4	Full Scale Limited Ventilation Fire Experiments	D J Millar
95/5	An Analysis of Domestic Sprinkler Systems for Use in New Zealand	F Rahmanian
96/1	The Influence of Non-Uniform Electric Fields on Combustion Processes	M A Belsham
96/2	Mixing in Fire Induced Doorway Flows	J M Clements
96/3	Fire Design of Single Storey Industrial Buildings	B W Cosgrove
96/4	Modelling Smoke Flow Using Computational Fluid Dynamics	T N Kardos
96/5	Under-Ventilated Compartment Fires - A Precursor to Smoke Explosions	A R Parkes
96/6	An Investigation of the Effects of Sprinklers on Compartment Fires	M W Radford
97/1	Sprinkler Trade Off Clauses in the Approved Documents	G J Barnes
97/2	Risk Ranking of Buildings for Life Safety	J W Boyes
97/3	Improving the Waking Effectiveness of Fire Alarms in Residential Areas	T Grace
97/4	Study of Evacuation Movement through Different Building Components	P Holmberg
97/5	Domestic Fire Hazard in New Zealand	KDJ Irwin
97/6	An Appraisal of Existing Room-Corner Fire Models	D C Robertson
97/7	Fire Resistance of Light Timber Framed Walls and Floors	G C Thomas
97/8	Uncertainty Analysis of Zone Fire Models	A M Walker
97/9	New Zealand Building Regulations Five Years Later	T M Pastore
98/1	The Impact of Post-Earthquake Fire on the Built Urban Environment	R Botting
98/2	Full Scale Testing of Fire Suppression Agents on Unshielded Fires	M J Dunn
98/3	Full Scale Testing of Fire Suppression Agents on Shielded Fires	N Gravestock
98/4	Predicting Ignition Time Under Transient Heat Flux Using Results from Constant Flux Experiments	A Henderson
98/5	Comparison Studies of Zone and CFD Fire Simulations	A Lovatt
98/6	Bench Scale Testing of Light Timber Frame Walls	P Olsson
98/7	Exploratory Salt Water Experiments of Balcony Spill Plume Using Laser Induced Fluorescence Technique	E Y Yii
99/1	Fire Safety and Security in Schools	R A Carter

99/2	A Review of the Building Separation Requirements of the New Zealand Building Code Acceptable Solutions	J M Clarke
99/3	Effect of Safety Factors in Timed Human Egress Simulations	K M Crawford
99/4	Fire Response of HVAC Systems in Multistorey Buildings: An Examination of the NZBC Acceptable Solutions	M Dixon
99/5	The Effectiveness of the Domestic Smoke Alarm Signal	C Duncan
99/6	Post-flashover Design Fires	R Feasey
99/7	An Analysis of Furniture Heat Release Rates by the Nordtest	J Firestone
99/8	Design for Escape from Fire	I J Garrett
99/9	Class A Foam Water Sprinkler Systems	D B Hipkins
99/10	Review of the New Zealand Standard for Concrete Structures (NZS 3101) for High Strength and Lightweight Concrete Exposed to Fire	M J Inwood
99/12	An Analytical Model for Vertical Flame Spread on Solids: An Initial Investigation	G A North
99/13	Should Bedroom Doors be Open or Closed While People are Sleeping? - A Probabilistic Risk Assessment	D L Palmer
99/14	Peoples Awareness of Fire	S J Rusbridge
99/15	Smoke Explosions	B J Sutherland
99/16	Reliability of Structural Fire Design	JKS Wong
99/17	Heat Release from New Zealand Upholstered Furniture	T Enright
00/1	Fire Spread on Exterior Walls	FNP Bong
00/2	Fire Resistance of Lightweight Framed Construction	PCR Collier
00/3	Fire Fighting Water: A Review of Fire Fighting Water Requirements (A New Zealand Perspective)	S Davis
00/4	The Combustion Behaviour of Upholstered Furniture Materials in New Zealand	H Denize
00/5	Full-Scale Compartment Fire Experiments on Upholstered Furniture	N Girgis
00/6	Fire Rated Seismic Joints	M James
00/7	Fire Design of Steel Members	K R Lewis
00/8	Stability of Precast Concrete Tilt Panels in Fire	L Lim
00/9	Heat Transfer Program for the Design of Structures Exposed to Fire	J Mason
00/10	An Analysis of Pre-Flashover Fire Experiments with Field Modelling Comparisons	C Nielsen
00/11	Fire Engineering Design Problems at Building Consent Stage	P Teo
00/12	A Comparison of Data Reduction Techniques for Zone Model Validation	S Weaver
00/13	Effect of Surface Area and Thickness on Fire Loads	H W Yii
00/14	Home Fire Safety Strategies	P Byrne
00/15	Accounting for Sprinkler Effectiveness in Performance Based Design of Steel Buildings in Fire	M Feeney

00/16	**A Guideline for the Fire Design of Shopping Centres**	**J M McMillan**
01/1	**Flamability of Upholstered Furniture Using the Cone Calorimeter**	**A Coles**
01/2	**Radiant Ignition of New Zealand Upholstered Furniture Composites**	**F Chen**
01/3	**Statistical Analysis of Hospitality Industry Fire Experience**	**T Y A Chen**
01/4	**Performance of Gypsum Plasterboard Assemblies Exposed to Real Building Fires**	**B H Jones**
01/5	**Ignition Properties of New Zealand Timber**	**C K Ngu**
01/6	**Effect of Support Conditions on Steel Beams Exposed of Fire**	**J Seputro**
01/7	**Validation of an Evacuation Model Currently Under Development**	**A Teo**
01/8	**2-D Analysis of Composite Steel - Concrete Beams in Fire**	**R Welsh**
01/9	**Contribution of Upholstered Furniture to Residential Fire Fatalities in New Zealand**	**C R Wong**
01/10	**The Fire Safety Design of Apartment Buildings**	**S Wu**

School of Engineering
University of Canterbury
Private Bag 4800, Christchurch, New Zealand

Phone 643 364-2250
Fax 643 364-2758